DISSERTATION

SUBMITTED TO THE

COMBINED FACULTIES FOR THE

NATURAL SCIENCES AND FOR MATHEMATICS OF THE

RUPERTO-CAROLA UNIVERSITY OF HEIDELBERG, GERMANY

FOR THE DEGREE OF

DOCTOR OF NATURAL SCIENCES

Dynamics and Architecture of the HOPS Tethering Complex in Yeast Vacuole Fusion

PRESENTED BY

DIPLOM-BIOCHEMIKER CLEMENS WERNER OSTROWICZ,

BORN IN KIEL, GERMANY

DISSERTATION

SUBMITTED TO THE

COMBINED FACULTIES FOR THE

NATURAL SCIENCES AND FOR MATHEMATICS OF THE

RUPERTO-CAROLA UNIVERSITY OF HEIDELBERG, GERMANY

FOR THE DEGREE OF

DOCTOR OF NATURAL SCIENCES

PRESENTED BY

DIPLOM-BIOCHEMIKER CLEMENS WERNER OSTROWICZ,

BORN IN KIEL, GERMANY

ORAL EXAMINATION:

Dynamics and Architecture of the HOPS Tethering Complex in Yeast Vacuole Fusion

Referees: Prof. Dr. Eduard Hurt

Prof. Dr. Christian Ungermann

Declaration

I herewith declare that I wrote this thesis independently and used no other sources and aids than those indicated.

April 28,2009 _____

(Clemens W. Ostrowicz)

Table of Contents

Publications and Manuscripts

Peplowska, K., Markgraf, D.F.*, **Ostrowicz, C.W.***, Bange, G., and Ungermann, C. (2007) The CORVET tethering complex interacts with the yeast Rab5 homolog Vps21 and is involved in endo-lysosomal biogenesis. *Dev. Cell* **12**, 739-750
*these authors contributed equally to this work.

Ostrowicz, C.W., Meiringer, C.T.A., and Ungermann C. (2008) Yeast vacuole fusion: a model system for eukaryotic endomembrane dynamics. Review. *Autophagy*. 4, 5-19.

Cabrera, M., **Ostrowicz, C.W.**, Mari, M., LaGrassa, T.J., Reggiori, F., and Ungermann C. (2009) Vps41 Phosphorylation and the Rab Ypt7 Control the Tageting of the HOPS Complex to Endosome-Vacuole Fusion Sites. *Mol. Biol. Cell* **20**, 1937-1948

Ostrowicz, C.W., Bröcker, C., and Ungermann C. (2009) The HOPS tethering complex consists of stable subcomplexes implicated in endolysosomal biogenesis. In preparation for submission.

Markgraf, D.F., Peplowska, K., Ahnert F., Mari, M., Griffith, J., Reggiori, F., **Ostrowicz C.W.** and Ungermann, C. (2009) Direct interaction of the CORVET subunit Vps8 and the Rab5 GTPase Vps21 tethers late endosomal compartments. In preparation for submission.

Summary

The evolvement of a complex endomembrane system, which is separating a variety of biochemical processes into distinct compartments, is a hallmark of eukaryotic cell development. Cellular homeostasis depends on the abilities of these lipid bilayer-enclosed organelles both to maintain distinct characteristics and to exchange materials. This is mainly achieved by a process called vesicular transport, which allows for a constant exchange of proteins, lipids and metabolites between different compartments. Lipid-bilayer enclosed vesicles bud from the donor compartment, are transported to the target compartment and fuse with its surrounding membrane. The basic machineries involved in the process in budding and fusion have been intensely investigated in the last years. However, our knowledge about the processes, which confer target specificity and regulate intracellular membrane fusion, is still limited. Before fusion of two-compartments can occur, they have to specifically recognize and bind each other to allow for subsequent SNARE[1]-induced fusion to take place. This early step in the fusion reaction is called tethering and involves the action of tethering factors and Rab GTPases.

In my research, I focused on the HOPS[2] protein complex that is implicated to function in the tethering process at the yeast vacuole, the fungal equivalent of lysosomes. To investigate the molecular properties that confer the functionality of this large hexameric complex, I established a method that allowed for the purification of substantial amounts of HOPS and investigated the interactions taking place between different subunits. This work paved the ground for electron microscopy analysis of the whole complex, which is currently performed and which yielded first, preliminary data. Furthermore, it allowed for the identification of the novel CORVET[3] tethering complex at the endosome, which has several subunits in common with the HOPS complex. I was able to show that chimeric complexes exist, harboring both HOPS- and CORVET-

[1] Soluble N-ethylmaleimide sensitive protein receptors

[2] Homotypic fusion and vacuole protein sorting

[3] Class C Core vacuole endosome tethering

specific subunits. This finding suggests that both complexes are dynamic and can interconvert.

During my studies on the subunits' interactions, I identified stable subcomplexes of the HOPS complex, for one of which I could show that it exists *in vivo*. The existence of such subcomplexes implies a much more dynamic functioning of the HOPS subunits than previously anticipated. This notion is further strengthened by my studies on the functionality of different subunits and subcomplexes. Intriguingly, my results show that the Rab Guanyl nucleotide exchange factor Vam6, which is needed to activate the vacuolar Rab Ypt7 for subsequent fusion and which is a component of the HOPS complex, loses its ability to interact with Ypt7 upon incorporation into a subcomplex or the fully assembled HOPS complex. In contrast to this, the subunit Vps41, which I could identify as a Rab effector, is active as a single protein and as part of the complex, suggesting that it might sequentially recruit the subcomplexes to assemble into the holo complex at sites harboring active Ypt7.

Another feature of Vps41 was addressed in my work. This protein was previously shown to be phosphorylated by the vacuolar casein kinase Yck3. I identified the phosphorylation sites in the Vps41 sequence, which allowed further studies on the effect of the phosphorylation on the functionality of the protein. In the phosphorylated state, the protein is displaced into the cytosol whereas it accumulates at endosomal-vacuolar fusion sites if phosphorylation is prevented. Intriguingly, we found that Ypt7 overexpression is able to partially rescue the loss of localization in the phosphomimetic mutant, indicating a cross-talk between these two layers of Vps41 regulation.

Zusammenfassung

Die Entstehung eines komplexen Endomembransystems, in dem eine Vielzahl biochemischer Prozesse in spezielle Kompartimente aufgeteilt werden, ist ein prägendes Merkmal der Entwicklung eukaryotischer Zellen. Die Fähigkeiten dieser von einer Lipid-Doppelschicht umgebenen Organellen sowohl ihre spezifischen Charakteristika zu erhalten, als auch Stoffe untereinander auszutauschen sind unabdingbar für die Erhaltung der zellulären Homöostase. Dies wird erreicht durch den sogenannten vesikulären Transport, der einen permanenten Austausch von Proteinen, Lipiden and Metaboliten zwischen verschiedenen Kompartimenten erlaubt. Membranumschlossene Vesikel knospen dabei vom Donorkompartiment ab, werden zum Zielkompartiment transportiert und fusionieren dort mit der Lipid-Membran. Die grundlegende Maschinerie, die für diese Prozesse verantwortlich zeichnet ist in den letzten Jahren intensiv erforscht und charakterisiert worden. Dennoch ist unser Wissen über die Prozesse, die die Spezifität der Fusionsprozesse vermitteln und diese regulieren nach wie vor sehr begrenzt. Bevor zwei membranumschlossene Kompartimente fusionieren können, müssen sie sich spezifisch erkennen und aneinander binden um die anschließende SNARE[1]-induzierte Fusion zu gestatten. Dieser frühe Schritt in der Fusionsreaktion wird als "Tethering" bezeichnet und umfasst die Wirkung von Tethering Faktoren und Rab GTPasen.

Wärend meiner Doktorarbeit beschäftigte ich mich hauptsächlich mit dem HOPS[2] Protein Komplex, der beim Tethering an der Hefevakuole, dem Äquivalent der Lysosomen höherer Eukaryoten, seine Funktion ausübt. Um die Eigenschaften des Komplexes, die für seine Funktion wichtig sind, näher untersuchen zu können, etablierte ich eine Methode, die die Aufreinigung größerer Mengen des Komplexes erlaubt und untersuchte, welche Untereinheiten miteinander interagieren. Diese Arbeiten schafften die Voraussetzungen dafür, dass nun elektronenmikroskopische Untersuchungen des gesamten Komplexes durchgeführt werden können, welche bereits erste preliminäre Daten lieferten. Darüber hinaus erlaubten meine Arbeiten die Identifizierung des bis

[1] Soluble N-ethylmaleimide sensitive protein receptors

[2] Homotypic fusion and vacuole protein sorting

dahin unbekannten, endosomalen CORVET[1] Tethering Komplex, der einige Untereinheiten mit dem HOPS Komplex gemein hat. Ich konnte zeigen, dass chimäre Komplexe existieren, die sowohl HOPS- als auch CORVET-spezifische Untereinheiten enthalten. Diese Entdeckung lässt vermuten, dass beide Komplexe dynamische Strukturen darstellen und ineinander umwandelbar sind.

Während meiner Studien zu den Interaktionen zwischen einzelnen Untereinheiten, entdeckte ich, dass HOPS aus stabilen Subkomplexen aufgebaut ist und ich konnte für einen von diesen bereits zeigen, dass er *in vivo* vorkommt. Die Existenz dieser Subkomplexe impliziert eine wesentlich dynamischere Funktionsweise des vakuolären Tetherings, als bisher vermutet. Dieser Eindruck wird weiterhin unterstützt durch meine Studien zur Funktionalität verschiedener Untereinheiten und Subkomplexe. Interessanterweise zeigen meine Ergebnisse, dass der Rab GEF Vam6, der zur Aktivierung des vakuolären Rab Proteins Ypt7 benötigt wird und ein Bestandteil des HOPS Komplexes ist, seine Fähigkeit mit Ypt7 zu interagieren verliert, sobald er in einen Subkomplex oder den HOS Komplex inkorporiert wird. Im Gegensatz dazu funktioniert die HOPS Komponente Vps41, die ich als Rab Effektor identifizieren konnte, sowohl als einzelnes Protein als auch als Bestandteil des HOPS Komplexes. Diese Ergebnisse deuten darauf hin, dass Vps41 dazu dienen könnte, die einzelnen Subkomplexe an Stellen mit aktiviertem Ypt7 zu rekrutieren und im Verlaufe dessen, der gesamte HOPS Komplex assembliert wird.

Eine weitere spezifische Eigenschaft der HOPS Untereinheit Vps41 wurde in meiner Arbeit näher charakterisiert. Frühere Arbeiten in unserem Labor haben gezeigt, dass dieses Protein von der vakuolären Casein Kinase Yck3 phosphoryliert wird. Mir ist es gelungen, die Phosphorylierungsstellen in der Vps41 Sequenz zu identifizieren. Dies erlaubte die Durchführung weiterer Studien zu dem Effekt der Phosphorylierung auf die Funktionalität des Proteins. Im phosphorylierten Zustand verliert Vps41 teilweise seine perivakuoläre Lokalisierung und liegt vornehmlich zytosolisch vor. Demgegenüber akkumuliert das nicht-phosphorylierte Protein zusammen mit anderen HOPS Untereinheiten an endosomal-vakuolären Fusionsstellen. In Übereinstimmung mit

[1] Class C Core vacuole endosome tethering

meinen oben genannten Ergebnissen konnte gezeigt werden, dass die Überexpression von Ypt7 die zytosolische Lokalisierung der phosphomimetischen Mutante teilweise rückgängig machen konnte. Dieses Ergebnis impliziert, dass über Yck3-vermittelte Phosphorylierung und die Interaktion mit aktiviertem Ypt7 die Lokalisierung und Funktionalität von Vps41 auf zwei Ebenen reguliert wird.

1 Introduction

Ever since evolution led to the development of intracellular membranes, living cells became able to efficiently separate metabolic and physiological entities, a feature their evolutionary predecessors where incapable of. A complex intracellular endomembrane network is a distinct property of all eukaryotic cells (Whittaker and Margulis, 1978; Woese et al., 1990). The DNA of eukaryotic cells resides in the most prominent membrane-enclosed compartment, the nucleus. Translation of proteins destined for organelles or the extracellular medium are translated on the rough endoplasmic reticulum and routed by vesicular transport to the Golgi apparatus. Inside the Golgi, proteins are further processed and modified before they get sorted to the plasma membrane, the endosomal compartment or the vacuole/lysosome. Next to mitochondria, the key players in the cellular energy metabolism, and chloroplasts in plant cells and eukaryotic algae, the above-mentioned organelles constitute the core components of the eukaryotic endomembrane system.

1.1 The Eukaryotic Endomembrane System

The boundary membranes of all intracellular organelles as well as the eukaryotic cell itself are comprised of lipid bilayers. A variety of proteins are embedded into or associated to the different membranes, both as structural as well as functional entities. At physiological temperature, lipid bilayers are dynamic structures and allow for lateral diffusion of lipids and proteins. The main lipid components of eukaryotic lipid bilayers are glycerolipids, sphingolipids and sterol derivatives. Different organelles' membranes harbor distinct lipid and protein compositions, which can diverge between the two membrane leaflets, allowing for separate functionalities on each side of the bilayer (Holthuis et al., 2003). Next to the distinct features of all organelles' membranes, their bilayer-enclosed lumina encompass different biochemical activities that are needed for synthesis and modification or breakdown of proteins, lipids and carbohydrates. By being performed in a highly ordered and regulated manner, these biologically essential functions allow for sustaining viability and progeny of the cell.

1.1.1 Intracellular Organelles

The genetic material of eukaryotes is kept separately from the cytosol in the nucleus, where replication as well as transcription of the DNA is taking place. The nuclear envelope is composed of a double membrane, which is continuously connected with the endoplasmic reticulum (ER). After the messenger-RNA is exported through the nuclear pores, translation of the RNA transcripts is carried out by ribosomes. Only in the case of translation of transmembrane proteins or proteins destined for the secretory pathway, the emerging amino acid chain is specifically recognized by the Signal Recognition Particle (SRP) ribonucleoprotein complex. The SRP binds to the SRP receptor on the ER membrane and subsequently hands over the ribosome to the translocon, which builds up a pore-like structure in the ER membrane and allows for the translocation of the nascent polypeptide chain across the ER membrane (Deshaies et al., 1991; Walter and Blobel, 1980). Inside the ER lumen, folding of the polypeptide chain takes place. Multiple chaperones facilitate correct folding, and disulphide-bond formation allows for stabilization of the tertiary protein structure. However, if polypeptides are misfolded and expose hydrophobic amino acid stretches that are normally secluded inside the protein's structure, aggregation can take place and subsequent impairment of the ER integrity could occur. To counteract these effects, eukaryotic cells employ the unfolded protein response (UPR) system. If the UPR is activated upon accumulation of misfolded proteins, production of chaperones is upregulated and the ER associated degradation pathway (ERAD) is activated, which leads to ubiquitination and subsequent proteasomal degradation (Vembar and Brodsky, 2008). If by these means, further misfolding cannot be prohibited and the cellular integrity is endangered, apoptotic cell death can be initiated by the UPR. In contrast to this, correctly folded proteins can be further modified in the ER by O- and N-glycosylation and are subsequently transported to the Golgi apparatus (Golgi) by COPII vesicular transport.

Other than the ER, the Golgi is not composed of a continuous membrane system but of several separate cisternae. In higher eukaryotes, these cisternae are closely located next to each other, thereby forming a stacked higher order structure. The Golgi is a polarized organelle, meaning that different cisternae harbor distinct biochemical properties. The part of the Golgi, which is receiving cargo from the ER and is often facing the ER, is referred to as the *cis*-Golgi. The part, which is distal to the ER and

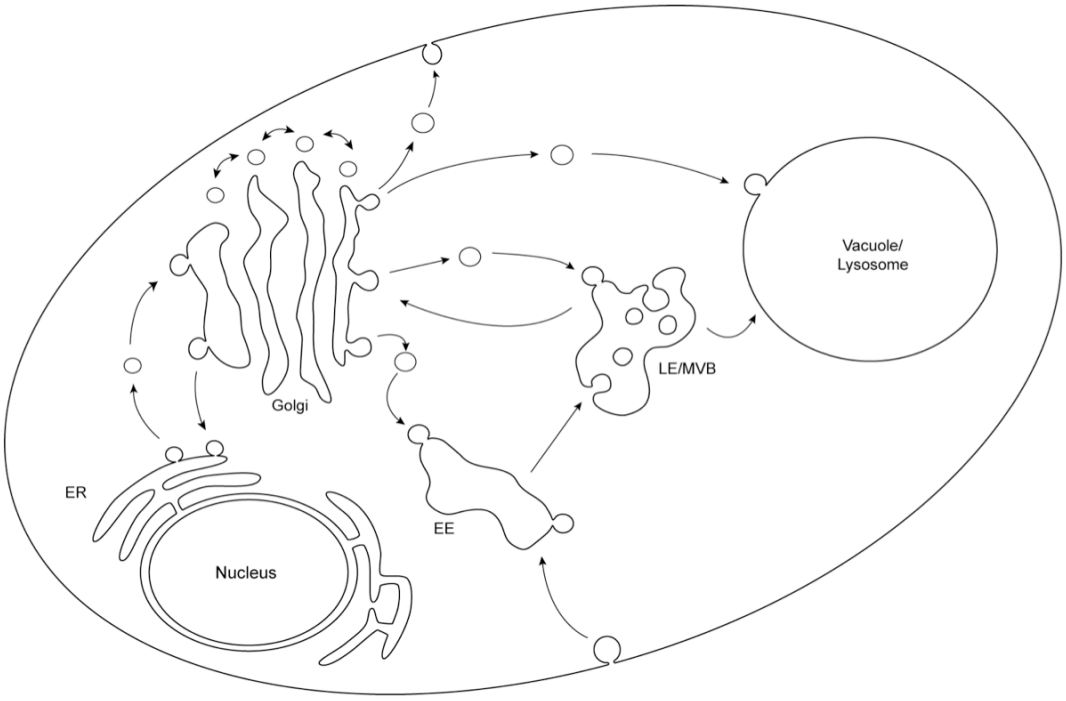

Figure 1.1 | **Overview of the endomembrane system in eukaryotic cells.** Organelles found in eukaryotic cells and of main interest for this study are schematically depicted. Note that distribution and shape of organelles can differ between species. EE=Early Endosome, LE=Late Endosome, MVB=Multi Vesicular Body, ER=Endoplasmic Reticulum. Figure adapted from Ostrowicz et al., 2008.

receives cargo after it has passed all other intermediate Golgi compartments, is referred to as the *trans*-Golgi. Since *cis*- and *trans*-Golgi are sites of specifically rapid vesicular turnover, these parts form bigger and more complex cisternae, called the *cis*- and the *trans*-Golgi-network (CGN and TGN, respectively) (see **Fig. 1.1**). Trafficking between the Golgi cisternae is taking place by anterograde and retrograde transport, which is mediated by coat protein complex II and I (COPII and COPI) vesicles, respectively. Furthermore, ER resident proteins, which escaped to the CGN are transported back as well by means of COPI vesicular transport.

Proteins that travel from the ER to the Golgi are prone to many different modifications. Further glycosylation takes place and certain proteins are proteolytically cleaved to remove signal peptides. These alterations can be observed in some cases by mobility shift in an electrophoretic chromatography setup and are often referred to as “maturation”. Next to the execution of modifications, the Golgi resembles the main

sorting station of the cell, leading to protein-specific transport to the plasma membrane, the endosomal compartment, the lysosome/vacuole, or back to the ER.

The endosomal compartment confers a similar sorting function as the Golgi. Upon endocytosis, proteins from the extracellular space as well as integral, plasma membrane (PM) resident proteins are transferred to the cytosol by endocytic vesicles that pinch off from the PM. These endocytic vesicles can either homotypically fuse to form an early endosomal compartment or fuse to pre-existing early endosomes. Proteins destined for degradation are retained in the endosome for degradation in the lysosome/vacuole. Due to the action of proton-pumps, the endosomal lumen is mildly acidified. Thus, endocytosed transmembrane receptors can undergo conformational changes that lead to the release of their substrate, which is retained in the endosome, while the receptor is recycled back to the plasma membrane. Similarly, biosynthetic cargo like the carboxypeptidase Y (CPY) is uni-directionally transferred from the TGN to the early endosome with the help of receptors. Subsequently, the cargo proteins dissociate off their receptors, which are efficiently transported back via vesicular transport (see **Fig. 1.1**).

The targeting of endocytosed transmembrane proteins to the vacuolar lumen eventually leads to their degradation. This process is initiated by the addition of a single ubiquitin moiety to or Lys-63-linked oligoubiquitination of the cytosolic part of the protein destined for degradation. Upon maturation of endosomes to the late endosomal compartment, the ubiquitin carrying proteins are further enriched on the endosomal membrane. This ubiquitin-enriched membrane is recognized by a subset of cytosolic proteins that can transiently associate with the endosomal membrane, the so-called Endosomal Complex Required for Transport (ESCRT) proteins. Four distinct ESCRT complexes are known to bind to the endosomal membrane and sequentially recruit each other in a well-defined order (Teis et al., 2008). The ESCRT-0 complex initiates this process by recognizing ubiquitinated cargo and phosphatidylinositol-3-phosphate, a lipid that is typically enriched on endosomal membranes. ESCRT-I and II act downstream of ESCRT-0 and are believed to further enrich or “trap” the ubiquitinated proteins. ESCRT-III finally leads to invagination of the endosomal membrane away from the cytosol into intraluminal vesicles, thereby forming Multivesicular Bodies (MVBs) (**Fig. 1.2**) (Hurley and Emr, 2006). Interestingly, recycling of cellular components is so elaborate that just before the invagination event, the ubiquitin is proteolytically cleaved from the invaginated cargo and is therefore made available for further endocytotic events (Amerik

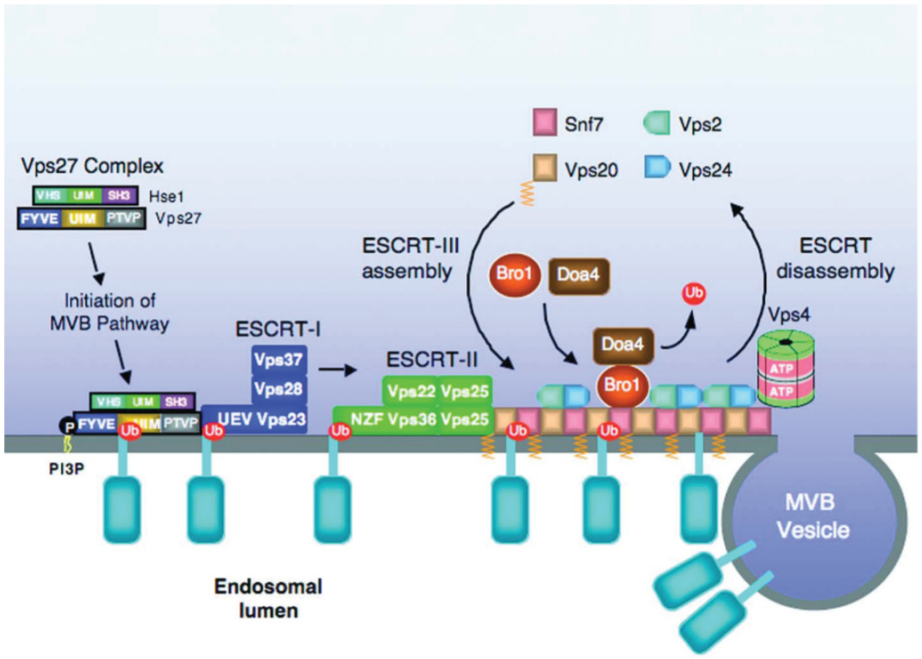

Figure 1.2 | **Formation of multi vesicular bodies in yeast.** Successive recruitment of ESCRT complexes –I, –II, and –III leads to enrichment of ubiquitinated cargo, deubiquitination by Doa4 and invagination of the endosomal membrane. The Vps4 AAA ATPase is required for ESCRT-III complex disassembly and therefore allows for the re-cycling of its subunits. Figure from Hurley and Emr, 2006.

et al., 2000). Whether MVBs as very late endosomes heterotypically fuse with the vacuole/lysosomes or must further mature to become indistinguishable from vacuole/lysosomes and finally homotypically fuse with this compartment, is currently under debate. However, there is strong evidence, that the latter is predominantly taking place (Peplowska et al., 2007; Rink et al., 2005).

The yeast vacuole corresponds to the lysosomal compartment of higher eukaryotes as a terminal organelle, responsible for the degradation and recycling of macromolecules. Moreover, it plays an important role as a storage compartment for amino acids and ions. It is therefore involved in detoxification, and pH- and ion-homeostasis of the cell. To maintain functionality of the vacuole, it constantly receives protein cargo from the biosynthetic pathway, which is transported via different routes from the Golgi either via the endosome by the CPY-pathway or directly from the Golgi by the AP3-pathway (Ostrowicz et al., 2008). These pathways are described in more detail in the next sections. Most of the vacuolar resident proteins are degradative enzymes like proteases, lipases, nucleases, and phosphatases needed for breakdown of various

substrates. Many of these enzymes reach the vacuole in an inactive state and are either activated by proteolytic cleavage or by the low vacuolar pH of down to 4.5. The low pH of the vacuolar lumen, which facilitates numerous acid catalyzed hydrolysis breakdown reactions, is primarily maintained by the vacuolar ("V")-ATPase, which couples the hydrolysis of ATP to directed proton transport across the vacuolar membrane. Next to its contribution to the numerous hydrolysis reactions taking place in the vacuolar lumen, the proton gradient is also used by various active transporters. These carry ions from the cytosol to the vacuolar lumen, therefore supporting the ion homeostasis of the cell.

1.1.1.1 Transport Pathways involving the vacuole*

The yeast vacuole, which resembles the lysosome of higher eukaryotes, is positioned at a crucial point of the eukaryotic endomembrane system. The two major trafficking pathways in the cell, the endocytic and the biosynthetic/secretory pathway target cargo to the vacuole/lysosome (**Fig. 1.3**). The metabolic function of the vacuole/lysosome has often been referred to as the cell's "stomach" or "sink". Nowadays, and to shed a more realistic light on this organelle, one would rather call it the major recycling facility of the cell. Its acidic pH is a prerequisite for the activity of the numerous hydrolases, i.e., nucleases, phosphatases, lipases and proteases within the vacuolar lumen, and the low molecular weight degradation products of these enzymes' catabolic activities are released into the cytosol for further use. Moreover, lysosomes are critical during starvation and for the degradation of cell surface receptors, thus allowing cells to respond to extracellular signals and adjust their response. Research on vacuole biogenesis and function was strongly promoted by several elegant genetic screens, which led to the identification of proteins involved in endocytosis (End), biosynthetic transport (Vps, Pep), vacuole inheritance (Vac), and vacuole morphology (Vam) in yeast (Bowers and Stevens, 2005). In many identified mutants, vacuole morphology is strongly perturbed. A morphology-based classification distinguishes normal (class A), partly (class B) and highly (class C) fragmented vacuoles from large (class D) vacuoles, and those having an enriched endosomal compartment (class E). The subsequent characterization of these genes unraveled the underlying machinery of a number of

* extract from Ostrowicz et al., 2008, written by the author of this thesis

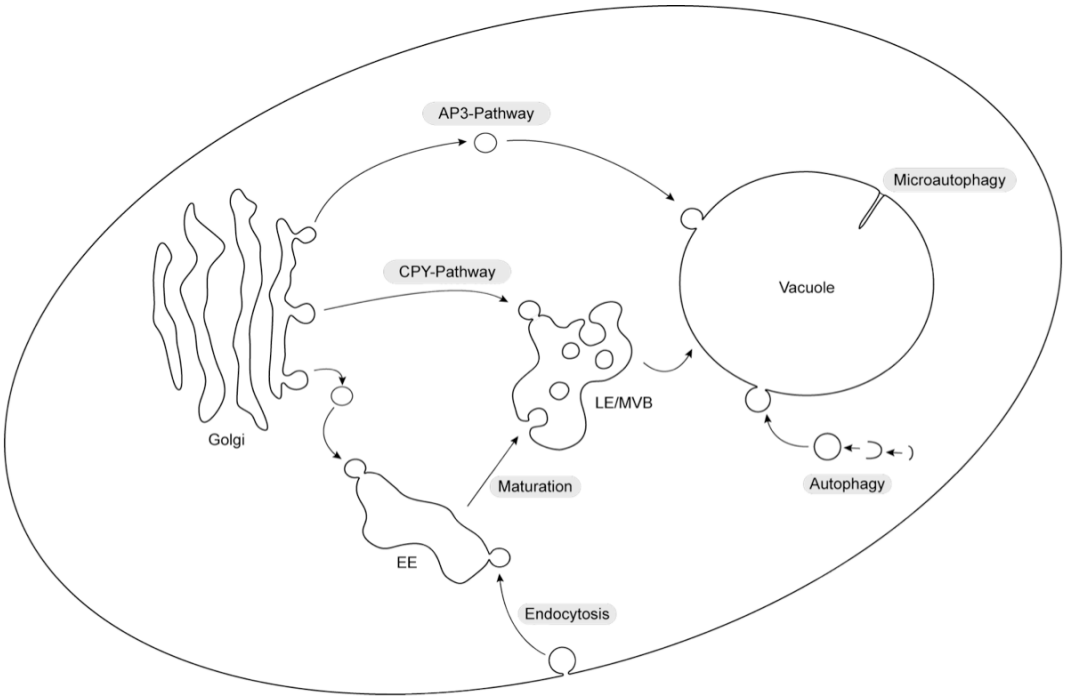

Figure 1.3 | **Transport pathways leading to the vacuole.** The vacuole receives cargo from a number of different routes, including the biosynthetic pathway, the endocytic pathway and autophagy. The cytoplasm to vacuole targeting (cvt-) pathway is not depicted, since the required machinery has a substantial overlap with the (macro-)autophagy machinery. Figure from Ostrowicz et al., 2008.

trafficking pathways that are critical for vacuole biogenesis, and in the case of the VAM genes, for vacuole fusion (Wada et al., 1992). Below, these trafficking pathways are briefly described. The vacuolar carboxypeptidase Y (CPY/Prc1) travels from the trans-Golgi-Network (TGN) to the late endosome, from where it is subsequently delivered to the vacuole (Rothman et al., 1989; Stevens et al., 1982). At the TGN, it is recognized by the receptor protein Vps10 (Marcusson et al., 1994), concentrated and packed into vesicles that pinch off from the TGN in an AP-1/clathrin-dependent manner. After fusion with the late endosomal compartment, Prc1 dissociates from its receptor and is then transported to the vacuole upon endosomal maturation. Vps10 is subsequently recycled back to the TGN with the help of the retromer complex (Seaman, 2005). Various other hydrolases have additionally been shown to interact with Vps10 and therefore follow the same route to the vacuole (Cooper and Stevens, 1996; Jørgensen et al., 1999). Consequently, this generic pathway has been termed the CPY-pathway after its most prominent cargo.

However, a small subgroup of vacuolar resident proteins, namely the *PHO8* gene product alkaline phosphatase (ALP), the soluble N-ethylmaleimide sensitive protein receptors (SNAREs) Vam3 and Nyv1 and the vacuolar casein kinase Yck3, which is palmitoylated at its C terminus, travel to the vacuole in a more direct trafficking event omitting the endosome (Darsow et al., 1998; Reggiori and Pelham, 2002; Sun et al., 2004; Wen et al., 2006). This pathway was termed the ALP- or AP-3-pathway after the adaptor complex, which is involved in the generation of vesicles at the TGN in a clathrin-independent fashion (Cowles et al., 1997a; Rehling et al., 1999; Stepp et al., 1997; Sun et al., 2004). Additional pathways are linked to the vacuole. The cytoplasm to vacuole targeting (Cvt) pathway and macroautophagy use a similar set of components to transport proteins to the vacuole (Klionsky et al., 1992; Klionsky, 2005; Scott et al., 1997; Scott et al., 1996; Scott et al., 2000). Whereas the Cvt pathway is a biosynthetic route to direct aminopeptidase I (Ape1) to the vacuole lumen, macroautophagy is a catabolic pathway, which plays a crucial role for cell survival upon starvation. In both cases, a double membrane of unknown origin engulfs organelles and cytosolic material (macroautophagy) or oligomeric Ape1 (Cvt pathway) and targets them directly to the yeast vacuole (Klionsky, 2005).

Considering the number of trafficking pathways leading to the vacuole, it is not surprising that the vacuole is a highly dynamic organelle (Weisman, 2006). During cell division, the vacuole fragments partially, producing vesicular and tubular structures, which are transported into the emerging bud. In order to control the overall shape of the vacuolar organelle, inherited vacuolar vesicles fuse later during cell division, maintaining a low copy number for this organelle (Conradt et al., 1992; Weisman et al., 1987; Weisman and Wickner, 1988). A number of proteins involved in inheritance have been identified in the past, including the vacuolar protein Vac8, the actin-binding Myo2 protein and its adaptor, Vac17 (Weisman, 2006). Moreover, the dynamin-homolog Vps1 has been implicated in vacuole fission (Baars et al., 2007; Peters et al., 2004). Vacuole fragmentation and fusion is also connected to osmoregulation, and to the synthesis and turnover of phosphatidylinositol-(3,5)-bisphosphate ($PI(3,5)P_2$) (Bonangelino et al., 1997; Bonangelino et al., 2002; Dove et al., 1997; Schott et al., 1999). Nevertheless, a clear concept of vacuole fission and fragmentation is still missing.

1.2 Membrane Trafficking

As outlined above, all intracellular organelles communicate to varying extents by exchanging proteins and lipids. Vesicles are employed as carriers in a variety of constitutive processes such as transport between the ER and the Golgi, as well as all Adaptor Protein (AP) associated transport steps, which are necessary for endo- and exocytosis, Golgi-to-endosome-, and Golgi-to-vacuole cargo transfer. In all of these cases, a distinct portion of the donor membrane is being pinched off during vesicle budding (**Fig. 1.4 a**). This process depends on the direct recognition of cargo by specific coat-forming proteins (in the case of COPI and –II transport) or AP complexes, which mediate interaction with the respective coat proteins. The nascent vesicles are subsequently enclosed by the coat proteins, which thereby facilitate the budding process.

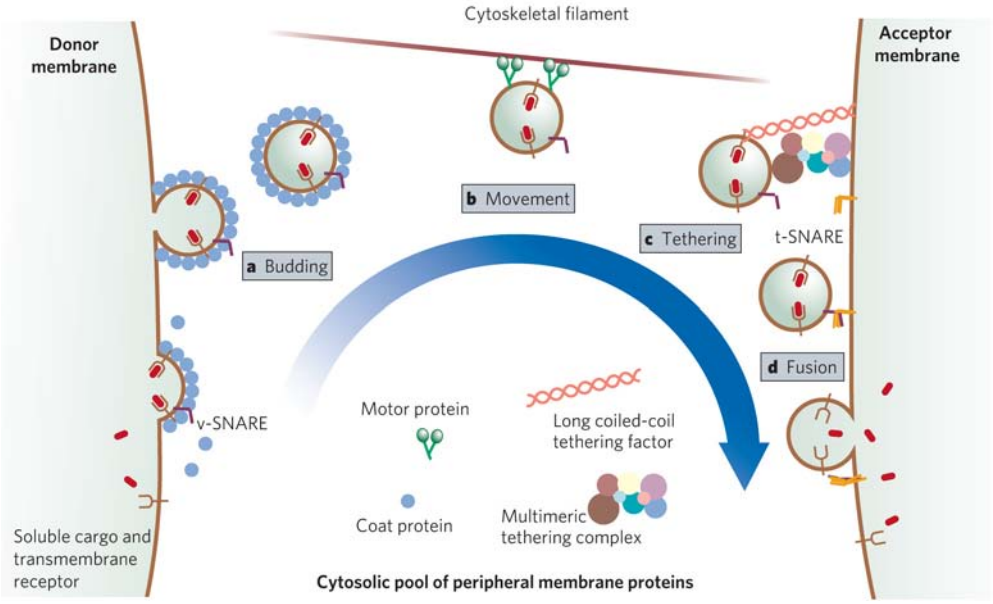

Figure 1.4 | **General principle of vesicular transport.** Transport vesicles carrying cargo proteins bud off from the donor membrane and move by active cytoskeletal transport and by diffusion to their target membrane. First membrane contact is initiated during tethering, which promotes SNARE trans-complex assembly and subsequent membrane fusion. Figure adapted from Behnia and Munro, 2005.

After complete separation from the donor membrane, vesicles are transported along the cytoskeleton to the target organelle.

To achieve fusion of the vesicular lipid bilayer with the organelle's membrane, several steps have to occur in a defined order. First, vesicle uncoating occurs. Second, a first step of recognition between vesicle and target compartment has to be initiated to ensure specificity of the subsequent fusion event. During this step, usually referred to as "tethering", the first physical interaction between the vesicle and its target membrane is established. Tethering, which is mediated by the concerted action of tethering factors and Rab (Ras-like in rat brain)-GTPases is a reversible process (**Fig. 1.4 c**). It is only after successful tethering that apposing membranes are brought into close enough contact to allow for interaction of cognate SNARE proteins that constitute the core machinery of membrane fusion. Partial assembly of the *trans*-SNARE complex leads to irreversible docking of the opposing membranes. Subsequent further assembly of the zipper-like trans complex ultimately leads to fusion and content mixing of the two compartments.

1.2.1 Vesicle Formation

Intracellular vesicles serve as the main carrier machinery in soluble and transmembrane protein as well as lipid transport between organelles. One remarkable example for vigorous production of vesicles is the TGN. As previously described, it serves as a sorting hub for a number of proteins either destined for the PM (exocytic pathway), the endosome (CPY pathway) or the vacuole (AP-3 pathway). How is specific recruitment of the correct cargo to these three different pathways achieved? Before the vesicle is shaped by the action of coat proteins, cargo proteins are specifically enriched in dedicated areas of the donor organelle membrane. Depending on their trafficking target, transmembrane proteins contain short, specific amino acid sequences in their cytoplasmic tail. Soluble proteins located in the lumen of organelles depend on the recognition by transmembrane receptors, which contain similar signal sequences in their cytoplasmic tails. Generally, these cytoplasmic signals are then recognized by soluble adaptor proteins, which are in turn recruited to the organellar membrane. It appears that mutual recruitment of cargo/cargo receptors and adaptor proteins leads to enrichment of cargo harboring the adaptor protein's specific signal sequence. Finally, next to cargo binding, the adaptor complexes are able to specifically interact with coat proteins to fulfill their function as adaptors. By recruiting coat proteins and other accessory proteins, the donor membrane is substantially remodeled and brought into the vesicular shape. The final step of membrane abscission has been reported to depend on the action of dynamin or related proteins for

example in clathrin-mediated endocytosis. In COPI- and –II-dependent transport, current evidence is suggesting the involvement of the respective initiating GTPases Arf1 and Sar1 in the final scission process (Beck et al., 2008; Lee et al., 2005).

1.2.1.1 Clathrin mediated vesicle formation

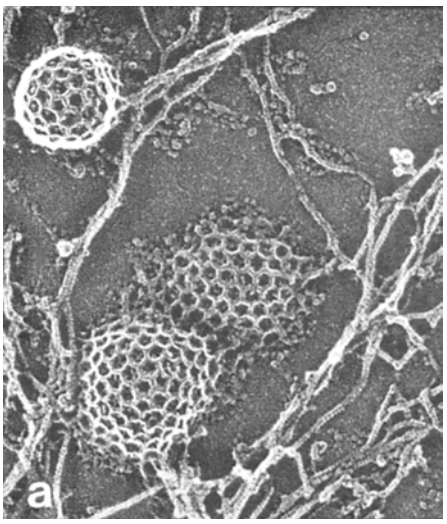

Figure 1.5 | **Clathrin coat assembly aids in formation of endocytic vesicles.** EM picture of the inner plasma membrane of chicken fibroblasts. Figure adapted from Heuser and Anderson, 1989.

One of the first coat proteins to be identified in the process of vesicle formation was Clathrin. Clathrin-coated-pits as the precursor state of Clathrin-coated vesicles (CCVs) were easily observed in electron microscopic (EM) visualizations of the intracellular side of the plasma membrane (**Fig. 1.5**) (Kanaseki and Kadota, 1969; ROTH and PORTER, 1964). Purified vesicles allowed for further characterization of the observed structures and finally led to the identification of one of the main proteinaceous factors involved in their formation (Pearse, 1976). Clathrin coats are assemblies of single Clathrin entities that each contain three clathrin heavy and three clathrin light chains, assembled into a typical triskelion or three legged structure (Kirchhausen and Harrison, 1981). Before coat assembly can occur, Adaptor Protein (AP) complexes are recruited to the donor membrane and specifically recognize Tyrosine-based YXXΦ- and dileucine D/EXXXLL-motifs on the cytoplasmic tails of cargo proteins. At the TGN, vesicles carry the AP-1 adaptor protein complex, whereas during clathrin-mediated endocytosis, clathrin is recruited to the plasma membrane by AP-2 complexes. Furthermore, Clathrin has recently been shown to form vesicles at the TGN in dependence of newly identified single-polypeptide GGA proteins (Costaguta et al., 2001; Hirst et al., 2001). Next to AP complexes, clathrin depends on a number of additional accessory proteins that support the formation of CCVs (**Fig. 1.6**).

Beside the AP-1 and -2 complexes, two additional homologous adaptor protein complexes, namely the AP-3 and AP-4 complexes, were described (Simpson et al., 1996).

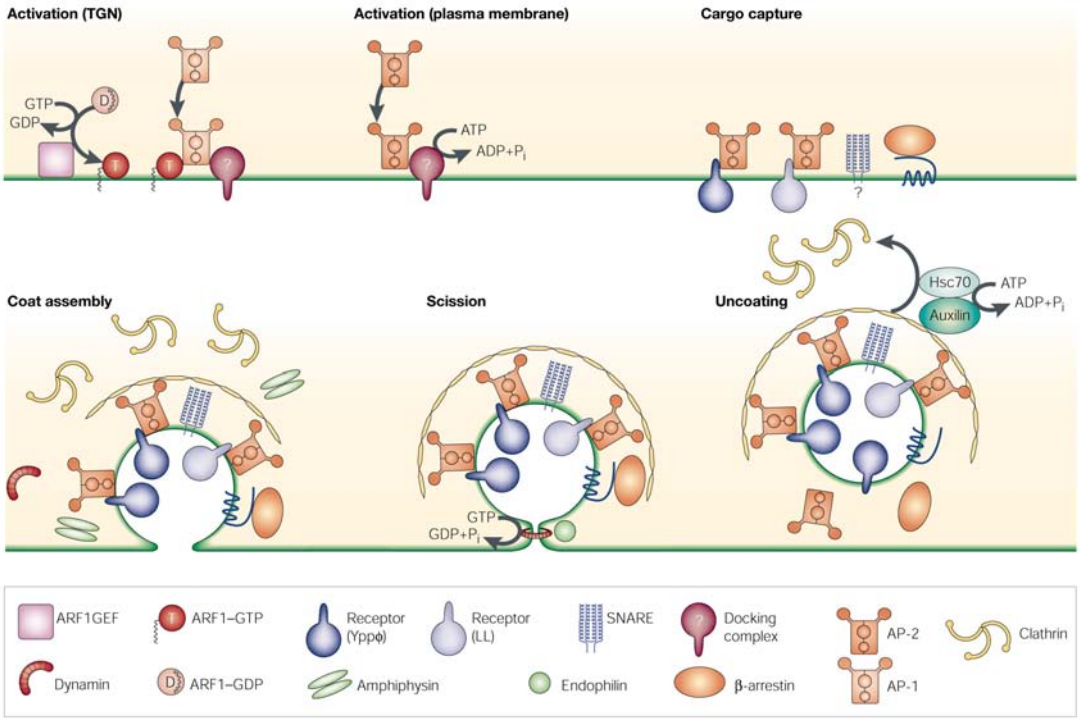

Figure 1.6 | **Adaptor protein complex dependent formation of Clathrin coated vesicles.** Several accessory factors that are known to be needed during CCV formation are depicted. Figure from Kirchhausen, 2000.

Whereas AP-3 is conserved from yeast to men, AP-4 is not present in yeast, fruit flies or nematodes. Both complexes are acting at the level of the TGN and have been reported to also act on endosomes in mammalian cells. The involvement of clathrin in the formation of vesicles in dependence of AP-3 and AP-4 remains controversial, although the AP-3 dependent ALP-pathway in yeast has been shown to be clathrin independent (Seeger and Payne, 1992; Vowels and Payne, 1998). Instead, a component of the vacuolar HOPS tethering complex, Vps41, appears to be involved in coat assembly and vesicle formation (Darsow et al., 2001; Rehling et al., 1999).

1.2.1.2 AP-3 dependent vesicle formation

In mammalian cells, the term Adaptor Protein 3 (AP-3) was used for two different adaptors involved in vesicle formation in the past. Originally, the single polypeptide clathrin adaptor AP 180/NP185 (Ahle and Ungewickell, 1986; Kohtz and Puszkin, 1988) was termed this way to stress its similarity with the AP-1 and -2 adaptors in that it binds

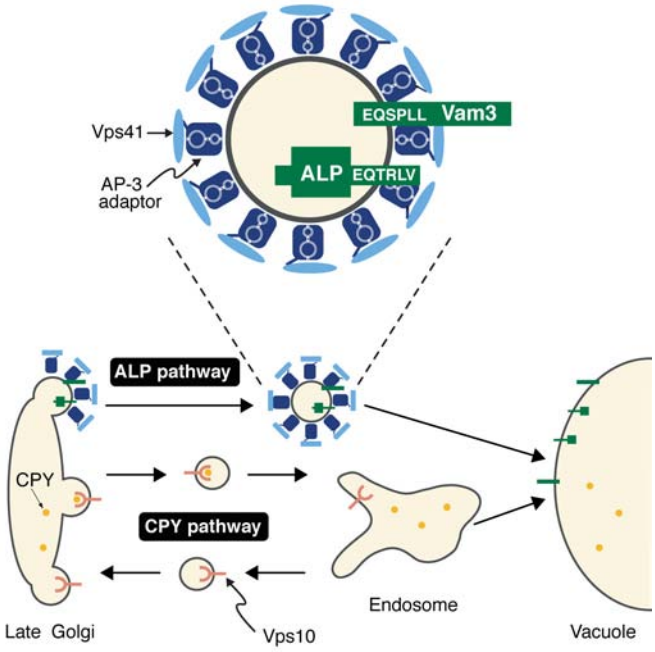

Figure 1.7 | **Possible mode of function of the AP-3 pathway.** At the late Golgi, proteins harboring specific di-leucine(-like) targeting motifs are recognized by the AP-3 adaptor complex. The HOPS subunit Vps41 binds to the AP-3 via its N-terminus and was proposed to fulfill a coat-like function. Figure from Rehling et al., 1999.

clathrin to form a coat (Murphy et al., 1991). In contrast to this similarity, AP 180 does not share structural or organizational features with the two previously identified APs, since it is not composed of four different proteins that assemble into a higher ordered structure to confer both cargo as well as clathrin specificity. Due to this disparity of features, the same name was later chosen by Robinson and colleagues (Simpson et al., 1997) for a novel adaptor protein complex that exhibited clear structural and functional homology with the AP-1 and -2 complexes. However, it was reported that the novel adaptor complex does not depend on clathrin in the formation of vesicles, a feature that made it unique among the classical APs. Although clathrin-independence was claimed for the AP-3-dependent pathway in mammalian cells, several publications still reported on a role of this coat protein during vesicle formation in this pathway (Dell'Angelica et al., 1998; Drake et al., 2000). As outlined above, the functioning of the AP-3 adaptor complex in the formation of vesicles remained obscure in mammalian cells. However, studies on the AP-3 complex in yeast yielded interesting insights into a possible alternative of AP-3 coat formation (Darsow et al., 2001; Rehling et al., 1999). Due to the robustness of the model system *Saccharomyces cerevisiae*, it was simple to probe for clathrin independence of the AP-3 pathway in yeast. A clathrin deletion mutant is viable in *S. cerevisiae* and studies of Seeger and Payne (Seeger and Payne, 1992) showed that alkaline phosphatase (ALP), the product of the *PHO8* gene, was transported to the vacuole unlike other biosynthetic cargo with wild type kinetics in cells lacking a functional clathrin heavy chain. In several following studies, the class B VPS protein Vps41 was identified as a required factor for a

functional AP-3 pathway in general (Cowles et al., 1997b) and, more specifically, by directly interacting with the AP-3 subunit Apl5 at the level of vesicle formation (Darsow et al., 2001; Rehling et al., 1999) (**Fig. 1.7**). Interestingly, Vps41 was also identified as a subunit of the hexameric HOPS tethering complex at the vacuole (Cowles et al., 1997b; Nakamura et al., 1997; Price et al., 2000a; Price et al., 2000b; Seals et al., 2000).

Compared to the generic CPY-pathway from the TGN to the vacuole, which utilizes AP-1 vesicles, few proteins have yet been identified as AP-3 cargo. The vacuolar transmembrane phosphatase ALP, the vacuolar SNAREs Vam3 and Nyv1 as well as the C-terminally palmitoylated Casein Kinase 3 Yck3 are transported directly from the TGN to the vacuole without passing the endosomal compartment. ALP harbors a dileucine-like LV motif as a recognition signal for the AP-3 complex (Vowels and Payne, 1998), whereas Vam3 contains a classical dileucine motif (Darsow et al., 1998). Nyv1 is sorted via the AP-3 pathway in dependence of an YXXΦ-like motif in its longin-domain (Wen et al., 2006) and Yck3 was the first yeast cargo protein identified to contain a classical YXXΦ-motif (Sun et al., 2004).

1.2.2 Vesicle targeting

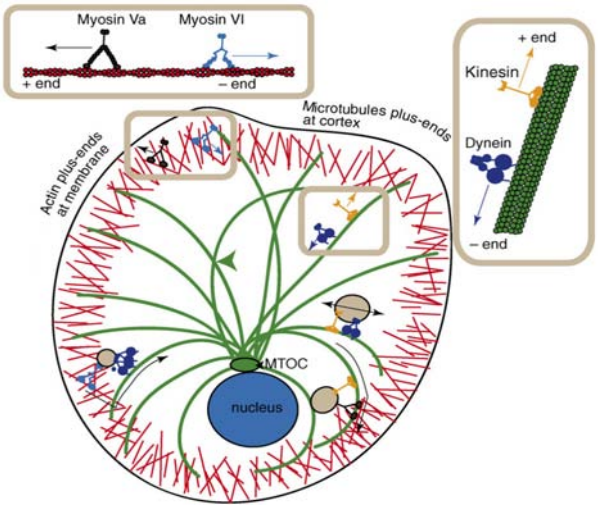

Figure 1.8 | **Distribution of different fibers and modes of vesicle transport in the cell.** Actin-dependent motor proteins aid in peripheral transport events e.g. after endocytosis. Vesicles can then be handed over to microtubule-dependent motor proteins. Figure adapted from Ross et al., 2008.

For transport of budded vesicles from the donor to the target compartment, motor-protein driven movement along actin filaments or microtubules is typically employed. In the case of actin filament based transport, myosin proteins serve as motors whereas dyneins and kinesins are associated with movement on microtubules (Pruyne et al., 1998; Ross et al., 2008). These motor proteins connect to vesicles and compartments by interacting with Rab GTPases, a class of proteins

that is as well involved in the tethering process upstream of membrane fusion (Hammer and Wu, 2002; Matanis et al., 2002; Schott et al., 1999). A switch between the associated kind of fiber and, consequently, the motor protein has been observed for example for endocytic vesicles that initially employ the cortical actin cytoskeleton during and shortly after endocytosis. For transport away from the cell cortex into the interior of the cell, myosin has to be exchanged for dynein so that movement along the centrically organized microtubules can occur (**Fig. 1.8**). How such exchanges are organized and which factors define, which motor protein dominantly acts on vesicles that harbor several different motor protein binding sites, remains to be elucidated. It is currently under debate if transport along cytoskeletal structures is a highly coordinated process or if a constant "tug of war" between different motor proteins is taking place (Ross et al., 2008).

1.2.3 Membrane Tethering

The transport of vesicles along the cytoskeleton is a process needed for targeting to the appropriate region inside the cell. However, before a subsequent fusion event with the correct target compartment can occur, the membranes destined for fusion have to specifically recognize each other. This step is critical to maintain organelle identity and therefore cellular homeostasis. It has been postulated in the past that SNARE proteins, which constitute the core machinery in intracellular membrane fusion, confer membrane specificity, but more recent work revealed that other factors are needed for this process upstream of SNARE function. Tethering of organelles, i.e. the reversible binding of matching membrane surfaces, appears to depend on the action of small Rab GTPases and tethering factors. For both of these groups of fusion factors, an increasing number has been identified in the past and I will present data in this study that allowed for the identification of a novel tethering complex a the endosome (see section 3.3). The diversity of Rab GTPases and tethering factors in eukaryotic cells allows for each organelle to harbor its individual set of these fusion factors, thereby mediating specificity in intracellular fusion events. In section 1.3, I will provide a detailed overview about tethering factors and Rab GTPases.

1.2.4 Membrane Fusion

The fusion of lipid bilayers in an aqueous environment is generally a thermodynamically unfavored process (Chernomordik and Kozlov, 2003). Although the rate of fusion of artificially produced liposomes can be increased chemically, the observed fusion rates are usually both kinetically and quantitatively low and do not compare to the speed and number of intracellular lipid bilayer fusion events. Taking into account the high density of transmembrane and membrane associated proteins, it becomes evident that fusion of intracellular compartments must rely on the concerted action of a highly organized protein machinery. Compartments destined for fusion need to be specifically brought into and retained in close proximity. For bilayer fusion to occur, apposing membranes have to be pulled together and eventually strongly deformed so that first the outer lipid layers can merge into a fusion stalk which is subsequently leading to a state called "hemifusion" (**Fig. 1.9**) (Chernomordik and Kozlov, 2003). It is now generally accepted that SNARE protein complex assembly is the minimal requirement for intracellular membrane bilayer fusion and I will discuss this process in more detail in section 1.5.

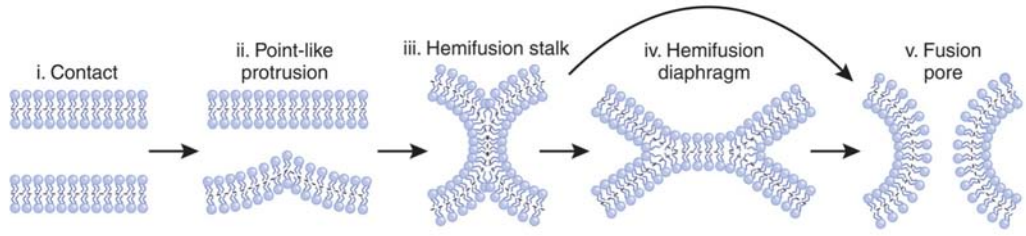

Figure 1.9 | **Stages of lipid bilayer fusion**. After first contact is established, a membrane protrusion helps minimizing the inter-membrane repulsion caused by the aqueous environment. After formation of a fusion stalk, the site of hemifusion can expand to a hemifusion diaphragm and subsequently to the formation of a fusion pore. Figure adapted from Chernomordik and Kozlov, 2008.

Several different physical models for the fusion of two membranes exist, and not all favor the existence of a hemifusion state. However, for vacuoles derived from *S. cerevisiae* this intermediate state of lipid bilayer fusion can be observed *in vitro*, if fusion speed is sufficiently reduced (Reese et al., 2005). Under physiological conditions, subsequent fusion of the second lipid layer is presumably taking place immediately after hemifusion. It is still under debate if this process requires additional downstream factors (Reese et al., 2005) or rather depends on the ability of SNARE transmembrane domains to self-interact

and oligomerize (Hofmann et al., 2006). However, fusion of artificial liposomes harboring SNAREs on their surface have been shown to be fusion competent, although efficiency and speed of fusion do not compare to biological systems (Nickel et al., 1999; Weber et al., 1998).

1.3 The Tethering machinery

1.3.1 Rab GTPases

Rab proteins are small monomeric GTPases that belong to the Ras superfamily. In yeast, eleven members of the Rab family have been identified, whereas multicellular organisms harbor a higher number of different Rabs, and many of these are believed to function in a tissue-specific manner (Fukuda, 2008). Most of the members of the Ras superfamily, like Rho, Ran or Sar/Arf GTPases, appear to be key regulators in a variety of intracellular events like cell morphogenesis and cytokinesis, nuclear transport, and vesicle formation. Rab proteins have been identified to regulate membrane trafficking and, more specifically, intracellular membrane fusion events. Like other GTPases, Rab proteins function as molecular switches. This is achieved by cycling between an active and inactive state, which are defined by the nucleotide that is bound to the protein. It is the nucleotide state, which also defines the localization of the Rab protein. Membrane anchoring is achieved by a double geranylgeranylation at the C-terminus, a modification, which is carried out by a cytosolic geranylgeranyltransferase. Rab escort proteins (REPs) bind to yet unprenylated Rab proteins, present them to the modifying enzyme and aid in the membrane targeting after geranylgeranylation has occurred. Next to REPs that are involved during the biogenesis of Rab GTPases, another kind of Rab binding protein has been described, the guanine nucleotide dissociation inhibitors (GDI) (Pfeffer et al., 1995; Takai et al., 1992). In yeast, only one Rab-GDI (Gdi1) has been identified (Garrett et al., 1994). Due to the strong hydrophobicity of the geranylgeranyl moiety, Rabs themselves are unable to leave the membrane. GDI only binds to the inactive, GDP-bound form of the Rab protein and at the same time mask its prenyl anchor, therefore allowing the protein to dissociate into the cytosol (**Fig. 1.10**). To prevent random re-association of Rabs onto membranes, they are believed to be recruited by GDI-displacement factors (GDFs) (Behnia and Munro, 2005). However, until today only one example of a protein

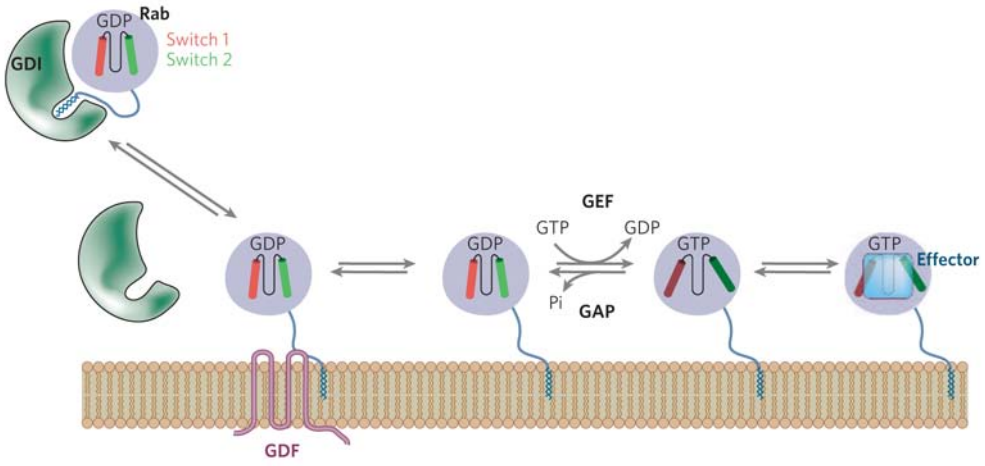

Figure 1.10 | **Rabs cycle dynamically between cytosol and target membrane.** The GDP-bound, inactive Rab protein is extracted from membranes by action of GDI, which binds the Rab and shields the prenyl anchor. GDFs are believed to recruit Rab proteins from the Rab-GDI complex and favor membrane association. Nucleotide exchange occurs with the help of a GEF and the GTP-bound Rab can then bind its effector. GTP hydrolysis is stimulated by a GAP, leading to a GDP-bound, inactive Rab. Adapted from Behnia and Munro, 2005.

harboring GDF activity has been described (Sivars et al., 2003) and it is currently under debate, if this activity is not possibly mediated by another group of Rab interactors, the guanyl nucleotide exchange factors (GEFs). GEF activity was described for a number of unrelated proteins and it seems that several different approaches for this intermolecular activity have developed during evolution (Bos et al., 2007). This fact strongly complicates the search for yet unidentified GEFs, or a clear characterization due to sequence or even structural similarities. GEFs specifically recognize Rab proteins and alter the nucleotide-binding pocket, thereby facilitating the removal of the bound nucleotide. As the next step, the GTPase is loaded again with guanly nucleotide due to its high affinity for this compound. Interestingly, both GDP and GTP are believed to bind equally well to the unloaded Rab and it is only the about ten-fold higher concentration of GTP in the cell which leads to an activation in the majority of nucleotide exchange reactions (Vetter and Wittinghofer, 2001). The GTP-bound Rab is in its active state and remains bound to its specific compartment until GTP hydrolysis occurs, rendering the protein a target for the GDI. The binding of GTP to the Rab protein leads to a conformational change of the protein, where the two switch domains are bend at flexible hinge regions due to charge-interactions with the γ-phosphate group of the GTP (Vetter and Wittinghofer, 2001). It is this activated conformation that is recognized by the Rab GTPase effector proteins, which are typically tethering factors or part of a tethering

complex that mediate the signaling of the active Rab protein to the downstream event of tethering (**Fig. 1.10**) (Behnia and Munro, 2005).

Since Rab proteins are comparably inefficient GTP hydrolyzing enzymes, they can stay in the GTP-bound, activated state for a long time. However, their intrinsic GTPase activity can be enhanced manifold by GTPase activating proteins (GAPs). These proteins complement the enzymatic active site of the Rab proteins. It has been reported that a Rab GAP contributes a glutamine residue, which orients the water molecule, which is needed for the hydrolysis reaction, whereas an arginine residue stabilizes the transition state by neutralizing negative charge at the γ-phosphate (Bos et al., 2007).

Compared to the protein classes of GEFs, GAPs and Rab effector proteins, GDFs are yet poorly characterized, in fact only one GDF has been identified in yeast (Sivars et al., 2003). It is puzzling, why it should be so difficult to identify a protein with a relatively clear expected phenotype for example upon deletion. If GDFs act specifically, a knockout should lead to a mis-localization of the total pool of affected Rab to the cytosol, since the protein could not be recovered from there after it was inactivated and extracted from the membrane by GDI (compare **Fig. 1.10**). Recently, Ralph Isberg and co-workers showed that the SidM protein of the intracellular pathogen *Legionella pneumophila* can act both as a GDF as well as a GEF protein for the human Rab1 protein (Machner and Isberg, 2007). In infected cells, it is efficiently recruited to the pathogen-containing replication vacuole by the SidM protein, which thereby allows the pathogen to hijack the intracellular trafficking machinery. Although SidM is a bacterial protein not involved in intrinsic trafficking events, it could serve as an example, which tells us that efficient localization and activation of a Rab protein mediated by a single factor is a functional approach. Hence, it appears likely that GEF proteins might as well act as GDFs therefore linking membrane recruitment to an immediate activation of the respective Rab protein. In this concept, Rab localization efficiency is increased due to a decreased risk of repeated membrane dissociation. Moreover, the specific recruitment of only one Rab protein to a defined compartment would in such a case only depend on one other factor that would have to localize independently.

1.3.2 Tethering Factors

The general mechanism of intracellular membrane tethering is defined by a process of reversible binding of apposite compartments destined for fusion, which involves tethering factors and in most cases members of the Rab GTPase family. Tethering occurs prior to the docking step, when *trans*-SNARE complexes start forming. In fact, tethering appears to be a prerequisite for efficient docking and proteins involved in tethering have been shown to bind SNAREs and are believed to facilitate binding of cognate SNAREs (Whyte and Munro, 2002).

To complicate matters, tethering events at different compartments were reported to involve a set of similarly functioning proteins such as Rabs, GEFs, and tethers, but the order of events and the precise functioning of these factors appear to substantially differ between organelles. In general, two classes of tethering factors have been described: long coiled-coil single polypeptide tethers that can form homodimers and large multi-subunit protein complexes. Among the first group are the early endosomal antigen 1 (EEA1) and p115 in mammalian cells and Uso1, a p115 homolog in yeast. EEA1 is implicated in homotypic tethering between early endosomes or endocytic vesicles. The C-terminal part of EEA1 contains a FYVE domain, which binds to phosphatidylinositol-3-posphate (PI(3)P) in the endosomal membrane bilayer. The rod-shaped homodimer sticks out into the cytosol and presents its N-terminus, which is able to specifically recognize and bind the endosomal Rab5, the mammalian Vps21 homolog.

The second class of tethering factors, the multi-subunit protein complexes, is characterized by a high degree of diversity among its members. It has to be noted, though, that all of the tethering complexes described here share a substantial conservation between species and some have been characterized in parallel for the mammalian system as well as in yeast. Other than for SNAREs and Rab proteins, most of these different complexes do not appear to be closely related, although some share similarity on a level of secondary structure (Whyte and Munro, 2002), implying a convergent development rather than a common ancestor (Koumandou et al., 2007). However, most tethering complexes were shown to interact with SNAREs and a specific Rab GTPase, either as a GEF, an effector or both (Kümmel and Heinemann, 2008; Whyte and Munro, 2002). The COG complex is needed for tethering events at the Golgi, the GARP complex acts in

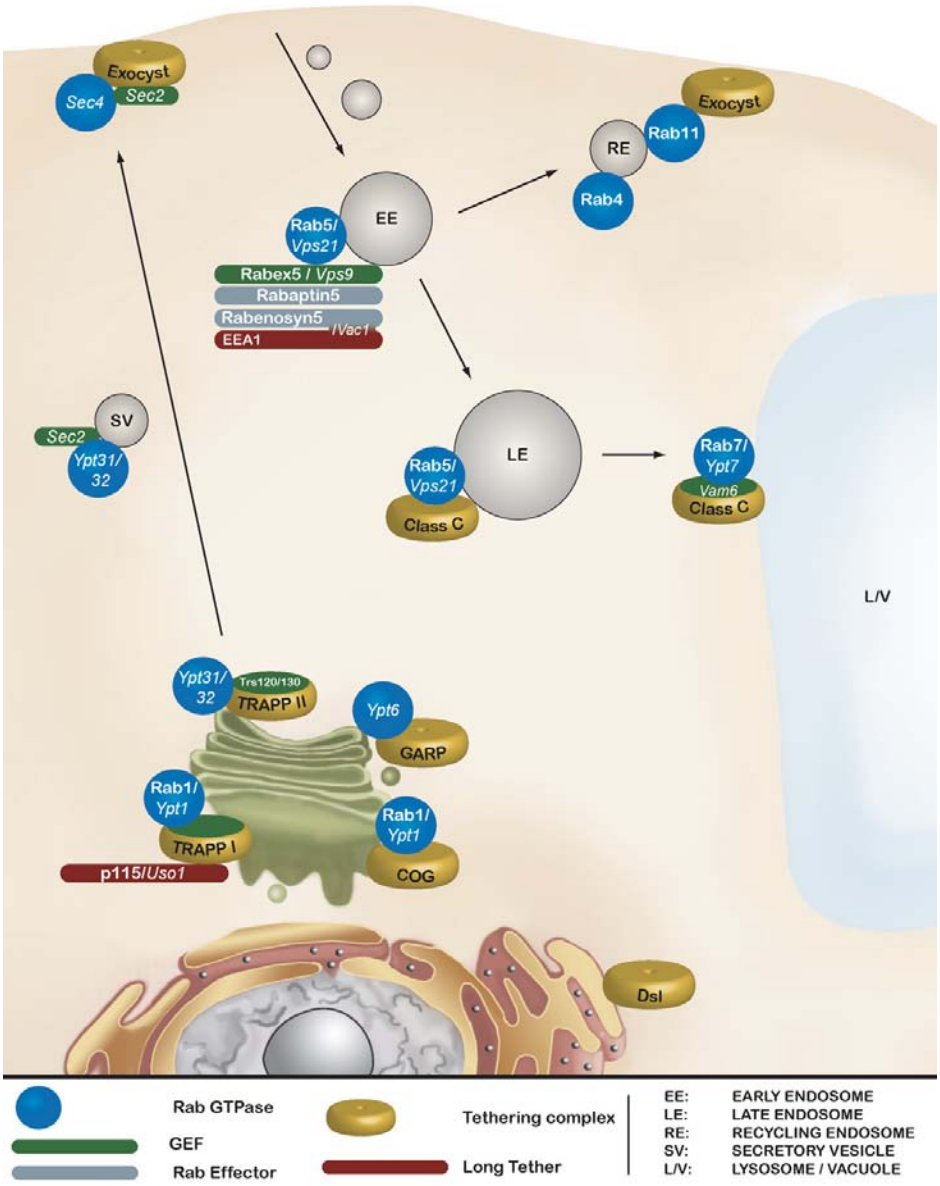

Figure 1.11 | **Rabs and tethering factors in eukaryotic cells.** Yeast Rab GTPase homologs are in italics. See figure legend for further details. Figure adapted from Markgraf et al., 2007.

endosome-Golgi transport, the TRAPP complexes are required for the biogenesis of the Golgi, the exocyst tethers vesicles destined for exocytosis, and the HOPS complex operates in the late endocytic pathway together with the novel CORVET complex and during homotypic vacuole fusion (**Fig. 1.11**). The Dsl-complex, which functions between the Golgi and the ER, is the only tethering complex described so far that is lacking a Rab binding partner. Interestingly, the Dsl complex consists of only three subunits, a small number compared to most other tethering complexes, and appears to interact notably tight with SNARE proteins, which might confer membrane specificity in this one special case

(Tripathi et al., 2009). In the following sections, I will present an overview of selected tethering complexes and their proposed mode of function.

1.3.2.1 The TRAPP complexes

Two of the best-characterized complexes involved in intracellular membrane tethering are the transport protein particle (TRAPP) complexes. Ten TRAPP subunits have been identified in yeast and the six smallest (Bet3, Bet5, Trs20, Trs23, Trs31 and Trs33) and one additional subunit of higher molecular weight (Trs85) form the TRAPP I complex, which has a role in ER to Golgi transport. Three additional subunits (Trs120, trs130 and Trs65) are added to TRAPP I to form the TRAPP II complex that is involved in trafficking at the later Golgi compartments (Sacher et al., 2008). Several studies dealing with the structural characterization of theses complexes yielded a very detailed picture of the subunits' assembly (**Fig. 1.12**) (Cai et al., 2008; Kim et al., 2006; Sacher et al., 2008). It appears that the core subunits of both TRAPP I and II form an elongated, rod-shaped structure (**Fig. 1.12 B**) (Kim et al., 2006). However, the functioning of the two complexes

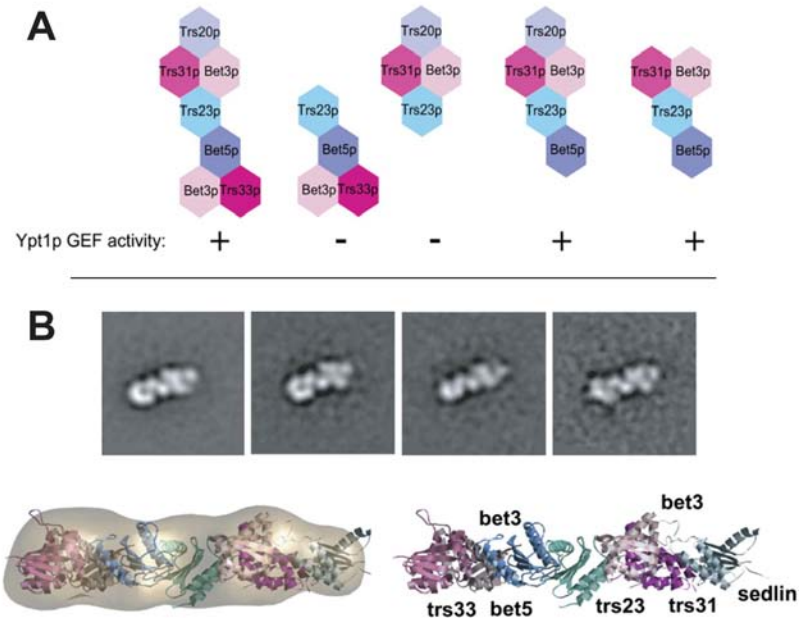

Figure 1.12 | **Architecture and structure of the TRAPP I complex.** Interactions between different subunits are depicted in **A**. Note that Ypt1 GEF activity relies on the assembly of four subunits. EM analysis of the yeast TRAPP I complex reveals its rod-shaped structure **B**, upper panel. Overlay of the crystal structure of human TRAPP subunits on the yeast TRAPP I EM structure **B**, lower panel. Sedlin is the mammalian ortholog of yeast Trs20. Figure adapted from Kim et al., 2006.

remains controversial. TRAPP I and II have been reported to harbor several interaction sites. The assembled TRAPP I complex was reported to exhibit GEF activity towards the Rab Ypt1. Interestingly, the active site is composed of the four TRAPP subunits, which are essential for cell viability (**Fig. 1.12 A**) (Kim et al., 2006). It appears straightforward that TRAPP II, which harbors the same four subunits, also acts as a Ypt1 GEF and this activity has been recently reported by the group of Susan Ferro-Novick (Cai et al., 2008). Nevertheless, these findings are in contrast to a previous study (Morozova et al., 2006), which reported on a switch of specificities of the GEF region in the complexes from Ypt1 to the Rabs Ypt31 and Ypt32, which act at later Golgi compartments, upon binding of the TRAPP II specific subunits. How these differing results can be explained remains controversial and before this specific question is addressed in an independent study, clarity will most likely not be achieved. An alternative explanation for the functioning of the three additional subunits in TRAPP II was proposed in the same study that found Ypt1 GEF activity in both complexes. TRAPP I and II had already been described to specifically bind to COPII and COPI vesicles via Sec23 and an unknown coat subunit, respectively (Cai et al., 2007b; Cai et al., 2005; Sacher et al., 2001). It was therefore proposed that transformation of TRAPP I to II does not alter its GEF specificity, but changes the mode of interaction with transport vesicles from COPII tethering at the early Golgi to COPI tethering at the intermediate and late Golgi. The functioning of the TRAPP I complex as tethering complex was proposed to be cooperating with the Golgi specific long tether and Ypt1 effector Uso1/p115, which is supposed to act as a long-range tether. After binding to the Ypt1-GTP positive vesicle, inactivation of Ypt1 could occur, leading to a conformational change in Uso1/p115, thereby bringing vesicles into closer proximity to the TRAPP complexes that then serve as GEFs for Ypt1 and re-activate the Rab, which initiates downstream events (maybe involving the COG complex, see below) that subsequently lead to fusion (Kim et al., 2006). However, no Ypt1 GEF acting upstream of TRAPP I was identified yet, a fact that is challenging this model. Clear biochemical evidence for such a two-step tethering event is largely missing, but it has been implicated in other studies of Golgi resident tethering factors (see below)

As pointed out above, solving a tethering complex's molecular structure can yield intriguing insights into its functionality, but cannot answer all the questions. In the case of the TRAPP complexes, which are examples for well-characterized complexes, it

becomes apparent that we are far from understanding the process of tethering to detail and that new questions arise with every new finding.

1.3.2.2 The COG complex

Next to the TRAPP complexes, a hetero-oligomeric complex composed of eight subunits has been identified to function at the Golgi apparatus with no preference for the *cis*- or *trans*- compartments. The conserved oligomeric Golgi (COG) complex is an effector of Ypt1-GTP, therefore functionally linking it to the Ypt1-GEF activity of the TRAPP complexes. It appears that the COG complex is specifically regulating intra-Golgi transport for example of Golgi-resident, intraluminal enzymes, since glycosylation of proteins is affected in COG mutants, but neither transport through the secretory pathway nor endocytic cycling of cargo appear to be profoundly disrupted (Ungar et al., 2002). Indeed, genetic interactions between COG subunits and coat proteins of COPI vesicles, which are the main retrograde transport carriers at the Golgi, have been reported (Kim et al., 2001; Ram et al., 2002). Moreover, the COG complex appears to interact with some but not all of the SNAREs implicated in trafficking to or from the *cis*-Golgi (Suvorova et al., 2002). In contrast to the TRAPP complexes, no GEF activity has been reported on COG subunits. It therefore appears likely that the Golgi-resident TRAPP complexes serve as Ypt1 GEFs thereby producing the activated Rab pool, which is then interacting with the COG tethering complex as their effector. Interestingly, also the COG complex has been found to interact with the COPI coat and with Golgi SNARE proteins, similar to the TRAPP complexes (compare section 1.3.2.1) (Suvorova et al., 2002). Therefore, it was suggested by Vladimir Lupashin and co-workers that the COG complex might have an additional

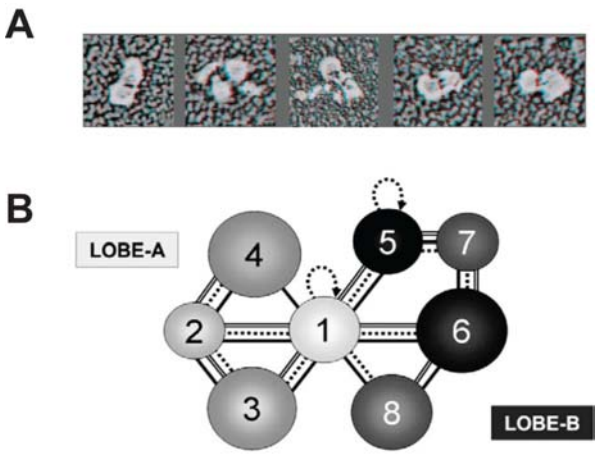

Figure 1.13 | **Structure of the COG complex.** EM analysis of purified and fixed COG complex **A** The two-lobed structure observed in **A** reflects the findings about the subunits' interactions depicted in **B**. Figure adapted from Ungar et al., 2006.

function during vesicle formation, a model that has been also developed for the GARP complex, which will be presented in the next section.

The COG complex has been structurally characterized by electron microscopy (**Fig. 1.13**) The complex harbors two connected lobes, a structure that is strikingly different to the structure of the TRAPP core complex that was outlined above (Kim et al., 2006; Ungar et al., 2002).

1.3.2.3 The GARP complex

The Golgi associated retrograde protein (GARP)/VFT (Vps fifty three) complex is composed of four proteins (Vps51, Vps52, Vps53 and Vps54) and three of these were initially identified as Class B proteins in a VPS-screen for defective vacuole protein sorting (Conibear and Stevens, 2000). Deletion of single or several subunits yields the same phenotype with inefficient CPY-pathway transport and missorting of Golgi resident proteins to the vacuole, consistent with the complex' functioning in retrieval of Golgi resident proteins from endosomes (Conibear and Stevens, 2000). Furthermore, the complex interacts with the GTP-form of the late Golgi Rab Ypt6/Rab6 and the SNARE Tlg1 that has also been implicated in this trafficking step (Conibear et al., 2003; Siniossoglou and Pelham, 2001; Siniossoglou and Pelham, 2002). The Ypt6 GEF heterodimer Ric1-Rgp1 appears to act independently of the GARP complex (Siniossoglou et al., 2000). Interestingly, the interaction with the SNARE Tlg1 depends on the smallest subunit of the complex (Vps51), which is not essential for assembly of the rest of the subunits (**Fig. 1.14 A**) (Siniossoglou and Pelham, 2002). Since the Ypt6 binding site is located in a different subunit (Vps52) that is part of the core complex, Pelham and co-workers suggest that Vps51 alone could bind to Tlg1 on recycling vesicles and that tethering is mediated by its interaction with the *trans*-Golgi resident GARP core complex (or the other way around, as implicated by Tom Stevens and co-workers, as in **Fig. 1.14 A**) and subsequent assembly into the full complex (Conibear et al., 2003; Siniossoglou and Pelham, 2002). A more recent study supports the idea of GARP subunit binding to endosomal structures upstream of the *trans*-Golgi, but suggests a different mode of action. Elizabeth Conibear and co-workers could show that a C-terminal domain of the core subunit Vps54 mediates localization to the early endosome and their results suggest that Vps54 is involved in the formation of retrograde vesicles at this compartment

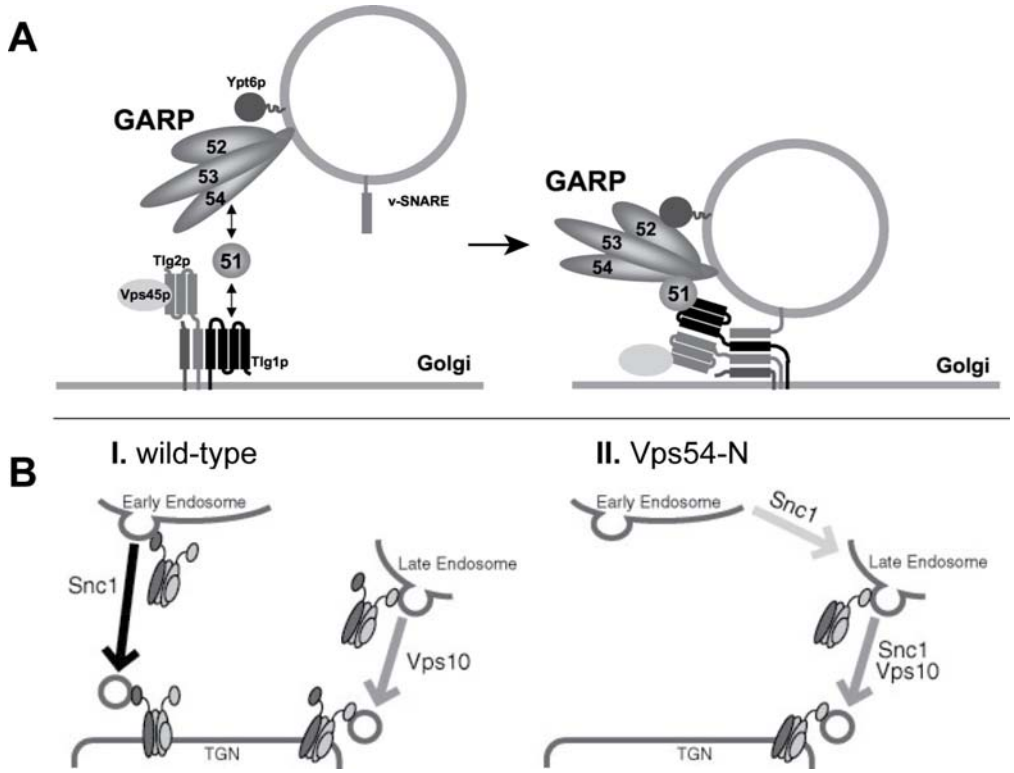

Figure 1.14 | **Two models of GARP functioning in endosome-Golgi tethering. A** The Tlg1-binding subunit Vps51 could independently localize and assemble into the GARP complex at site of tethering with the preassembled core complex. **B I** Alternatively, fully assembled GARP complex is needed on both membranes for proper tethering. **B I.** and **II.** GARP seems to harbor two distinct interaction sites for early and late endosomal retrograde vesicles. Figures adapted from Conibear et al., 2003; and Quenneville et al., 2006.

(**Fig. 1.14 B**). The deletion of this region (Vps54-N, see **Fig. 1.14 B II.**) did not impair overall complex assembly and yielded no obvious effect on retrograde transport from late endosomes, but had an effect as soon as functioning of the retromer was impaired, a protein complex that is needed for late endosomal retrieval pathways (Quenneville et al., 2006). The group proposes a model in which the GARP complex is recruited to retrograde vesicles at the site of their formation and even plays a role in cargo sorting or vesicle budding. This hypothesis is substantiated by a study from Howard Riezman and colleagues, who have previously shown that COG complex subunits not only interact with the COPI coat but seem to be needed for proper cargo sorting at the site of vesicle formation at the ER (Morsomme and Riezman, 2002). In both of these studies, single subunits of tethering complexes have been shown to interact with factors involved in vesicle formation. Therefore, Conibear argues that this is clear evidence that vesicles destined for a specific organelle do not only need Rab GTPases as tethering effectors on

their membrane but also need to harbor the corresponding tethering complex, to allow for a homotypic tethering event between vesicle and target compartment. This intriguing hypothesis could explain why several tethering complex's subunits have been described to interact with coat proteins although it is believed that coat disassembly efficiently occurs prior to tethering, making it unlikely that this interaction plays a role directly during tethering. However, the data leave enough space for the alternative hypothesis of tethering complex assembly during tethering as proposed by Hugh Pelham for the GARP complex and as has been observed in the case of the exocyst complex (see next section).

1.3.2.4 The exocyst complex

The majority of subunits of the exocyst complex has been identified in a screen for temperature sensitive mutants that fail to secret proteins (TerBush et al., 1996). The fully assembled complex consists of eight subunits, which appear to be conserved from yeast to man, a typical feature of tethering complexes. The exocyst is mainly found at the plasma membrane, at sites of pronounced exocytosis for example the bud tip in *S. cerevisiae* due to expansion of the cell wall. Consequently, several studies in other model systems also imply a functioning of the exocyst in membrane and protein retrieval from recycling endosomes and in cytokinesis, where secretion is enhanced at the midbody (Gromley et al., 2005; Prigent, 2003). Interestingly, members of the exocyst have been observed to reach the site of exocytosis via different routes and assemble into the full complex during exocytic vesicle tethering (Boyd et al., 2004; Finger et al., 1998). Two subunits (Sec3 and Exo70) appear to be directly recruited to sites of exocytosis by the Cdc42, Rho1, and Rho3 GTPases, which are regulators of cell polarity (**Fig. 1.15 A**). The six other subunits are attached to exocytic vesicles, which are targeted via Actin cables to the plasma membrane (Boyd et al., 2004; Finger et al., 1998). This model was challenged by a recent study, which doubts that Sec3 is localized independent of exocytic vesicles, based on immunofluorescence experiments compared to GFP-tagged proteins in the original work (Finger et al., 1998; Roumanie et al., 2005). However, the idea of a spatial landmark for exocytic vesicles at the plasma membrane made of Sec3 and Exo70 remained widely accepted. Furthermore, the exocyst subunit Sec6 appears to interact with the plasma membrane SNARE Sec9, another common feature among tethering complexes (Sivaram et al., 2005). The interaction of a subset of exocyst subunits with Rho-GTPases is a rather unique characteristic, but it is apparent that tethering of vesicles,

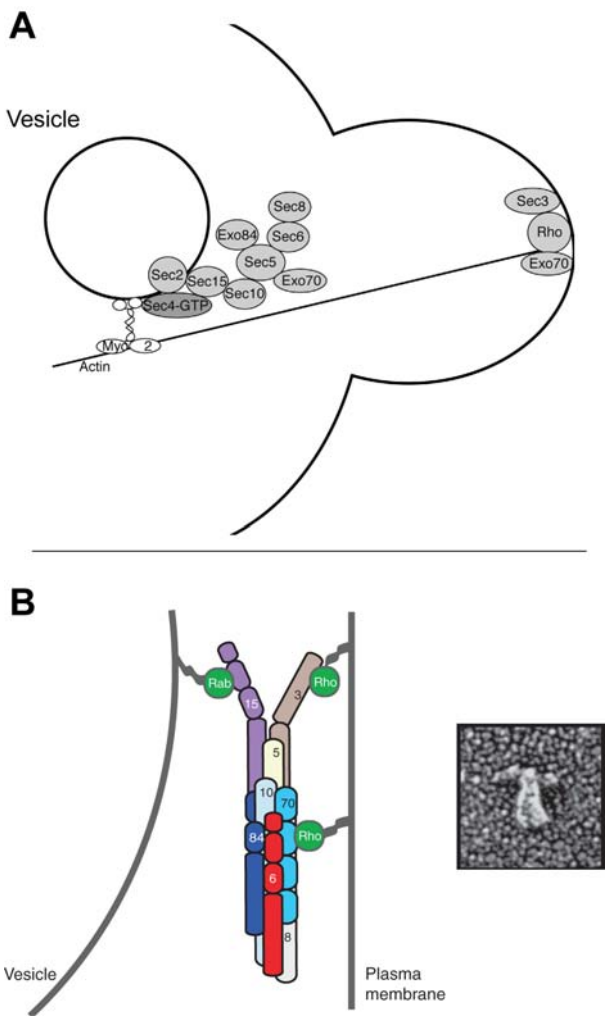

Figure 1.15 | **The Exocyst tethering complex assembles at sites of secretion. A** Sec3 and to some part, Exo70 are believed to localize to sites of exocytosis due to Rho-GTPase binding, whereas the other subunits preassemble and travel via exocytic vesicles before complex assembly occurs during tethering. **B** EM analysis of assembled and fixed exocyst complex (right) and model of interactions during complex assembly (left). Note that the subunits are believed to form rod-shaped structures. Figure adapted from Munson and Novick, 2006.

which act in a number of cell cycle dependent, spatially restricted processes, has to be controlled by GTPases that connect to these layers of intracellular controlling.

The membrane recruitment of the vesicular exocyst subcomplex has also been studied to some extent. Data from the lab of Peter Novick showed that the exocyst recruiting Rab GTPase Sec4 is activated by a protein (Sec2) (**Fig. 1.15 A**), which is recruited to membranes by interacting with the *trans*-Golgi resident, activated form of the Rab Ypt32 (Ortiz et al., 2002) (compare section 1.3.2.1). The authors of that study therefore suggest that it might be a common theme that such Rab cascades determine functioning and directionality of intracellular trafficking events (Markgraf et al., 2007). Further evidence for this mechanism was provided more recently by a study in which interaction of Sec2 with the exocyst subunit Sec15, the direct Sec2-GTP effector was shown to disrupt Ypt32-Sec2 interactions after recruitment of Sec15 by activated Sec4 (Medkova et al., 2006). However, whether the GEF activity of Sec2 was altered subsequently of Sec15/exocyst binding, was not assessed. Taken together, the exocyst is recruited by a Rab after its activation by a transiently interacting GEF, which gets initially recruited by an upstream Rab GTPase, an intriguing mechanism that

elegantly includes the proposed upstream activity of the TRAPP II complex (compare section 1.3.2.1).

The exocyst is structurally characterized to some extent (**Fig. 1.15 B**). EM studies revealed a rod shaped structure with two juxtaposed extensions that are believed to represent the GTPase binding sites. The crystal structure of some exocyst subunits was solved and it appears that they predominantly form elongated α-helical bundle structures, which were proposed to pack against one another along their length to form a structure that could fit the EM data (Munson and Novick, 2006).

1.3.2.5 The HOPS tethering complex*

Tethering events at the vacuole/lysosome are mediated by the C-Vps/HOPS (homotypic fusion and vacuole protein sorting) protein complex, which is well conserved among species. In yeast, this complex consists of six subunits ranging from 79 to 123 kDa in size. Four of its subunits belong to the class C gene family, which result in the most fragmented vacuole phenotype if deleted Raymond, 1992 p03219; Robinson, 1991 p04163; Preston, 1992 p04164}, whereas the two additional subunits, Vps41/Vam2 and Vps39/Vam6, are class B genes (**Fig. 1.16**) (Nakamura et al., 1997). The HOPS complex was characterized as a 700 kDa hetero-oligomeric complex that binds the vacuolar Rab GTPase Ypt7 in its GTP form (Peplowska et al., 2007; Seals et al., 2000; Wurmser et al., 2000), this study.

All six HOPS proteins have been characterized in some detail, even though their precise function still needs further clarification. Vps11/Pep5 and Vps18/Pep3 both contain C-terminal RING-H2 domains. Mutations in the RING domain of Vps18 lead to vacuole fragmentation and missorting of proteins to the vacuole (Rieder and Emr, 1997), indicating an essential role of these domains in complex assembly or protein function. RING domains are present in ubiquitin ligase proteins, and the mammalian Vps18 protein has indeed been shown to promote ubiquitination (Yogosawa et al., 2006). In contrast to the tethering complexes introduced above, the HOPS complex harbors a subunit that belongs to the Sec1/Munc18 (SM)-protein family (Vps33). Members of this protein

* extracted and modified from Ostrowicz et al., 2008, written by this thesis' author.

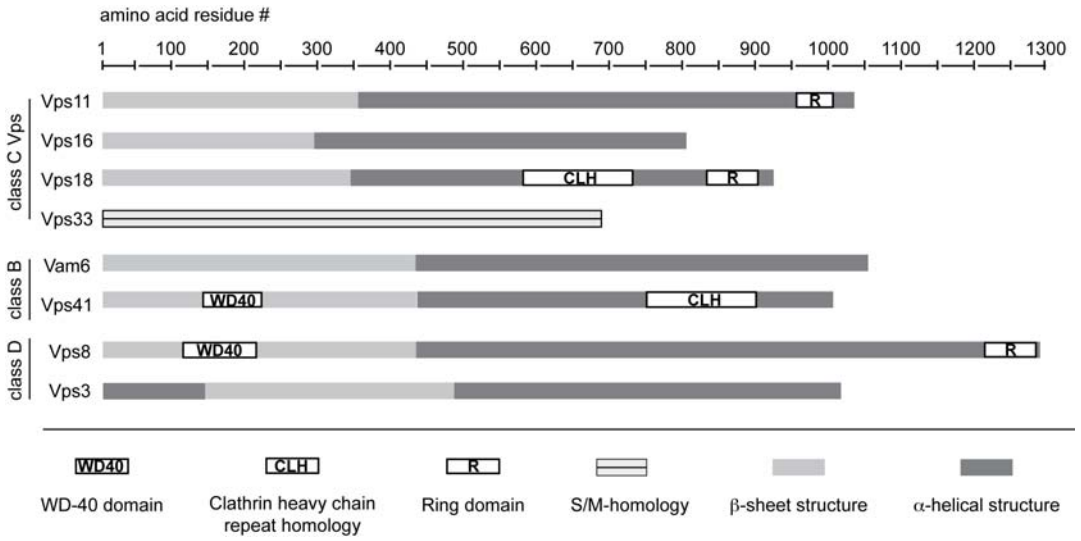

Figure 1.16 | **Schematic overview of the HOPS/CORVET complex subunits.** Note the similarity of secondary structure arrangement, despite very limited sequence similarity. Depicted domains were identified using the SMART sequence analysis tool (http://smart.embl-heidelberg.de/). The Class D genes Vps3 and Vps8 are subunits of the homologous CORVET tethering complex, which was identified in this thesis' work and are depicted for comparison.

family bind SNAREs and are believed to act as chaperones for unassembled SNAREs and to promote efficient *trans*-SNARE-complex assembly (Dulubova et al., 2003; Rizo and Südhof, 2002; Scott et al., 2004; Shen et al., 2007). Indeed, a recent study from the group of Bill Wickner provided evidence for a SNARE-complex proofreading function of the HOPS complex (Starai et al., 2008). They observed that SNARE complexes including mutated SNAREs led to fusion in the *in vitro* vacuole fusion assay, but were blocked upon HOPS addition. Interestingly, this observation was only observed if complete HOPS was added and not in the case of Vps33 addition (Starai et al., 2008). Moreover, Vps33 contains an ATP binding site (Banta et al., 1990; Gerhardt et al., 1998). The subunit Vps16 remains the least characterized HOPS subunit, lacking clearly characterized motifs.

The Class B protein Vps41 has several N-terminal WD-40 domains, which are most likely part of a large β-propeller structure (**Fig. 1.16**) (McMahon and Mills, 2004). In addition to its role in vacuole fusion, the protein is required for the formation of AP-3 vesicles at the late Golgi (compare section 1.2.1.2). In this context, Vps41 has been discussed as a coat protein because specific mutants abolish AP-3 vesicle generation, a feature that was also observed for other tethering complexes' subunits (compare sections 1.3.2.1, 1.3.2.2 and 1.3.2.3) (Darsow et al., 2001; Rehling et al., 1999). The other Class B

subunit Vam6 was shown to exhibit guanyl-nucleotide exchange factor activity (GEF) for Ypt7 (Wurmser et al., 2000). Interestingly, all HOPS subunits (with the exception of Vps33) seem to share a common domain structure with the N-terminus being rich in β-sheets and a predominantly α-helical C-terminus, consistent with the idea of a common ancestor or convergent evolution (Koumandou et al., 2007). Furthermore, Vps41 and Vps18 share a limited sequence similarity with the clathrin heavy chain and are harboring a CLH (clathrin heavy chain repeat homology) domain inside their α-helical C-terminal region. This repeat was shown to mediate interactions between clathrin heavy chains during coat assembly (Ybe et al., 1999). *In silico* analysis revealed that although sequence similarity of the HOPS subunits is low, it appears likely that all of them (despite Vps33) share an N-terminal β-propeller and an adjacent α-solenoid structure (**Fig. 1.16**) (http://bioinf.cs.ucl.ac.uk/psipred/). This kind of arrangement of β-sheets and α-helices has also been observed for protein coats like clathrin, COPI and II, and nuclear pore complex proteins (Devos et al., 2004).

The mechanism of HOPS function on vacuoles is not resolved. Based on the GEF activity of Vam6, it was believed that HOPS activates Ypt7 at the vacuole and binds to it in the GTP-bound form, a model that is challenged by data from this study (see section 3.5). Indeed, binding of HOPS to the membrane is reduced in the absence of Ypt7 (Price et al., 2000a), but it has not been tested whether the identified affinity of HOPS for phospholipids (Stroupe et al., 2006) accounts for the residual association of HOPS with vacuoles. Potentially, it is a combination of several interactions, including its binding to SNAREs (Dulubova et al., 2001; Laage and Ungermann, 2001; Sato et al., 2000; Stroupe et al., 2006). HOPS is thought to act as a tether, which spans the distance between vesicles and the vacuole or two vacuoles during homotypic fusion. During this event, first contact between vacuoles seems to be reversible (Ungermann et al., 1998b). Because Ypt7 appears to be required on both vacuoles (Mayer and Wickner, 1997), and HOPS binds to Ypt7-GTP (Seals et al., 2000), tethering could occur by transient dimerization of HOPS. It is also possible that HOPS is binding asymmetrically to SNAREs and Ypt7, and the symmetric requirement of Ypt7 would not be exclusively related to HOPS function. In a recent study from the Wickner lab, it was shown, that high concentration of SNAREs due to overproduction on the vacuolar membrane can circumvent the need for Ypt7 (Starai et al., 2007). The authors conclude that the Rab might have a regulatory role by enriching SNAREs, HOPS and regulatory lipids at the site of fusion, the so-called vertex-

enrichment. It should be noted that it was shown previously that HOPS, SNAREs and Ypt7 accumulate in an interdependent manner at the vacuole docking site (or the vertex ring) (Wang et al., 2003b), indicating a strong crosstalk among, and potentially, multimerization of, these proteins. However, like for *in vitro* fusion of liposomes, which are bearing only SNARE proteins on their surface, the presented system of overproduced SNAREs only provides another evidence that these proteins constitute the core fusion machinery and that Rabs and tethering complexes are needed to mediate specificity and increase efficiency of the fusion reaction.

Regulation of the HOPS complex function occurs on several levels. During the fusion reaction, HOPS is released from vacuoles (Price et al., 2000a), which might explain the ATP-dependent dynamics of Vps33 observed *in vivo* and *in vitro* (Gerhardt et al., 1998). Moreover, the membrane association of the HOPS complex is regulated by the vacuolar casein kinase Yck3 (LaGrassa and Ungermann, 2005). Yck3 phosphorylates the HOPS subunit Vps41 on the vacuolar membrane, which attenuates fusion in wild type conditions. Yck3 knockout leads to a strong accumulation of Vps41 at vacuole contact sites, whereas overexpression of the kinase strongly reduces fusion and these phenotypes can now be recapitulated using Vps41 mutants (Cabrera et al., 2009), this study. The data obtained in these studies allowed further characterization of the mode of function of Vps41 phosphorylation and yielded intriguing insights into a possibly general scheme of controlling membrane localization of factors not only involved in membrane tethering (see section 3.1).

1.4 The yeast vacuole as a model system for intracellular membrane fusion*

Analysis of vacuole fusion was greatly facilitated by the invention of an *in vitro* fusion assay (Conradt et al., 1992; Haas et al., 1994). For this assay, vacuoles from two yeast strains with a different genetic background are employed. One of these strains lacks the major phosphatase Pho8, which usually serves as a degradative enzyme cleaving phosphoester bonds in the lumen of the vacuole. The other strain lacks the major vacuolar protease Pep4, which is needed for the activation of other hydrolases, including Pho8; it therefore accumulates inactive pro-Pho8. Upon mixing of the vacuoles purified from the two strains in a fusion reaction, the vacuoles fuse, and Pep4 removes the pro-peptide from Pho8. Fusion activity can then be measured using p-nitrophenylphosphate as a Pho8 substrate, which becomes yellow upon dephosphorylation. Thus, the amount of generated p-nitrophenol can be directly linked to the rate of fusion between the two pools of vacuoles. The advantages of this *in vitro* fusion assay are manifold: It is relatively easy to perform and basically every strain with the depicted background can be assayed for fusion activity, allowing for the efficient screening of fusion relevant open reading frames (ORFs). Furthermore, chemical compounds and proteins such as antibodies and fusion factors can simply be added to the reaction to investigate their influence on the fusion rate. However, since the assay employs biological reaction partners certain shortcomings are unavoidable: Mutants with altered vacuole morphology may have vacuoles deficient in Pho8 or Pep4, since both marker proteins have to be sorted to the vacuole, and some endosomal proteins affect vacuole morphology (Peplowska et al., 2007; Raymond et al., 1992). Inhibitors applied in the assay may inhibit Pho8 or Pep4 activity rather than the targeted fusion factor (Jun and Wickner, 2007; Merz and Wickner, 2004a). Usually, the latter is controlled by lysing vacuoles prior to fusion in the presence of the inhibitor, such that Pep4-dependent activation of Pho8 can be measured independent of fusion. An alternative content mixing assay has been presented recently. For this assay, two segments of β-lactamase were fused to the transcription factors Fos or Jun and targeted

* extracted and modified from Ostrowicz et al., 2008, written by the author of this thesis.

to the vacuole, where the formation of the Fos-Jun complex reconstitutes β-lactamase activity (Jun and Wickner, 2007). This assay shows the same kinetic properties as the Pho8-based assay, but β-lactamase activity seems to be less sensitive to inhibitors directed against fusion factors. In addition, lipid mixing assays have been developed, which allow a resolution of lipid and content mixing (Jun and Wickner, 2007; Reese et al., 2005). In some studies, the *in vitro* fusion assays have been complemented by the visual examination of vacuole fusion under the fluorescence microscope (Jun and Wickner, 2007; Mayer and Wickner, 1997; Merz and Wickner, 2004b; Reese et al., 2005; Wang et al., 2002b). Fused vacuoles increase in volume and populations can then be analyzed. *In vivo* vacuole fusion during osmotic stress is used as an additional measure. If exposed to hyperosmotic stress, vacuoles fragment, but fuse again, if the cells are subsequently placed into low osmotic medium afterwards (Bonangelino et al., 2002; Wang et al., 2001b). Neither alternative assay can be easily manipulated nor permit a kinetic analysis of the fusion reaction, but they may be valuable to complement the content and lipid mixing assay. In the following sections, I will discuss the present knowledge on vacuole fusion factors and give insight into the fusion mechanism and its regulation.

1.4.1 Stages of vacuole fusion*

A series of events occurs prior to lipid bilayer mixing (**Fig. 1.17**). It is still under debate if distinct steps follow a defined order or if the fusion rather arises through cooperative action of fusion factors involved in different steps of the reaction (Jun et al., 2006). It seems plausible that fusion occurs at least partly in a consecutive order of events, since inhibitors to intermediate steps will block the subsequent fusion reaction (Conradt et al., 1994; Haas et al., 1994). As observed in the *in vitro* vacuole fusion assay, these steps are termed priming, tethering, docking and fusion/bilayer mixing (Wickner, 2002) and will be introduced below.

* extracted and modified from Ostrowicz et al., 2008, written by the author of this thesis.

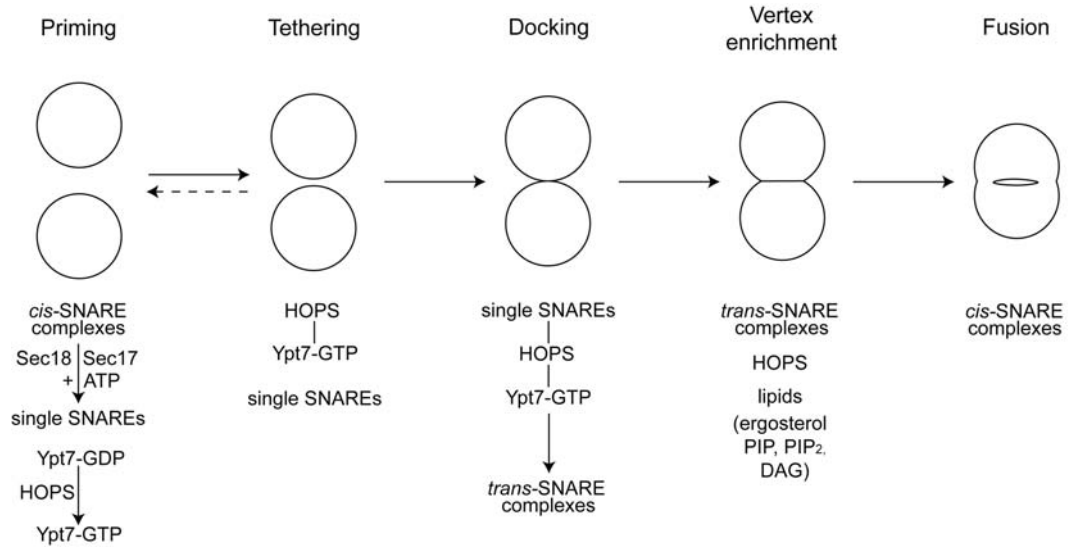

Figure 1.17 | **Stages of in vitro vacuole fusion.** The key players of vacuole fusion are depicted below the cartoon. Several additional accessory factors that are implicated in this process are omitted for reasons of clarity. Figure adapted from Ostrowicz et al., 2008.

1.4.1.1 Priming*

In the ATP-dependent priming reaction, vacuoles are prepared for the first contact and subsequent fusion. A number of fusion factors that reside on the vacuole in an inactive state are now activated in an ATP dependent manner (Haas and Wickner, 1996; Mayer and Wickner, 1997; Mayer et al., 1996; Price et al., 2000a; Ungermann et al., 1998a; Ungermann and Wickner, 1998). The NSF-homolog Sec18, an AAA ATPase, disassembles *cis*-SNARE complexes with the help of its co-factor Sec17 (**Fig. 1.17**), which is released from vacuoles during the priming reaction (Mayer et al., 1996). In this reaction, the soluble SNARE Vam7 dissociates from the complex but stays partially bound to the vacuole membrane (Boeddinghaus et al., 2002; Ungermann and Wickner, 1998). In addition, the dynamin-like Vps1 protein, which binds to Vam3 on vacuoles, is released from this site (Peters et al., 2004). After disassembly, SNAREs are in an active, fusion-competent state. A couple of additional reactions like palmitoylation of the Vac8 fusion factor and Vam10 function have also been connected to priming (Kato and Wickner, 2003; Veit et al., 2001).

* extracted and modified from Ostrowicz et al. 2008, written by the author of this thesis.

1.4.1.2 Tethering*

Tethering - the reversible but distinct contact between vacuoles - is dependent on the fully assembled HOPS tethering complex and the small Rab GTPase Ypt7, present in its GTP-form on both membranes (Mayer and Wickner, 1997; Ungermann et al., 1998b). The HOPS complex is a large hexameric protein complex, consisting of the four C-Vps proteins (Vps11, 16, 18, 33), Vps41, and Vam6 (Seals et al., 2000; Wurmser et al., 2000). The complex has a molecular mass of approximately 700 kDa, and may be present in an even larger complex on membranes (Price et al., 2000a). Compared to the much smaller SNARE complex, the large size of the HOPS complex is believed to enable it to reach over much bigger distances, which predestines it for mediating first contacts between vacuoles (**Fig. 1.17**) (Cai et al., 2007a). At present it is not clear, if the bridging by one HOPS complex is sufficient for efficient vacuole tethering or whether the HOPS complex dimerizes during tethering. A major problem in addressing the tethering stage in the vacuole fusion assay is to dissect tethered from docked vacuoles, which already contain *trans*-SNARE complexes.

1.4.1.3 Docking and fusion*

During docking, unpaired SNAREs that were made available during vacuole priming assemble into *trans*-complexes between opposing membranes. According to several studies, it seems that the Q-SNAREs Vam3, Vam7 and Vti1 on one membrane pair with the R-SNARE Nyv1 from the other membrane (**Fig. 1.17**) (Collins and Wickner, 2007; Dietrich et al., 2005; Fratti et al., 2007; Ungermann et al., 1998b). This arrangement is sufficient to drive liposome fusion using purified SNAREs (Fukuda et al., 2000). The proteins form a zipper-like complex, which propagates from the N-terminal, cytoplasmic side to the transmembrane proximal part of the SNARE domain (Fasshauer et al., 1999; Fasshauer et al., 1997a; Fasshauer et al., 1997b). Most likely, assembly of the complex creates sufficient physical constraints on the vacuolar membrane to drive lipid bilayer mixing (Jahn and Scheller, 2006; McNew et al., 2000; Pobbati et al., 2006; Weber et al., 1998). It should be noted that the liposome fusion assay, which has been employed to

* extracted and modified from Ostrowicz et al., 2008, written by the author of this thesis.

demonstrate SNARE-dependent fusion *in vitro*, is dependent on the vesicle preparation and SNARE density on the liposome (Chen et al., 2006; Dennison et al., 2006). It therefore seems likely that additional factors promote SNARE-mediated fusion *in vivo*. Furthermore, inhibitors and mutants that allow SNARE pairing but block lipid mixing have been described in the literature (Bayer et al., 2003; Collins and Wickner, 2007; Jun and Wickner, 2007; Reese et al., 2005). It is presently unclear how vacuole fusion is triggered once the fusion process is initiated.

A number of factors such as the HOPS complex, the SNAREs, and Ypt7 specifically enrich on a structure surrounding the future fusion site (Wang et al., 2003b; Wang et al., 2002b). The formation of the vertex-ring (compare section 1.3.2.5) leads to a flattening of the vacuole boundaries and therefore enlarges the contact zone between the fusion-destined vacuoles. Fusion of vacuoles was shown to leave membrane fragments within the organelle, which leads to the formation of intraluminal membranes (Wang et al., 2002b). The concerted enrichment of several factors at the fusion site may support the SNARE-driven fusion process. *In vivo*, such enrichment has, for example, been shown for the HOPS subunit Vps41, the docking factor Ccz1 and for the Vac8 fusion factor (LaGrassa and Ungermann, 2005; Tang et al., 2006; Wang et al., 2003a; Wang et al., 2002a).

1.5 SNARE function in vacuole fusion*

SNAREs are membrane-anchored proteins that share a conserved coiled-coil domain adjacent to their transmembrane domain, which is required for regulated fusion of lipid bilayers. They are classified as either Q- or R-SNAREs, depending on whether they contain a glutamine or arginine residue at a conserved position within their SNARE domain (**Fig. 1.18 B**) (Fasshauer et al., 1998; Weimbs et al., 1997). According to their localization, they are also referred to as vesicle (v)- and target (t)-SNAREs (Rothman, 1994). Most R-SNAREs are acting as v-SNAREs, while most Q-SNAREs form t-SNARE complexes. The fusion-competent assembly of SNAREs from opposing membranes, termed the *trans*-SNARE complex or SNAREpin (Weber et al., 1998), in general consists of three Q- and one R-SNARE (**Fig. 1.18 A**). Once the bilayers have fused and all

* extracted and modified from Ostrowicz et al., 2008, written by the author of this thesis.

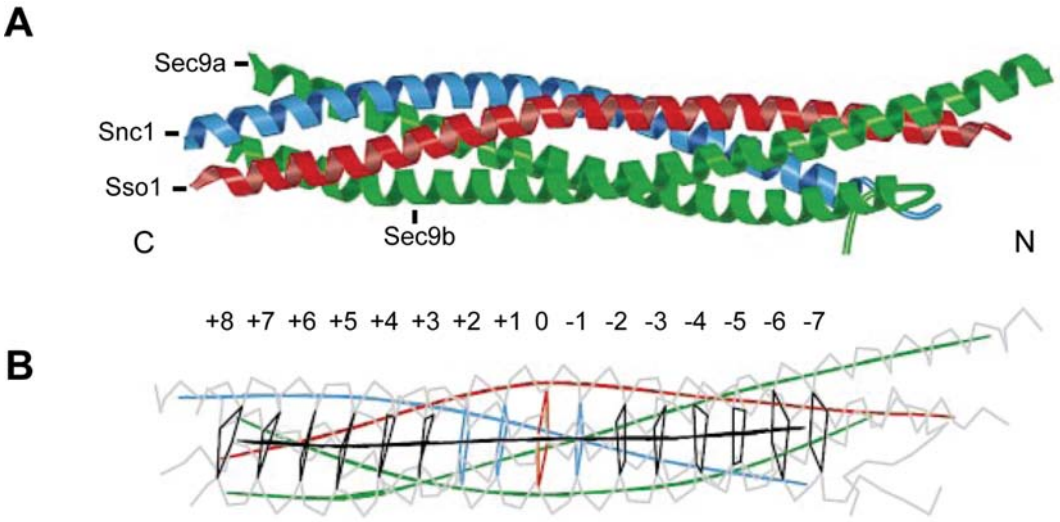

Figure 1.18 | **Structure of an assembled SNARE complex. A** Upon assembly, SNAREs form a 4-helix bundle, which shapes into a circular cylinder of approximately 120Å length. Zippering starts for all components at the membrane-distal N-terminus and proceeds to the C-terminus, which is anchored to the membrane in most cases. **B** In the center of the SNARE complex (referred to as "0-layer"), the Q- and R-residues, which are responsible for the modern classification of SNAREs, are involved in an ionic interaction. The surrounding layers are held together by leucine-zipper-like hydrophobic interactions, therefore shielding the 0-layer from the aqueous environment. Figure adapted from Sutton et al., 1998.

SNAREs are located within the same membrane, the still-assembled SNARE-complex is termed a *cis*-SNARE complex. SNAREs are recycled for further rounds of fusion by disassembly of the *cis*-SNARE complex by NSF/Sec18 and α-SNAP/Sec17 (Söllner et al., 1993a; Söllner et al., 1993b) (**Fig. 1.19**).

Studies on vacuole fusion clarified the order of events leading to membrane fusion, when it became clear that the yeast NSF and α-SNAP-homologs Sec18 and Sec17 act prior to docking and not during fusion (Mayer and Wickner, 1997; Mayer et al., 1996) (**Fig. 1.19**). Later on, five SNAREs were identified on yeast vacuoles that are involved in the fusion reaction: three Q-SNAREs (Vam3, Vam7 and Vti1) and two R-SNAREs (Ykt6 and Nyv1) (Darsow et al., 1997; Nichols et al., 1997; Sato et al., 1998; Ungermann et al., 1998a; Ungermann et al., 1999). The Q-SNAREs Vam3, Vam7 and Vti1 form complexes either with Nyv1 or Ykt6 (Dietrich et al., 2005; Fukuda et al., 2000). Whereas the Nyv1 complex is driving homotypic vacuole fusion, the Ykt6 complex is implicated in other fusion reactions at the vacuole (Dilcher et al., 2001) and palmitoylation (Dietrich et al., 2004).

1.5.1 SNAREs during priming*

Every vacuole fusion event leads to the accumulation of the SNARE-complex on the same membrane – the *cis*-SNARE complex, which is associated with Sec17 (Ungermann et al., 1998a; Wang et al., 2000) and the HOPS complex (Laage and Ungermann, 2001; Price et al., 2000a). For further rounds of fusion to occur, the *cis*-SNARE complex is disassembled by the ATPase Sec18/NSF (Ungermann et al., 1998a) (**Fig. 1.19**), which

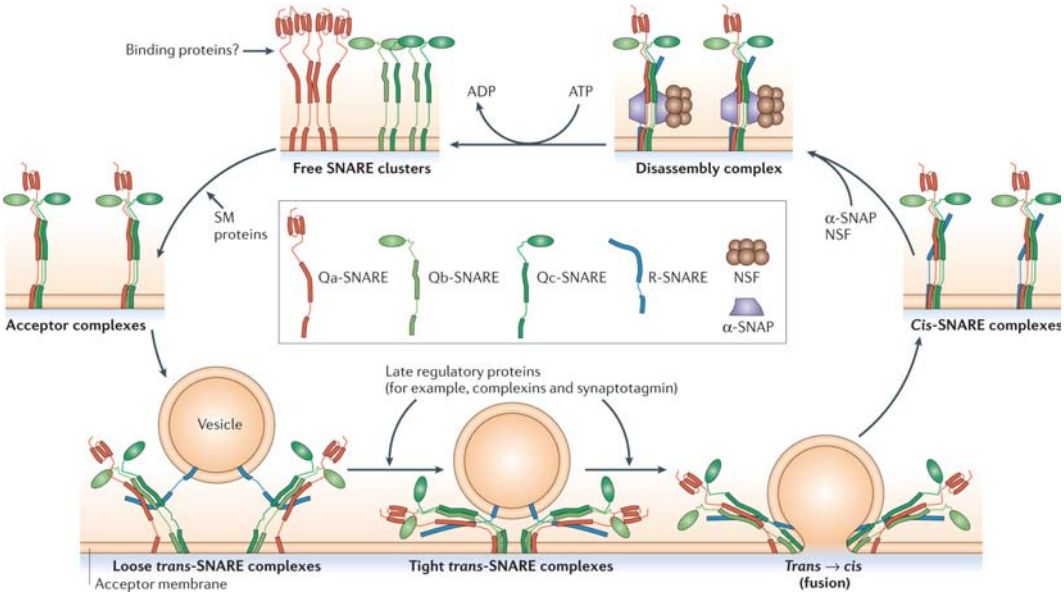

Figure 1.19 | **General model of SNARE mediated vesicle fusion and recycling of SNAREs.** *Cis*-SNARE complexes from previous fusions are disassembled by the action of Sec18/NSF and its co-factor Sec17/α-SNAP. Free Q-SNARE form pre-complexes, which are believed to be chaperoned by Sec1/SM-proteins. Upon successful tethering, R- and Q-SNAREs are brought into sufficient proximity to form trans-complexes. The energy released during complex formation is exerted to drive lipid bilayer fusion. Figure adapted from Jahn and Scheller, 2006.

leads to the release of Sec17/α-SNAP (Mayer et al., 1996; Wang et al., 2000), and the HOPS complex (Price et al., 2000a) as well as the soluble SNARE Vam7 (Boeddinghaus et al., 2002; Ungermann et al., 2000; Ungermann and Wickner, 1998). Vam7 lacks a transmembrane domain, but contains a phosphatidylinositol-3-phosphate (PI(3)P) binding module, a PX domain, at its N-terminus, which is required for membrane binding

* extracted and modified from Ostrowicz et al., 2008, written by the author of this thesis.

(Cheever et al., 2001; Lee et al., 2006; Song et al., 2001). Following its release, Vam7 is specifically recruited to the docking site (Boeddinghaus et al., 2002). Moreover, Vam7 initiates docking of vacuoles in conjunction with Ypt7 (Ungermann et al., 2000), while the free Q-SNARE Vam3 engages in binding to the HOPS complex (Laage and Ungermann, 2001; Sato et al., 2000), which subsequently leads to the docking of vacuoles. It is possible that that the N-terminal domain of Vam3 has a critical role in this process. Mutant vacuoles carrying Vam3 without this domain show reduced *trans*-SNARE pairing, HOPS binding and fusion (Laage and Ungermann, 2001). It should be noted, however, that another study did not find impaired fusion in a similar mutant (Wang et al., 2001a).

1.5.2 SNAREs during tethering, docking and fusion*

The events taking place during vacuole fusion downstream of priming can be divided into two steps (1) the reversible tethering of vacuoles mediated by HOPS and (2) the irreversible pairing of SNAREs between vacuoles *in trans*. Initial tethering of vacuoles occurs at specific sites and is mediated by the Rab Ypt7, but apparently occurs independent of SNARE function (Ungermann et al., 1998b; Wang et al., 2002b) (Wang et al., 2003b). Following this, Vam3 and Vam7 regulate each other's enrichment at these initial contact sites, whereas Vti1 assembly seems to be regulated by a different mechanism (Wang et al., 2003b). Ypt7 is thought to orchestrate the associations between the Q-SNARE and HOPS thereby bridging the transient tethering with the irreversible step of *trans*-SNARE complex formation (Collins et al., 2005). Lipid rearrangements are important for these events to proceed (Fratti et al., 2004; Jun et al., 2004; Kato and Wickner, 2003; Lee et al., 2006; Wang et al., 2003b; Wang et al., 2002b). SNARE pairing between vacuoles can be detected using SNARE deletion strains or assays with tagged SNAREs (Collins and Wickner, 2007; Dietrich et al., 2005; Ungermann et al., 1998b). Each of these assays shows a Sec17-Sec18, ATP-, and Ypt7-dependent accumulation of SNARE complexes, which are also detectable when fusion inhibitors are added to the reaction.

* extracted and modified from Ostrowicz et al., 2008, written by the author of this thesis.

2 Rationale

Eukaryotic cells harbor a diversity of intracellular organelles that need to function in a concerted manner to support cellular homeostasis. The efficient exchange of matter of various kinds is a crucial prerequisite to sustain communication between organelles. Components contained in compartments continuous with the cytosol can freely diffuse or be actively transported through membrane-spanning pores and channels. Luminal contents as well as membrane lipids and transmembrane proteins rely on active vesicular transport for proper trafficking between organelles. This transport system is defined by a number of highly complex and precisely regulated processes involving proteins, protein modifications, and lipids. Intracellular membrane fusion is one of the key processes during trafficking next to vesicle budding and transport. Mainly at this stage, specificity of trafficking appears to be achieved. Although numerous different SNARE proteins, which constitute the core fusion machinery, exist in eukaryotic cells, most of these share a high degree of structural homology and the process of *trans*-SNARE-complex formation or "zippering" appears to follow a general scheme. Furthermore, most SNAREs, if belonging to the same SNARE family (R, Qa, Qb or Qc), seem to be redundant in function, i.e. are able to functionally replace a different SNARE protein. Hence, directionality and specificity of vesicular transport and homotypic organelle fusion events must rely on a machinery that is different from the fusion-promoting SNARE complexes. The primary recognition event of apposing membranes is mediated by the action of Rab GTPases and tethering factors. Although most Rab GTPases are homologous, they appear to function in a non-promiscuous manner and interact with a defined tethering effector in most cases. Other than the two protein families of SNAREs and Rabs mentioned above, not all tethers appear to be related and, in some cases, rather seem to be the product of convergent evolution. Together with their molecular interaction partners, the Rab proteins, it is these factors that are now generally accepted to confer organelle and vesicle identity. The molecular complexity of many tethers and the lack of a common molecular scheme for tethering events have made the investigation of this crucial step in membrane fusion an intricate scientific challenge. Previous work on tethering complexes like the exocyst at the plasma membrane and the GARP-complex at the Golgi has revealed a sequential functioning of subunits and the existence of defined

subcomplexes towards the assembly of the holo complexes, which are functionally linked with the fusion process (see sections 1.3.2.3 and 1.3.2.4). Fusion events at the yeast vacuole and at the homologous lysosome of higher eukaryotes are dependent on the multi-subunit HOPS tethering complex. Only little data was obtained for the functioning of single HOPS subunits in the past and most studies were dealing with the analysis of the full complex's function (see section1.3.2.5). Since nothing is known about the complex's structure and possible assembly routes, and our knowledge about regulation of its function is limited, I was striving to answer the following questions:

1. What is the molecular structure of single HOPS subunits?
2. What is the overall quaternary structure of the HOPS complex?
3. Which subunits interact and what is the stoichiometry of these interactions?
4. Do stable subcomplexes exist?
5. Do yet unidentified HOPS interactors exist?
6. How is HOPS activity regulated?

3 Results

3.1 Regulation of the HOPS tethering complex by Yck3-mediated phosphorylation of its subunit Vps41

Previous studies in our lab revealed the existence of a mechanism that regulates the vacuolar HOPS tethering complex function during homotypic vacuole fusion (LaGrassa and Ungermann, 2005). Upon transfer to a medium of high osmolarity (e.g. 0.4M NaCl), the yeast vacuole fragments and does not fuse back unless osmotic stress is released. Although the mechanisms leading to fragmentation are not yet clearly elucidated, it appears that the massive production of phosphatidylinositol-3,5-bisphosphate ($PI(3,5)P_2$) on the vacuolar membrane and massive flux of water from the vacuolar lumen to the cytosol are involved in this process (Ostrowicz et al., 2008). If the cells are transferred to medium with normal osmolarity after osmotic stress, vacuoles rapidly fuse back. This process relies on the *bona fide* vacuole fusion machinery including the HOPS complex and the vacuolar set of SNAREs (Vam3, Vti1, Vam7, Nyv1/Ykt6). In a screen for impaired fragmentation during salt stress, a strain lacking the yeast casein kinase 3 (Yck3) was identified by our lab to exhibit premature vacuole back-fusion during continuous high osmolarity (LaGrassa and Ungermann, 2005). Yck3 was previously identified as a non-transmembrane cargo of the AP-3 pathway. The protein gets palmitoylated at its C-terminus and is mainly found on the vacuolar membrane facing the cytosol (Sun et al., 2004). In contrast to this, possible targets or cellular functions of Yck3 beyond its activity as a casein kinase were not described. In further experiments employing the *in vitro* vacuole fusion assay, it could be shown that Yck3 exerts its function during tethering, since vacuoles with surplus Yck3 cannot dock and vacuoles lacking Yck3 are not susceptible to two classical fusion inhibitors, Gdi1 and Gyp7-47, known to act at the tethering stage of the fusion reaction. Furthermore, the HOPS subunit Vps41 was identified as a phosphorylation target, since a GFP-fusion protein changed localization in a yck3Δ strain, whereas other fusion factors did not. Moreover, Vps41 was observed previously to change its mobility in SDS-PAGE if vacuole containing fractions were incubated with ATP (Price et al., 2000a); this effect could now be shown to rely on

the existence of Yck3 in the vacuole preparation: Vps41 from yck3Δ vacuoles did not exhibit the "up-shift", which was observed for wt vacuoles (LaGrassa and Ungermann, 2005). After the elucidation of this crucial layer of regulation during vacuole tethering, it was critical to identify the phosphorylation target sequence in Vps41. This appeared to be especially important, since Yck3, a as a casein kinase, is believed to possibly act on a number of target proteins, which makes it difficult to clearly assign effects of manipulations on Yck3 solely to its action on Vps41. To substantiate the findings about Yck3 and to gain further insight into the molecular processes underlying our observations, it would be useful to perform further studies with variants of Vps41, which are unable to get phosphorylated or contain acidic amino acids at the phosphorylation site, mimicking a constitutive phosphorylation.

3.1.1 Identification of phosphorylation sites in Vps41

The most straightforward approach to determine the sites of phosphorylation in Vps41 seemed to perform mass spectrometry with the up-shifted fraction of Vps41 in comparison to non-phosphorylated protein. For this approach, subcellular fractionation of a yeast strain overexpressing Vps41 was performed. In this procedure, cells are subjected to cell wall digestion and subsequent mild rupture of the resulting spheroblasts. Hence, cellular organelles are released into the lysis buffer and can be separated by differential centrifugation. The P13 fraction, which is the resulting pellet from a centrifugation of 13,000xg and contains vacuoles to a high extent, is then incubated with ATP to allow for *in vitro* phosphorylation of Vps41 by the Yck3 kinase. This approach was also used for the experiments in which Vps41 phosphorylation was assayed analytically. In the case of mass spectrometry sample preparation, a much higher amount of cell material was used (approx. 2000 OD-Units vs. 60 OD-Units for standard subcellular fractionation), to allow for the subsequent purification of Vps41 with α-Vps41 antibody coupled sepharose and for visualization by Coomassie staining on an SDS-PAGE gel (**Fig. 3.1**). The resulting gel was sent for further mass spectrometry analysis (MALDI-TOF and ESI-MS/MS) to Christian Preisinger, a protein phosphorylation specialist in the collaborating group of Francis Barr (at that time: Max-Planck-Institute, Martinsried, Germany).

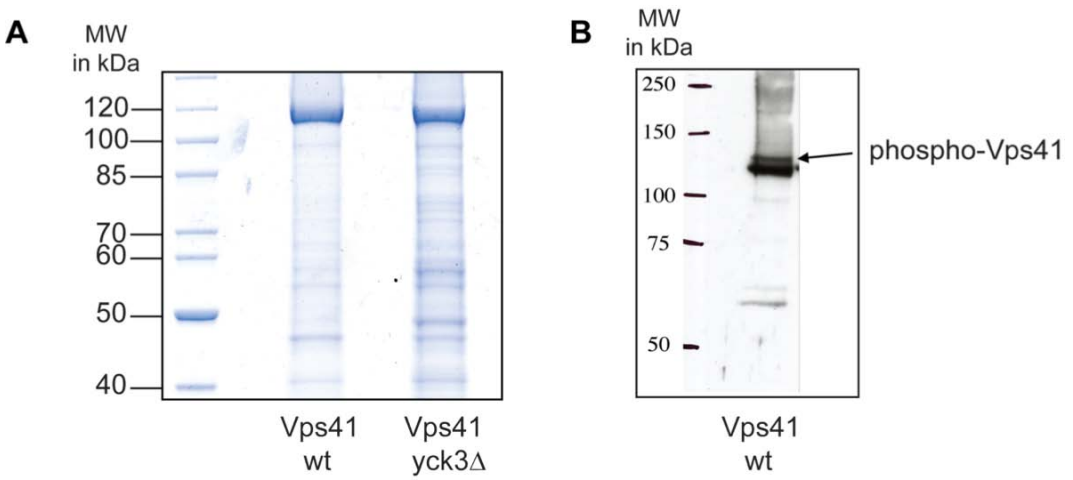

Figure 3.1 | **Purified Vps41 samples after ATP incubation used for mass spectrometry analysis. A** P13 fractions of a wild-type yeast strain and of a yck3Δ mutant were incubated with ATP and Vps41 was subsequently purified using an anti-Vps41 affinity column. **B** Western blot of the wt samples decorated against Vps41. Note the small percentage of upshifted protein.

Unfortunately, the results of the mass spectrometry analysis did not lead to clear results. One major drawback was the low amount of phosphorylated specimen, which could also not be raised in subsequent experiments. Furthermore, the results from Munich revealed that Vps41 is constitutively phosphorylated independent of Yck3 activity at several serine residues at its amino terminus, complicating a clear identification of transiently phosphorylated residues.

To circumvent the shortcomings of the mass spectrometric approach, we decided to single out the most promising phosphorylation sites in Vps41 by in silico prediction using the web-based NetPhos service (http://www.cbs.dtu.dk/services/NetPhos/). Since Vps41 is a large protein of 992 amino acids and contains a substantial amount of serine and threonine residues, 87 and 53, respectively, the incidence for a predicted phosphorylation site was relatively high. We employed a score threshold of 0.5 with 1 being the highest and 0 being the lowest score. Netphos predicted 40 serine residues and 9 threonine residues to be possible phosphorylation targets (**Fig. 3.2**).

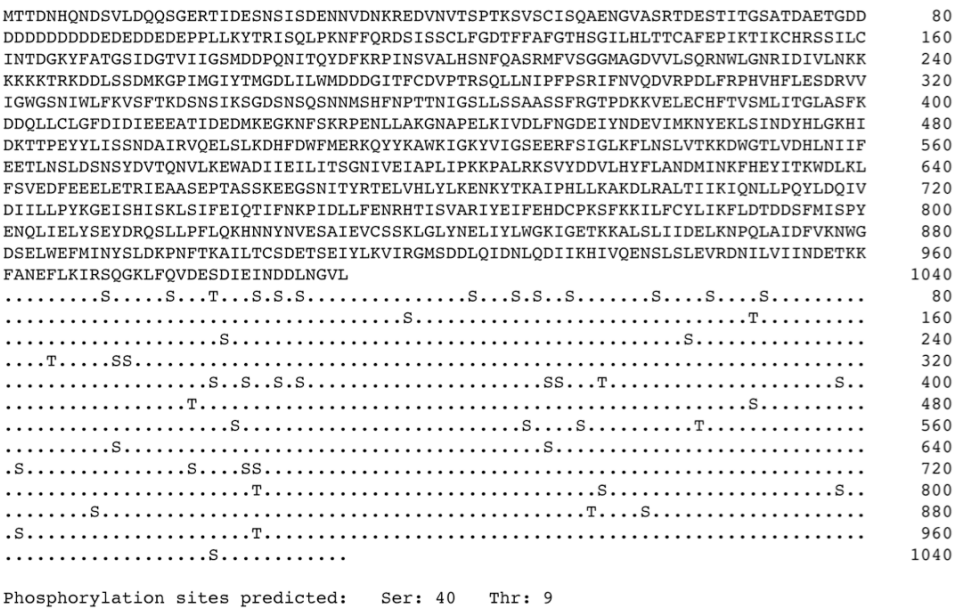

Figure 3.2 | **Prediction of Vps41 phosphorylation sites by the NetPhos algorithm.**

Following the most promising predictions, we prepared mutants of the VPS41 coding sequence by the use of site-directed mutagenesis. Several neighboring potential phosphorylation sites were simultaneously altered to narrow down the search for potential sites in a first approach, therefore decreasing the number of constructs that would have to be prepared (**Table 3.1**).

Table 3.1 **Phosphorylation site mutants of Vps41**

strain	residues altered	working name
CUY1919	T662, S663, S664, T665, S669	S663-664-669-T662-665A
CUY1920	S794, S798	S784-798A
CUY1921	S364, S367, S368, S371, S372, T376	S364-367-368-371-372-T376A
CUY1922	S118, S120, S121	S118-120-121A
CUY1924	none	wt

Due to the results obtained from the mass spectrometric approach, we decided to disregard the most amino terminal residues in our future experiments and focused on the

four potential phosphorylation sites listed in **Table 3.1**. The mutated sequences were cloned into genomically integrative vectors under the control of the constitutive NOP1 promoter and transformed into a *vps41* deletion strain. The resulting mutants were subjected to cell lysis and the P13 fraction was incubated with or without ATP (**Fig. 3.3**).

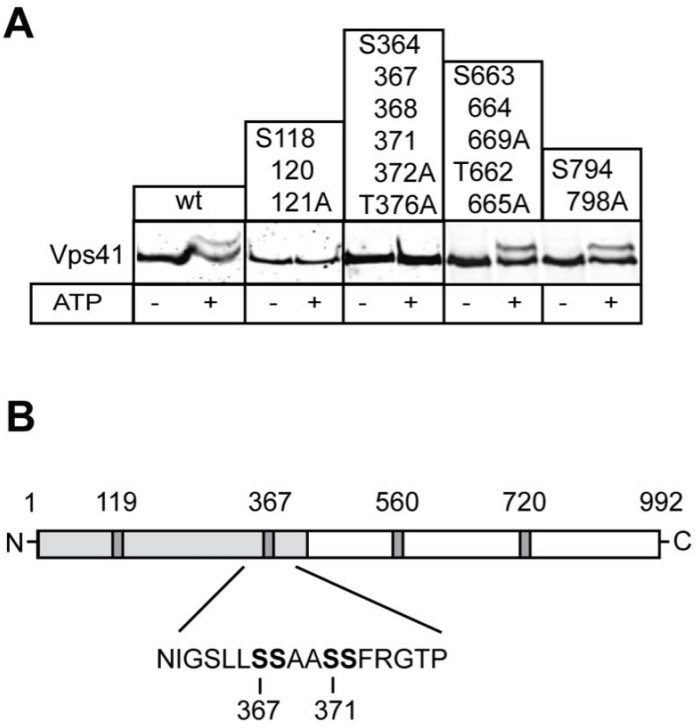

Figure 3.3 | **Analysis of putative phosphorylation sites in Vps41. A** P13 fractions of the indicated strains were incubated with and without ATP, subjected to SDS-PAGE and Western blotting. **B** Scheme of the analyzed Phosphorylation sites. Adapted from Cabrera et al., 2009. Experiment conducted by the author of this thesis.

Two potential sites yielded a change in SDS-PAGE mobility compared to the wild type if mutated into alanine. During further analysis of the two phosphorylation-impaired mutants, fluorescence microscopy of FM 4-64-stained cells revealed, that the S118-120-121A mutant had strongly fragmented vacuoles, reminiscent of the phenotype observed upon deletion of the *vps41* gene. In contrast to this, the S364-367-368-371-372-T376A mutant exhibited normal vacuolar morphology. A GFP-tagged version of this Vps41 variant specifically localized to one or few punctate structures adjacent to the vacuolar membrane. Strikingly, this resembled the exact phenotype observed in a *yck3* deletion background (**Fig. 3.4**).

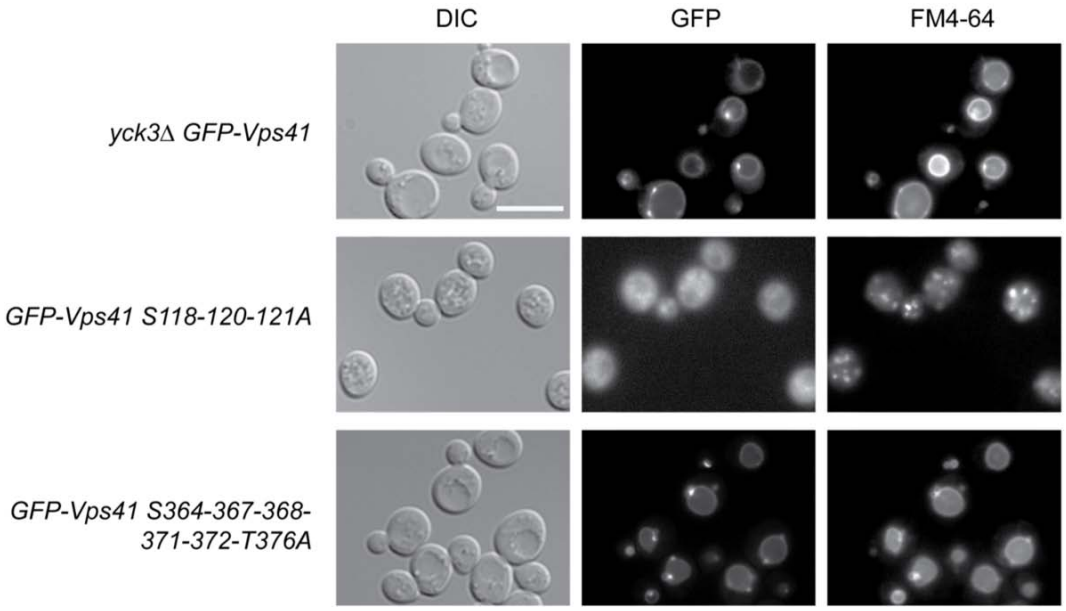

Figure 3.4 | **Microscopic analysis of the two putative phosphorylation mutants that showed impaired upshift.** Log-phase cells were subjected to FM 4-64 staining and analyzed by fluorescence microscopy. Size bar: 10μm

We therefore concluded that we identified the correct phosphorylation site. Further experiments with single and dual amino acid residue alterations (**Fig. 3.5**) revealed that the minimal mutation needed to diminish SDS-PAGE up-shift as well as a change in

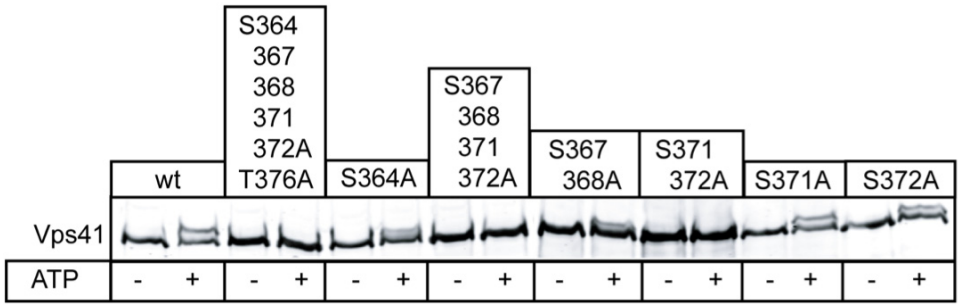

Figure 3.5 | **Analysis of single and dual amino acid alterations to assess the minimal phosphorylation site.** Indicated mutants were subjected to up-shift analysis as described above. Adapted from Cabrera et al., 2009. Experiment performed by Dr. Margarita Cabrera.

intracellular localization of the GFP-tagged Vps41 protein, is the mutation of the sequence coding for amino acid residues S367, S368, S371 and S372.

This finding was the basis for several additional experiments performed by Dr. Margarita Cabrera in our lab, which elucidated the major effects of Vps41 phosphorylation in the endolysosomal system (Cabrera et al., 2009). Furthermore, *in silico* analysis of the Vps41 sequence revealed that this protein harbors a putative ALPS motif (Drin et al., 2007), which could form an amphipathic helix that inserts into lipid bilayers. Intriguingly, this motif is located exactly at the phosphorylation site. Further studies currently under way in our lab aim at the elucidation of the effect of Yck3 mediated phosphorylation on the integrity of the ALPS motif. Possibly, this connection is only one example of a general scheme of controlling the association of proteins to intracellular membranes (see discussion).

3.1.2 The vacuolar fusion factor Mon1 is a substrate of Yck3

Next to Vps41, there was no substrate known to be phosphorylated by the Yck3 kinase, contradictory to our knowledge about casein kinases as promiscuous kinases with usually several possible target substrates. However, in several studies by the lab of Dan Klionsky, it has been reported that the prevacuolar/vacuolar fusion factor Mon1, which is known to interact with another factor, Ccz1, exhibits a change in SDS-PAGE mobility upon incubation of vacuole containing fractions with ATP (Wang et al., 2003a; Wang et al., 2002a). Since this phenotype is reminiscent of the effect we observed for Vps41, we sought to elucidate if the observed up-shift is dependent on Yck3 activity. To test this, P13 fractions from wild type and *yck3*Δ cells were incubated with and without ATP. To facilitate detection of Mon1 and Ccz1, a TAP tag was fused to the C-terminus of both proteins in the respective strain backgrounds. Indeed, I was able to observe a clear change of SDS-PAGE mobility for a fraction of the Mon1 protein upon ATP incubation. This up-shift was not visible in the *yck3* deletion background. In contrast to this, no change in SDS-PAGE mobility could be detected for the Mon1 binding partner Ccz1 under any circumstances (**Fig. 3.6 A**)

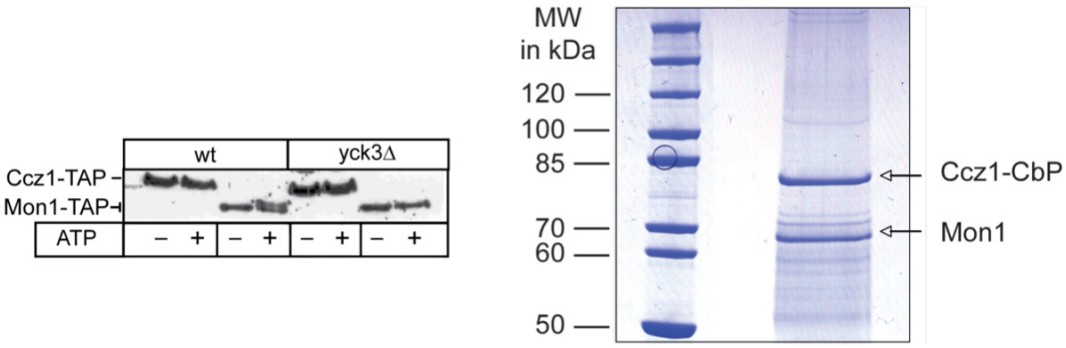

Figure 3.6 | **Probing for Yck3-dependence of the Mon1 upshift. A** Indicated strains were subjected to the up-shift assay as described above. **B** The Mon1-Ccz1-complex was successfully purified from a Ccz1-TAP strain. A full TAP experiment was performed and eluates were analyzed by SDS-PAGE and Coomassie staining.

This data suggests that Mon1 is another substrate of Yck3, which exhibits a biochemically well-detectable effect upon phosphorylation. Furthermore, I was able to purify the Mon1-Ccz1 complex from a strain harboring a TAP-tagged version of Ccz1 (**Fig. 3.6 B**). No unknown interactors could be identified using mass spectrometry.

Recent work by Alexey Merz and colleagues (Brett et al., 2008) suggests that the vacuolar Q-SNARE Vam3 is another phosphorylation target of Yck3, with a putative function of Yck3 in controlling the vacuolar SNARE machinery next to its effect on the HOPS tethering complex (Brett et al., 2008). However, further studies on the effect of Yck3-mediated phosphorylation of Mon1 performed by Dr. Margarita Cabrera and a diploma student in our lab did not yield any further advances on the subject yet.

3.2 Purification of HOPS complex and its subunits for crystallization and electron microscopy analysis

One aim of my thesis was the production of sufficient amounts of single HOPS subunits so that crystallization trials and subsequent X-ray analysis could be carried out. The elucidation of protein structures can provide substantial help in understanding the functioning of proteins and protein complexes on a molecular level. In several studies it was shown that the HOPS complex at the yeast vacuole fulfills a major function in the process of tethering. The complex was demonstrated to interact with the activated form of the vacuolar Rab GTPase Ypt7 and to be able to interact with SNARE complexes

(Collins et al., 2005; Price et al., 2000a; Seals et al., 2000); yet the precise molecular events taking place during tethering and subsequent docking remained obscure. I sought to disclose the mechanism of tethering by providing information about the molecular details of the involved factors.

3.2.1 Recombinant expression of HOPS subunits

The smallest subunit of the HOPS complex is the Sec1/Munc18-homolog Vps33 with an apparent molecular weight of 79kDa. The other subunits' molecular weights range from 93kDa (Vps16) to 123kDa (Vam6). Hence, it becomes clear that recombinant expression of these proteins in standard expression systems like *Escherichia coli* is not an easy task. Moreover, HOPS subunits might not be very soluble proteins, since they appear to act as peripheral membrane proteins *in vivo*. Although the production of small quantities of some proteins was reported on (Darsow et al., 2001), the amounts and the quality of a protein needed for crystallization trials exceeds everything yet obtained from recombinant expression systems. To succeed in the production of these complicated proteins, different approaches were employed to find the most appropriate method of production as well as purification of HOPS proteins.

3.2.1.1 Bicistronic expression

In a study by Lutzmann *et al.* (Lutzmann et al., 2002) it was reported that the expression of nuclear pore complex subunits could be greatly improved by bicistronic co-expression of several proteins in one *E. coli* cell. Moreover, the assembly of nuclear pore subcomplexes could be followed by these means in the recombinant expression system. To adopt this elegant system for the HOPS subunits, I constructed a bicistronic plasmid based on the pET24d-system. The background plasmid was a kind gift from Professor Ed Hurt. It contained the sequence for an N-terminal GST-fusion protein tag combined with a TEV protease cleavage site for the first gene to be introduced. For bicistronic expression, an additional ribosomal binding site had to be introduced into the primers employed for the cloning of the second gene of interest (Lutzmann et al., 2002). The bicistronic co-overexpression of recombinant proteins that form subcomplexes has several advantages: (i) if the proteins are well interacting, they might aid in the process of protein folding in the cell, by specifically chaperoning already folded domains, (ii) the

two proteins should be expressed to roughly the same concentration in the cell, since they are translated from the same mRNA molecule and (iii) only one protein must harbor an affinity purification tag, since the second protein will be co-purified as long as native purification conditions are employed. Since our knowledge of the HOPS subunits and the interactions taking place between these were very limited and partially wrong at this stage of my studies, I chose the two subunits Vps41 and Vam6 to be co-expressed in E. coli (Nakamura et al., 1997; Price et al., 2000b). These two subunits were reported to act together in the "Vps41/Vam6" complex and reasoned to transiently interact with the class C-VPS proteins. Unfortunately, the co-overexpression of these two proteins did not lead to an increase in expression or purification efficiency of Vps41 or Vam6. Furthermore, induction could only be monitored on Western blot level, so that this approach was not followed on. During further work in this study on the interactions taking place between the HOPS complex subunits and the subcomplexes that stably form, it turned out that Vps41 and Vam6 do not directly interact, clearly explaining the above-mentioned results.

3.2.2 Purification of HOPS proteins from yeast

The Tandem Affinity Purification technique allows for the efficient native purification of proteins and their interactors from cell lysate. Two different affinity tags are fused in tandem to either the N- or C-terminus of the protein of interest. Both tags are separated by a protease cleavage site, which allows for the native elution from the first affinity column (compare methods section 5.3.12.1). The classical TAP tag consists of a calmodulin-binding-peptide (CbP) a TEV-protease cleavage site and an additional protein A tag, derived from *Staphylococcus aureus*, which binds to the constant region of IgG antibodies. One advantage of the TAP method over other, classical purification procedures is that the proteins can be purified to a high degree of purity because background impurities are diminished due to two different affinity matrices. Another improvement over some other methods for analytical protein purification is that the proteins of interest are generally eluted natively, so that downstream analysis can be performed with functional proteins. During my studies dealing with the architecture of the HOPS complex, I employed the TAP method, using a protocol that had been adapted from the original method for the work with membrane-associated proteins by the group of Prof. Ed Hurt (see methods section 5.3.12.1). The TAP technique proved useful for answering many questions about the interactions taking place between the different

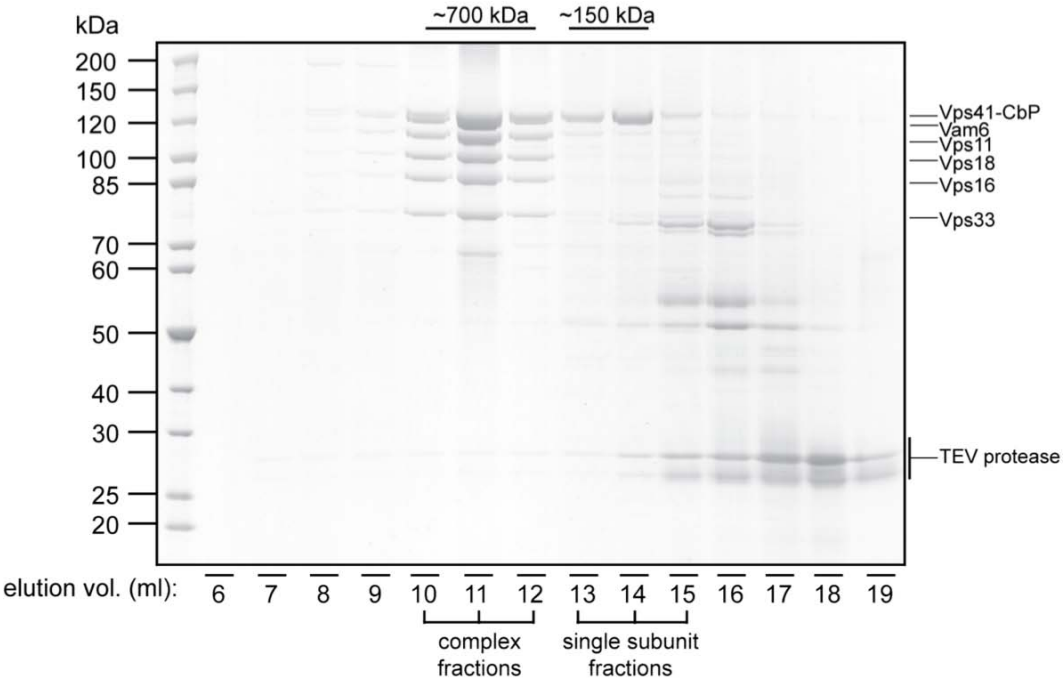

Figure 3.7 | **Purification of the HOPS tethering complex.** TAPurification was performed with a strain harboring a TAP-tagged version of Vps41. The TEV eluate was used to perform a size exclusion chromatography (gelfiltration). 100% of the elution fractions were TCA-precipitated and loaded onto a precast 4-12% SDS-PAGE gel (Invitrogen, Karlsruhe, Germany) that was subsequently stained with Coomassie.

HOPS subunits and was especially powerful in combination with the gelfiltration method, which allows for the sizing of protein complexes and the separation of proteins and complexes by molecular weight. As depicted in **Fig. 3.7**, the TAP method allowed me to efficiently purify the full native HOPS complex. For this experiment, I used TEV eluate from a purification employing a strain harboring a TAP-tagged version of Vps41. The eluate was applied to a Superose 6 column (GE healthcare, Munich, Germany) and isocratic gelfiltration was performed. Since I employed the same buffer for the elution as for protein purification, the UV absorption that was monitored during the column run was strongly quenched due to the contained detergent. Therefore, no useful UV-absorption pattern for the column elution can be presented. The complex containing fractions 10-12 approximately correspond to a molecular weight of 700 kDa, as it was determined using calibrating protein complexes of that size. The single Vps41 protein elutes shortly after in fraction 13-14, which corresponds to a molecular weight of approximately 150-100 kDa. All other bands that can be observed on the SDS-PAGE gel in **Fig. 3.7**, most likely represent impurities resulting from unspecific binding to the IgG-sepharose matrix. Single subunits that could have dissociated off the complex are hard to detect (besides

Vps41, which was specifically pulled down in this experiment), suggesting a very stable interaction of the HOPS subunits. Interestingly, no other major bands can be detected in the complex fraction, indicating that all other HOPS-interactors, which were described before, are only transiently binding. The one additional band that can be seen in fraction 12 at a size of approximately 70kDa represents a chaperone, which was only sometimes detected in the HOPS purifications and most likely represents an artifact of the purification procedure. Further results from these experiments are presented in the following sections. Next to the usefulness of the TAP method for analytical protein complex purification, I utilized this procedure for the purification of overproduced proteins from *S. cerevisiae*, for which recombinant expression in *E. coli* proved unsuccessful before (see section 3.2.1).

3.2.2.1 Purification of Vps41 for crystallographic trials

Overproduction in *S. cerevisiae* can be performed by several methods. Transformation with multi-copy plasmids like the 2µ plasmids leads the occurrence of several copies of the gene of interest in a single cell, which consequently results in increased expression levels due to a higher number of mRNA transcripts. Unfortunately, these plasmids are normally not retained in the cell unless selectivity pressure is applied, making the use of selective minimal media unavoidable, which very often leads to slow growth and reduction of cell mass yield. Another possibility is the genomic integration of a highly active promoter upstream of the gene of interest. The advantage of this method is the robustness of the genomic DNA alteration and the possibility to use complex media, which results in higher viability of cells, leading to faster cell growth and higher cell densities. Due to these benefits, I decided to utilize the *GAL1* gene promoter. This promoter is induced upon addition of galactose to the growth medium in the absence of glucose, which represses transcription of genes, which are under the control of the *GAL1* promoter.

Since the Vps41 protein is of major interest for our understanding of the functioning of the HOPS complex and vacuole tethering *per se*, it was chosen as the main target to be tested for overproduction in yeast. Indeed, the protein proved to be well-expressed and soluble after purification with detergent-containing buffer. As observed in

Fig. 3.8, galactose induced overexpression of Vps41 led to a substantial increase in protein yield with the standard purification procedure.

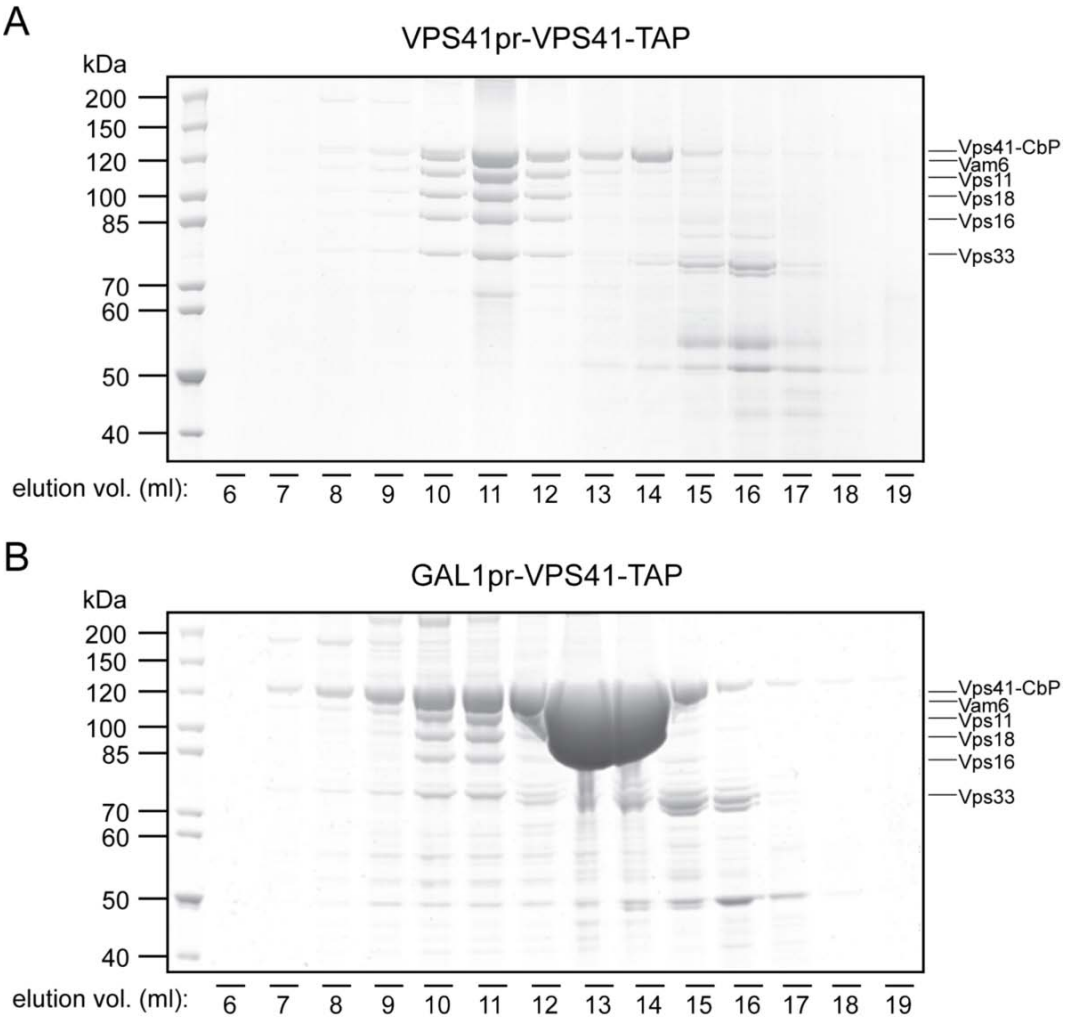

Figure 3.8 | **Effect of Gal-overproduction on the protein yield in a Vps41-TAP purification from yeast.** Same amounts of TEV eluate were applied to a Superose 6 column in **A** (compare **Fig. 3.7**) and **B**. The amount of purified complex is equal in both cases, whereas Vps41 is highly enriched in **B** due to GAL1pr overproduction.

3.2.2.2 Screening for optimal purification conditions for Vps41

Although the first results from the galactose overproduction of Vps41 appeared to be promising in that the acquired protein amounts could be suitable for crystallographic trials, further experiments were necessary, to optimize the purification conditions. The amount of obtained protein should be maximized and at the same time, buffer conditions,

such as detergent type and concentration, and salt strength should be as close as possible to the optimal starting conditions for crystallographic trials. For this purpose, small-scale TAP experiments (Mini-TAPs, see section 5.3.12.2) with cells from the *GAL1pr-VPS41* strain were performed until the TEV elution step. Several different conditions could be tested in parallel by this approach, allowing for a more rapid determination of optimal buffer conditions.

Different detergents that were especially suitable for protein crystallographic experiments were screened for best performance during lysis and purification. In all cases, the end concentration of the detergent was at least two times the critical micelle concentration (CMC). One first experiment, in which the standard nonionic detergent IGEPAL-630 was exchanged for the zwitterionic detergent CHAPS, revealed that this detergent was suitable for lysis and IgG-sepharose binding of Vps41-TAP. Unfortunately, CHAPS inhibited the TEV protease that was used to elute the protein natively from the IgG-beads. This example shows that a detailed examination of all purification steps has to be carried out, before a single component can be deliberately altered.

To determine the optimal detergent for Vps41 purification, I screened a number of different substances (**Table 3.2**), which had been used in crystallization trials before

Table 3.2 **Detergents used for Vps41 purification**

detergent	chemical name
Cymal-5	5-Cyclohexyl-1-pentyl-β-D-maltopyranoside
DDM	n-Dodecyl-β-D-maltopyranoside
Fos-Choline-12	n-Dodecylphosphocholine
LDAO	n-Dodecyl-N,N-dimethylamine-N-oxide
NDDM	n-Nonyl-β-D-glucopyranoside
UDDM	n-Undecyl-β-D-maltopyranoside

and had proven to be compatible with this procedure. Interestingly, the different detergents that were used for this screen revealed partially striking differences in their

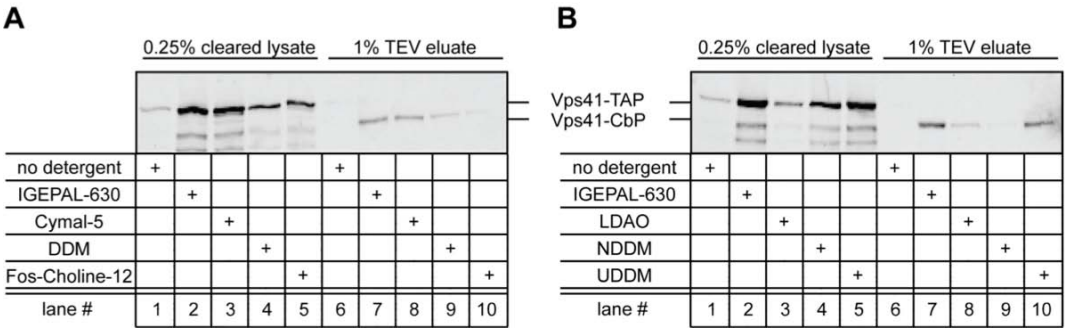

Figure 3.9 | **Analysis of different detergents during cell lysis and protein purification.** The Mini TAP protocol was performed with buffer containing the indicated detergents in **A** and **B**. The indicated amounts were subjected to SDS-PAGE and Western blotting. The membrane was decorated with anti-Vps41 antibody afterwards.

ability to support the solubility of the target protein and, even more noticeably, to allow for efficient TEV cleavage (**Fig. 3.9**).

Even though NDDM and UDDM do only slightly differ in the length of their carbon chain (compare **Table 3.2**), they solubilize Vps41 differently and show a stark difference in supporting the TEV cleavage reaction. The detergent LDAO, which has proven useful for solubilizing and crystallizing transmembrane proteins, does apparently not support solubilization of the membrane associated Vps41. The sugar-based detergent UDDM matched the good solubilization properties as well as the good support of the TEV protease activity of IGEPAL-630 and was chosen as the detergent of choice for subsequent purifications for crystallization trials.

Another crucial property of the purification buffer is its salt strength. For crystallization, it is useful to have a low starting concentration of salts to allow for facile

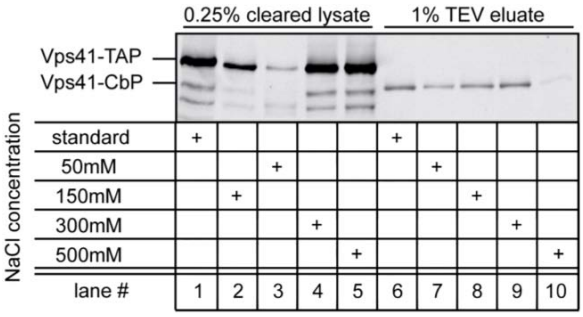

Figure 3.10 | **Influence of the NaCl concentration on the efficiency of the Mini-TAP protocol.** The experiment was performed as in Fig. 3.8, but with different NaCl concentrations.

screening of the right crystallization conditions. Originally, the TAP procedure was conducted using 300mM NaCl in all buffers. Since this is a rather high concentration above the physiological salt strength, I tested different NaCl concentrations for the effectiveness of Vps41 solubilization and efficiency of TEV cleavage (**Fig. 3.10**).

Evidently, the salt strength has profound influence on the Vps41 solubilization properties of the buffer. 500mM NaCl extracts the protein best from the membrane fraction (**Fig. 3.10** lane 5 compared to 1-4), although only slightly better than 300mM NaCl. The TEV elution, on the other hand, is strongly inhibited by the high salt concentration (lane 10), whereas 300mM NaCl seem to be tolerated by the TEV protease (lane 9). The beneficial effects of a low salt concentration on the TEV cleavage reaction become clear by the comparison of lanes 7-9 with lanes 2-4 (note the change in loading order). Even though the cleared lysate, which was used for loading the IgG sepharose, contained much less protein in the case of lanes 2 and 3, the protein amounts eluted by the TEV treatment do not reflect these strong differences but appear relatively similar (compare lanes 7 and 8 to lane 9).

Although a substantial amount of work was invested on the investigation and optimization of the purification conditions of Vps41 from yeast, crystallization of the protein was not yet possible. Purified samples were sent to the group of Professor Roger Goody (Max-Planck-Institute, Dortmund, Germany) and different crystallization conditions were tested without success. Future crystallization trials could be more successful, since only a limited number of conditions were tested in this first approach. The purification routine that I established for Vps41 could also be applied for other subunits to successively determine the HOPS complex subunits' structures.

3.2.2.3 Purification of HOPS complex for electron microscopy

The impressive advances on the protein yield that became possible by genomic integration of the *GAL1* promoter in front of the Vps41 coding region led me to generate a strain harboring all six HOPS subunit genes under the control of the *GAL1* promoter. Since each of these genomic alterations is dependent on the use of an antibiotic or auxotrophy marker, we decided to generate two parent strains with each containing three subunits' genes under the *GAL1* promoter control. For the creation of the "all-GAL-HOPS" strain, these two parent strains would have to be mated, which would result in a

diploid strain containing all six genomic alterations. Indeed, I was successful in the production of both parent strains and, consequently, the all-GAL-HOPS strain. First purification trials showed that the resulting yield of purified HOPS complex was at least ten- to fifteen-fold increased compared to the wild-type purification (**Fig. 3.11**). Despite

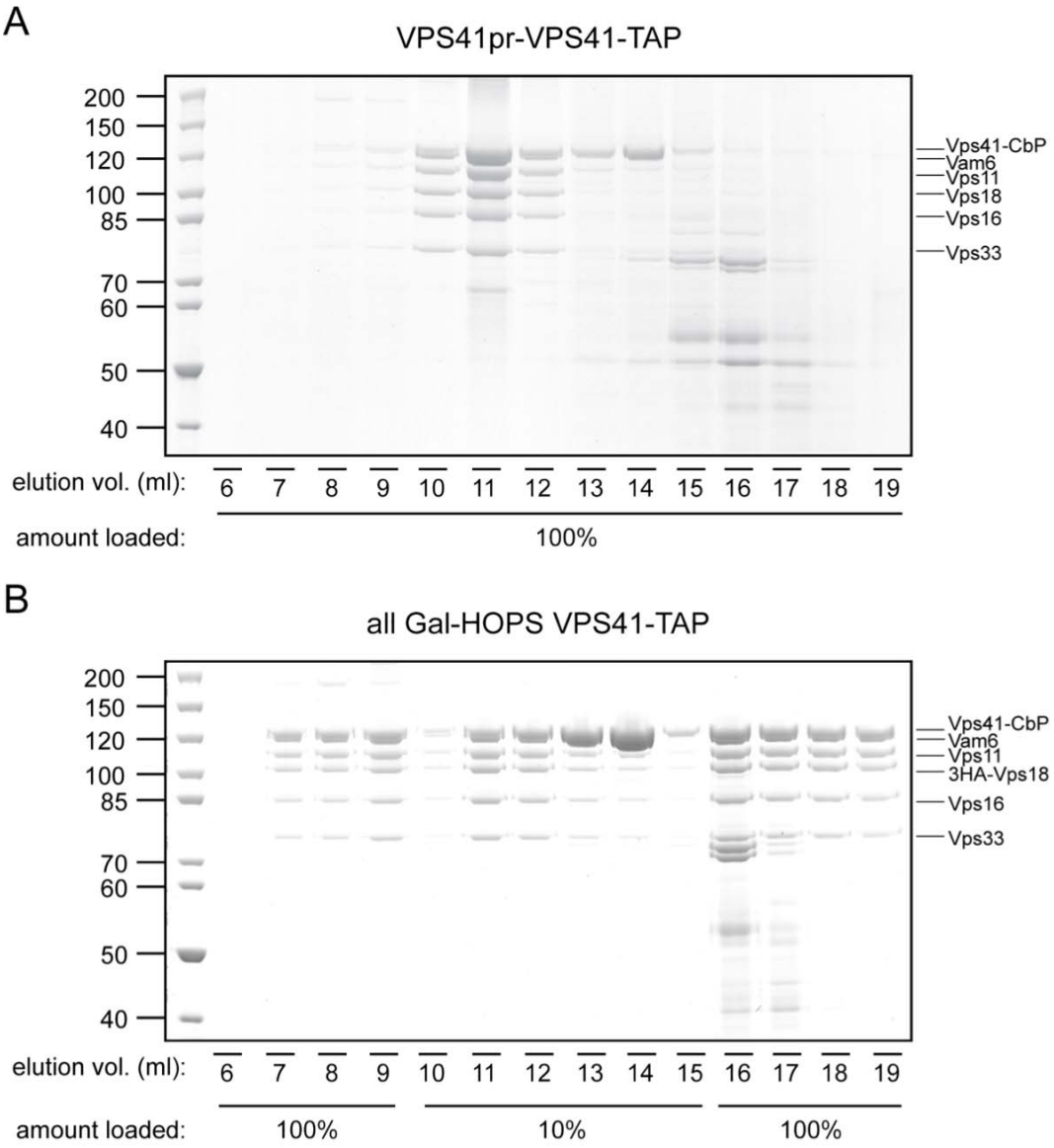

Figure 3.11 | **Effect of Gal-overproduction of all HOPS subunits on the protein yield in a TAP purification from yeast.** Same amounts of TEV eluate were applied to a Superose 6 column in **A** and **B**. The amount of purified complex is highly enriched in **B** due to *GAL1*pr overproduction of all subunits. Note that in the main complex fractions, only 10% of the fractions were loaded on the gel compared to 100% in **A.** The complex proteins observed in **B** in fractions 6-9 and 16-19 most likely occur due to the column's inability to efficiently separate higher protein amounts of the complete complex.

this multiplication of purified protein amounts, crystallization of the whole complex did not appear feasible until now, since the total amounts do still not compare to the yields accomplished for the single subunit Vps41 (compare section 3.2.2.1). Nonetheless, analysis of the HOPS complex structure by electron microscopy is under way. My successor colleague Cornelia Bröcker is currently performing several experiments in collaboration with Dr. Stefan Raunser at the Max-Planck-Institute in Dortmund. First negative stain results were just recently obtained and are depicted in **Fig. 3.12**.

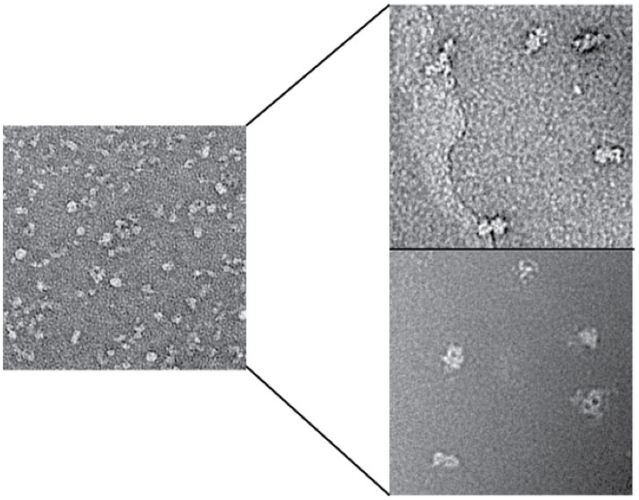

Figure 3.12 | **Preliminary negative stain EM-data of the HOPS complex.** Provided with kind permission by Cornelia Bröcker. EM analysis was performed by Dr. Stefan Raunser.

3.3 Identification and characterization of the novel CORVET tethering complex and intermediate complexes

3.3.1 Vps3 interacts with the class C Vps proteins

The establishment of methods needed to tackle the challenges of protein overproduction and complex purification mentioned above served as powerful tools for further characterization of the HOPS tethering complex. One incidental finding of a former co-worker of mine, Dr. Karolina Peplowska (now Max-Planck-Institute, Martinsried, Germany), gave rise to a number of experiments that finally led to the identification of three novel protein complexes with homology to the HOPS tethering complex (Peplowska et al., 2007). Together with me, she performed a tandem affinity purification of the class D protein Vps3, that had been previously described by our lab to be involved

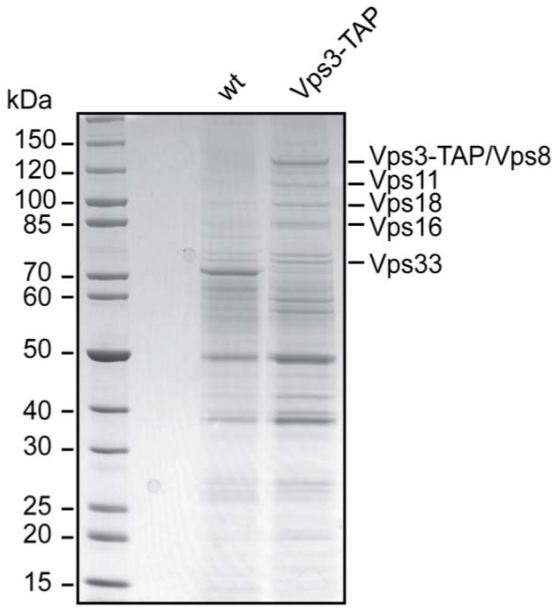

Figure 3.13 | **Vps3 binds to the class C-Vps proteins and Vps8.** A standard TAPurification was performed with a strain harboring a TAP-tagged version of Vps3. Adopted from (Peplowska et al., 2007). Experiment was conducted by this thesis' author together with Dr. Karolina Peplowska.

in the process of vacuole fragmentation upon osmotic stress (LaGrassa and Ungermann, 2005). Intriguingly, we found that Vps3 does interact with the class C Vps proteins Vps11, Vps16, Vps18 and Vps33, all of which are main components of the HOPS complex (**Fig. 3.13**). Additionally to the class C Vps proteins, the class D protein Vps8 was identified to interact with Vps3. Vps8 had been previously identified to bind to the class C Vps proteins by Elizabeth Jones and co-workers (Subramanian et al., 2004), a finding that I could confirm with my own TAP experiments before (**Fig. 3.14**).

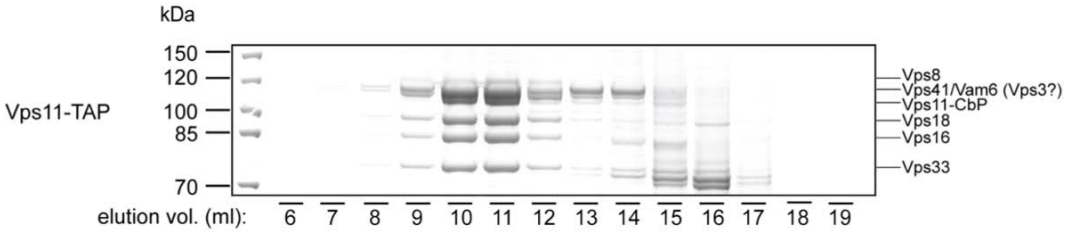

Figure 3.14 | **Vps8 is contained in Vps11-TAP TEV eluate.** Gelfiltration analysis of a Vps11-TAP TEV eluate. Vps8 was identified via mass spectrometry. Vps3 is most likely present on the gel together with Vps41 and Vam6 but could not be detected by the mass spectrometric analysis.

3.3.2 Vps3 is a subunit of a novel HOPS homologous complex

Based on our findings of the interaction of Vps3 with Vps11, -16, -18, and -33, we decided to investigate to which extent these proteins act together. For this purpose, I performed IgG-sepharose pull-downs and subsequent TEV protease cleavage with cell lysates from strains harboring a TAP-tagged version of Vps3 or Vps8. The eluates where applied to a Superose 6 size exclusion column (compare section 3.2.2.1) to determine the size of putative protein complexes and the stoichiometry of the involved proteins. Indeed, I was able to show that Vps3 and Vps8 are both part of a protein complex of an approximate molecular weight of 700kDa, comparable to the HOPS tethering complex (**Fig. 3.15**). Interestingly, Vps3 is not found in equal amounts as the other subunits in the complex containing fractions, as judged by the strength of the Coomassie stained bands (**Fig. 3.15**, compare fractions 10-12 in **A** and **B**). Yet in both the Vps3- as well as the Vps8-TAP gelfiltration, Vps3 is observed in a peak of higher retention, resembling lower molecular weight fractions of 100-150kDa. In the case of the Vps8 purification, the amount of Vps3 eluting in this second peak corresponded well with the amount of the other subunits still present in the complex (**Fig. 3.15**, compare fractions 10-12 with 13-14

in **B**), indicating that it was part of the complex during the purification procedure but dissociated either during TEV elution at 16°C or upon injection on the gel filtration column due to the strong dilution effect. In the case of the Vps3-TAP size exclusion, more Vps3 is found in the single protein fractions 13 and 14 than the other proteins in the complex fractions 10-12, most likely because not all of the Vps3 molecules are included in the complex *in vivo*, resulting in non-equimolar amounts on the SDS-PAGE gel.

Beside this very specific characteristic, comparison with the results of the gelfiltration experiments obtained for the HOPS complex reveals that the observed complexes show a strong similarity in their biochemical properties *in vitro* (**Fig. 3.15**,

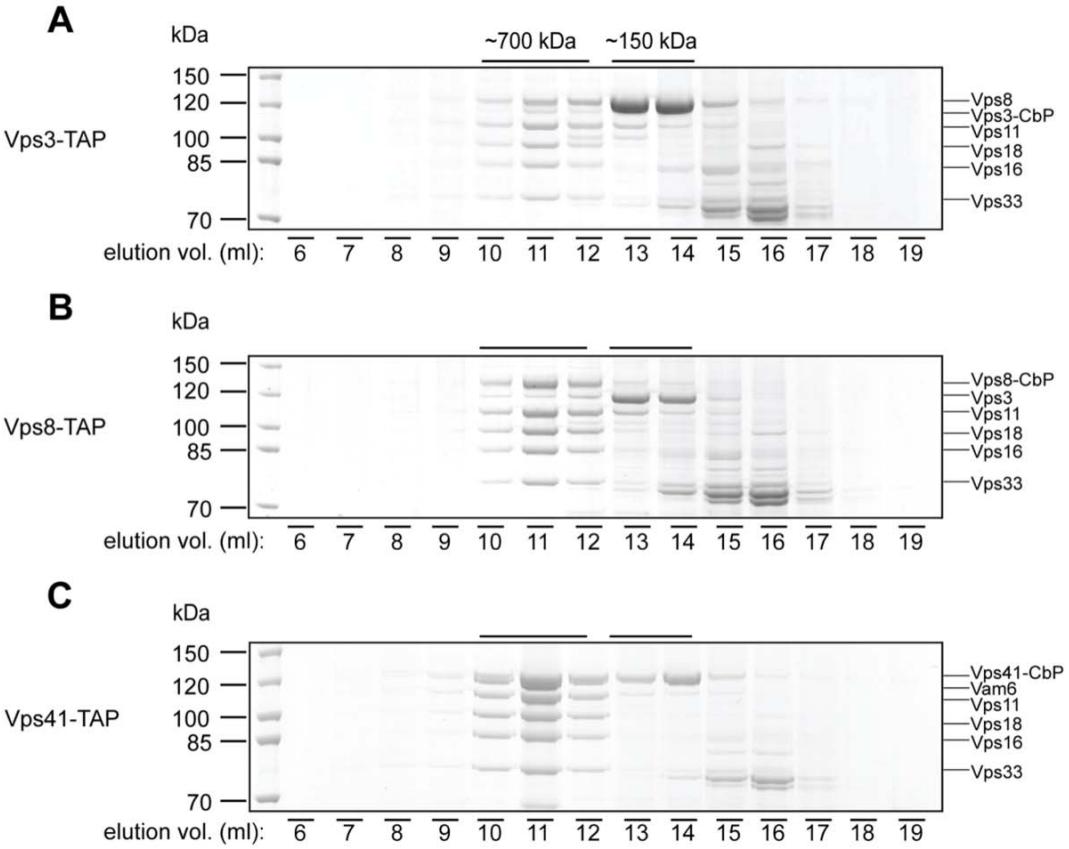

Figure 3.15 | **Identification of the Vps3-Vps8-Class C complex.** TEV eluates from TAPurifications of the indicated strains were subjected to SDS-PAGE and subsequent Coomassie staining. Note that all complexes elute in fractions corresponding to approx. 700kDa and show equal elution patterns.

compare **A** and **B** to **C**). Both Vps3 and Vps8 have previously been shown to act at the level of endosomes (Subramanian et al., 2004), and are needed for proper sorting of cargo to the vacuole (Rothman et al., 1989). Owing to these facts and the involvement of the

Class C Vps proteins, we decided to term this novel complex CORVET (class C core vacuole/endosome tethering).

3.3.3 Identification of intermediate complexes

The striking similarity between the CORVET and the HOPS complex led us to analyze the sequence similarities between the four subunits that are specific for each of the two complexes. Although all of these proteins share a certain similarity, the strongest similarity was found between Vps3 and Vam6 as well as Vps41 and Vps8 (Peplowska et al., 2007). This indicated that the respective subunits could fulfill comparable functions and might be involved in interactions with similar subunits. We therefore wondered, if next to the CORVET and HOPS complex, mixed complexes could exist and if we were

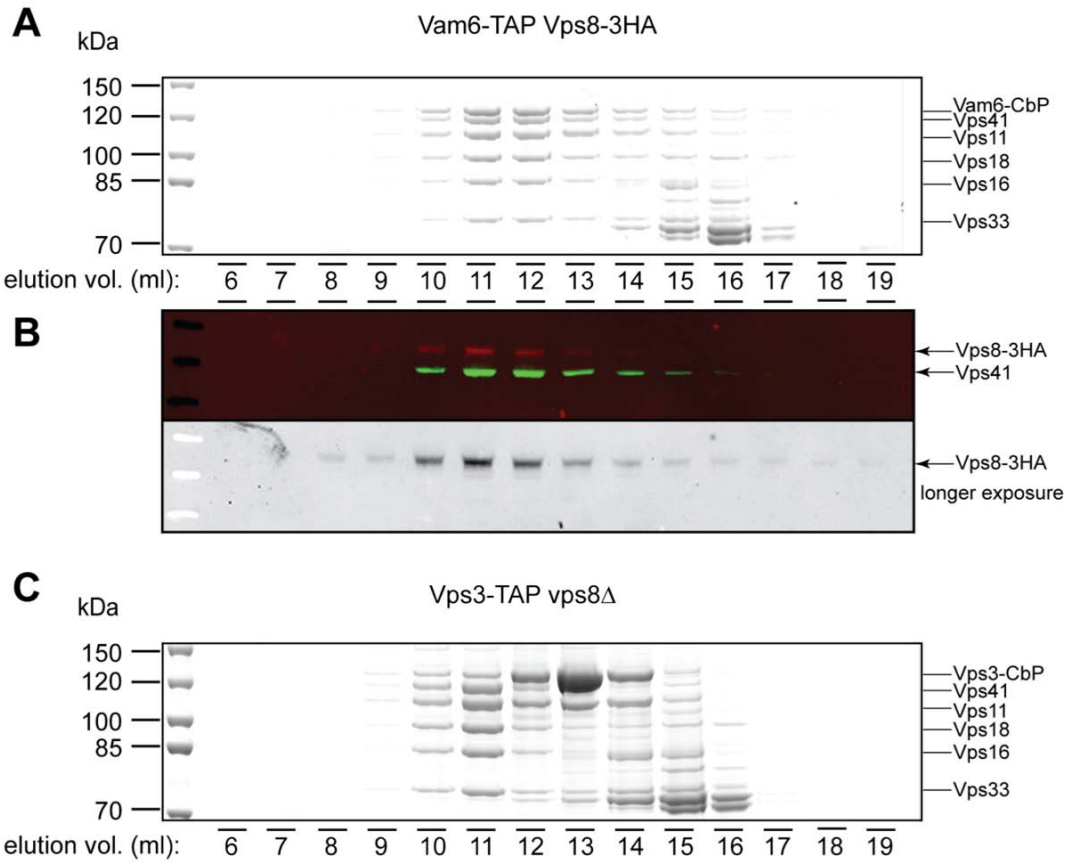

Figure 3.16 | **Identification of two intermediate complexes. A-B** The Vps8-Vam6 intermediate complex could not be identified on Coomassie levels**.** Therefore, I employed an HA-tagged version of Vps8. **B** 20% of the gelfiltration elution fractions were subjected to SDS-PAGE and Western blotting and subsequently decorated with anti-HA antibody (mouse, red) and anti-Vps41 antibody (rabbit, green). Antibodies were visualized using fluorescent secondary antibodies and a LiCor Odyssey scanner. **C** The Vps3-Vps41 intermediate complex is readily detectable in a vps8Δ strain.

able to detect those. Indeed, I was able to show that an HA-tagged version of Vps8 is specifically co-eluting with the complex purified with Vam6-TAP from an otherwise unaltered strain background (**Fig. 3.16 A**). Since the HOPS complex is primarily purified under these conditions, Vps8-3HA is not detectable on a Coomassie-stained SDS-PAGE gel, but can be identified on Western blot level using a specific anti-HA antibody (**Fig. 3.16 B**). In order to probe for the existence of the other putative mixed complex, I chose a vps8Δ strain with a TAP-tagged version of Vps3 and performed an IgG-sepharose affinity purification with TEV elution and subsequent gelfiltration. In this case, the purified complex could be well observed on a Coomassie stained SDS-PAGE gel (**Fig. 3.16 C**) and proteins were identified via mass spectrometry. Together with Vps3, Vps41 and the class C Vps proteins were retained on the IgG-sepharose matrix and eluted together from the gelfiltration column in a single peak. Again, Vps3 dissociates partially from the complex as it has been observed in section 3.3.2.

3.4 Identification of stable HOPS subcomplexes

3.4.1 Deletion of single HOPS subunits reveals the existence of stable subcomplexes

In my efforts to unravel the interactions and transformations taking place in the course of tethering complex conversion from the endosomal CORVET to the vacuolar HOPS complex (Peplowska et al., 2007), I was confronted with several interesting findings. My first observation was the existence of a stable subcomplex comprised of Vam6, Vps11 and substoichiometric amounts of Vps18 in a deletion mutant of the HOPS subunit Vps41 (**Fig. 3.17** compare **A** and **B** (wild-type condition) to **C** (vps41Δ)). In order to uncover additional stable subcomplexes and to address the question of the HOPS complex architecture I asked which subunit interactions would survive the single gene deletion of other subunits. I found that only subunits Vam6 and Vps33 could be removed without subsequent loss of other subunits from the core complex (**Fig. 3.18**). In the case of Vam6, this finding can be explained at least partially by its replacement by Vps3, which leads to the formation of the previously identified intermediate complex (Peplowska et al., 2007). In support of previous findings (Rieder and Emr, 1997), I observed that deletion of *VPS16* caused Vps33 to vanish from the complex

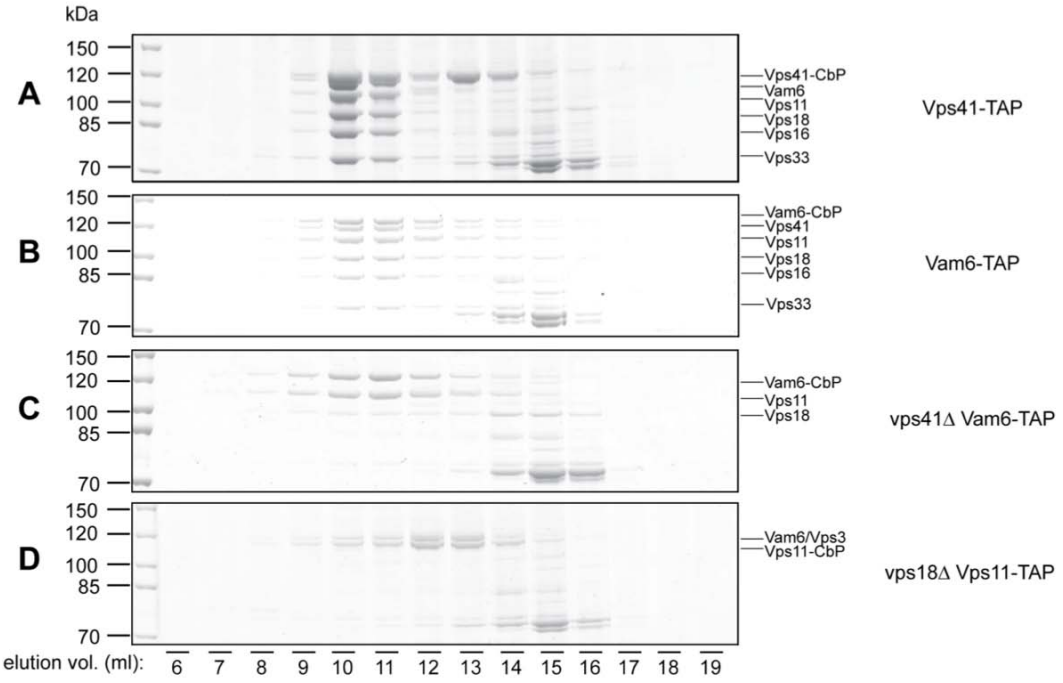

Figure 3.17 | **Identification of stable HOPS subcomplexes by deletion mutant analysis.** As described in previous experiments, TEV eluates from TAPurifications of the indicated strains were applied onto a Superose 6 column and elution fractions were put on an 4-12% SDS-PAGE gel and subsequently stained with Coomassie.

(**Fig. 3.19**), suggesting that Vps33 binding to the HOPS complex is solely dependent on its interaction with Vps16 and that Vps33 is not needed to maintain a stable core complex. The resulting tetrameric subcomplex consists of the two class C Vps proteins Vps11 and Vps18 as well as Vam6 and Vps41, indicating that Vps16 and Vps33 are

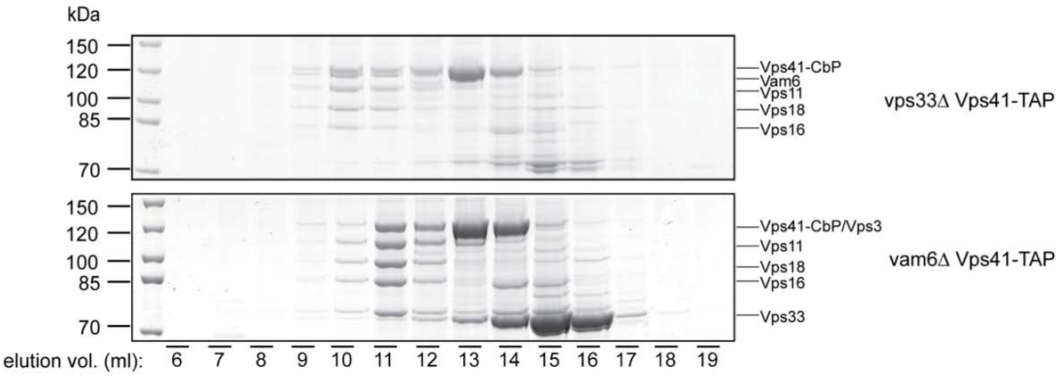

Figure 3.18 | **Vps33 and Vam6 are the most peripheral subunits and their absence only slightly impairs complex stability.** TEV eluates from TAPurifications of the indicated strains were applied onto a Superose 6 column and elution fractions were put on an 4-12% SDS-PAGE gel and subsequently stained with Coomassie. Note that complexes elute slightly different due to the employment of two different Superose 6 columns.

dispensable for the remaining interactions to occur. Single deletion of the remaining Class C-Vps genes (i.e. *vps11* or *vps18*) resulted in hardly or no detectable residual subcomplexes except for the dimeric subcomplex Vps11-Vam6 in vps18Δ (**Fig. 3.17 D**). This data led to a basic model of HOPS subunit interactions (see discussion section 4.4). This model gained refinement due to additional co-overexpression studies (see below).

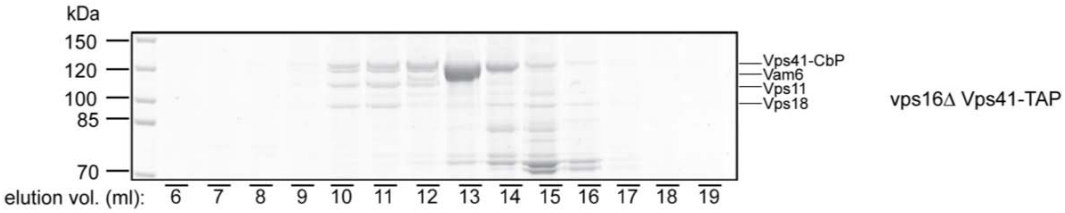

Figure 3.195 | **Vps33 binds to the HOPS complex via Vps16.** TEV eluates from TAPurifications of the indicated strains were applied onto a Superose 6 column and elution fractions were put on an 4-12% SDS-PAGE gel and subsequently stained with Coomassie.

3.4.2 Overexpression of apposite subunits allows formation of stable subcomplexes

The intriguing findings about the existence of stable subcomplexes in single HOPS subunit deletion strains led me to survey the possibilities to express and overproduce those in cells with wild type background. My aim was to confirm our previous results, to gain further insight into the organization of HOPS and its corresponding subcomplexes, and to be able to produce larger amounts for further biochemical characterization. Therefore, I tested the ability of the HOPS subunits to form stable subcomplexes in the relative absence of other HOPS subunits. Indeed, upon expression of specific doublets, one triplet and one quadruplet of HOPS subunits under the strong, inducible *GAL1* Promoter, I observed formation of stable subcomplexes (**Fig. 3.20**, summarized in **Table 3.3**). In the case of the two doublets Vps11-Vam6 and Vps16-Vps33 (**Fig. 3.20**, lane 2 and 3), a near 1:1 stoichiometry of the purified proteins is observed, indicating that these proteins do form very stable interactions.

Table 3.3. **Co-overexpression of HOPS complex subunits**

strain	genotype	scheme
CUY2724	BY4727, *vps11pr::HIS3-GAL1pr vam6pr::NatNT2-GAL1pr VAM6::TAP-URA3*	
CUY3238	CUY1772 X CUY2858, *vps33pr::HIS3-GAL1pr vps16pr::KanMX-Gal1pr VPS16::TAP-URA3*	
CUY3361	CUY3050 X CUY2873, *vps11pr::HIS3-GAL1pr vps18pr::KanMX-GAL1pr-3HA vam6pr::NatNT2-GAL1pr VAM6::TAP-URA3*	
CUY3447	CUY3050 X CUY3435, *vps11pr::HIS3-GAL1pr vps18pr::KanMX-GAL1pr-3HA vps41pr::TRP1-GAL1pr vam6pr::NatNT2-GAL1pr VAM6::TAP-URA3*	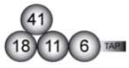
CUY3448	CUY2489 X CUY3435,*vps11pr::HIS3-GAL1pr vps16pr::NatNT2-GAL1Pr vps18pr::KanMX-GAL1pr-3HA vps41pr::TRP1-GAL1pr vam6pr::NatNT2-GAL1pr VAM6::TAP-URA3*	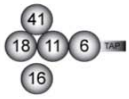
CUY2675	CUY2489 X CUY1953, *vps11pr::HIS3-GAL1pr vps16pr::NatNT2-GAL1Pr vps18pr::KanMX-GAL1pr-3HA vps41pr::TRP1-GAL1pr VPS41::TAP-URA3 vam6pr::KanMX-GAL1pr vps33pr::HIS3-GAL1pr*	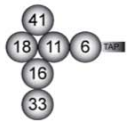

Furthermore, it seems most likely that the two proteins of each pair represent at least one of their respective primary interaction partners in the assembled HOPS complex. If

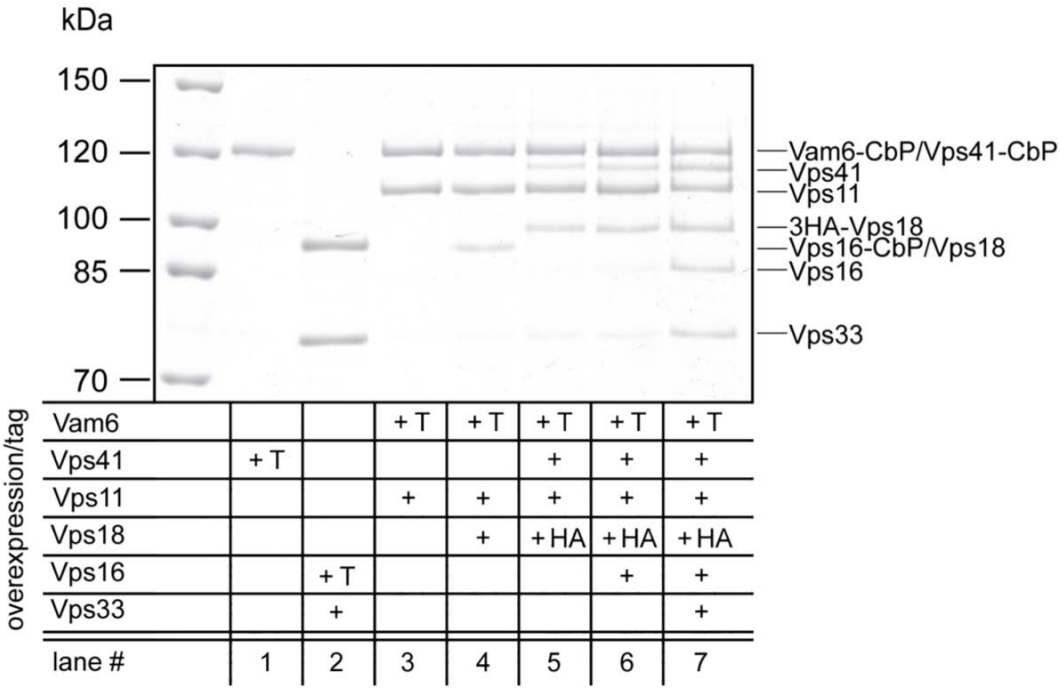

Figure 3.20 | **Co-overexpression of cognate subunits allows for purification of highly pure subcomplexes.** Strains harboring the indicated genomic alterations (compare **Table 3.3**) were purified using the Mini TAP protocol. Both purification steps were employed and the resulting final EGTA eluates were TCA-precipitated. Different amounts were loaded on a 7% SDS-PAGE gel to achieve comparable signals. The gel was stained using the linear Sypro Orange stain to allow for better comparison of signal strengths for different proteins.

Vps18 is co-overexpressed with Vam6 and Vps11 (**Fig. 3.20**, lane 4), a similar picture as in the *vps41* deletion background is observed (compare section 3.4.1), indicative of a mixed population, where only part of the Vps11-Vam6 complex binds Vps18. Also Vps41 only associates with a fraction of the total Vps11-Vam6 complex (**Fig. 3.20**, lane 5). Its co-overexpression does not alter the amount of bound Vps18 significantly and it appears that the two proteins interact in a similar ratio with the Vp11-Vam6 subcomplex. This finding either indicates that Vps41 binding to the HOPS complex is mediated by interactions with Vps18 alone or that its binding site is comprised of Vps18 and Vps11 together. Since no direct interaction between Vps41 and Vam6 was detectable in any of our essays before, we could exclude that Vam6 contributes substantially to Vps41 binding to the complex (see also discussion section 4.4). To further elucidate this, we assayed for Vps41 interactors in different overexpression backgrounds. Vps41 overproduction in the *GAL1*pr-*VAM6*-*VPS11* background did not lead to a trimeric subcomplex and co-overexpression of Vps18 and Vps41 did not yield a dimeric subcomplex, indicating that Vps41 does not exclusively bind to either C-Vps subunit.

The additional co-overexpression of Vps16 (**Fig. 3.20**, lane 6) does not lead to the formation of a pentameric subcomplex as it was observed for the *vps33* deletion strain (compare section 3.4.1). A possible explanation for this obvious difference could be that Vps16, if overproduced without its binding partner Vps33, forms aggregates that do not participate in the generic subcomplex assembly. One indication that further substantiates this idea is that a very small portion of Vps33 and Vps16 does associate to the Vps11-Vps18-Vam6-Vps41 subcomplex, which means that binding of Vps16 is restricted to the amount of available Vps33. If Vps16 is not overexpressed, it does not seem to be dependent on Vps33, most likely because its cytosolic concentration is much lower, which would prohibit its presumed aggregation. The Vps33 dependence of overexpressed Vps16 becomes even more apparent in the purification made from a strain co-overexpressing all six subunits of the HOPS complex. Here, all subunits are pulled down to a similar extent (**Fig. 3.20**, lane 7). Also the association of Vps18 and Vps41 are increased in this expression background. Hence, Vps16 and Vps33 seem to stabilize interactions of Vps18 and Vps41 with the complex. This notion is well supported by the deletion experiments, where the overall ratio of complex to single protein is reduced in the *vps33*Δ and *vps16*Δ strains (compare section 3.4.1 **Fig. 3.18** and **3.19** fractions 10/11 versus 13/14).

A substantial amount of information about the architecture of the HOPS complex could be obtained using the deletion and co-overexpression approach. To further strengthen the data and to rule out that secondary unspecific effects led to the observed results, I decided to further substantiate the data with Yeast-2-Hybrid analysis of selected binding partners (**Fig. 3.21**)

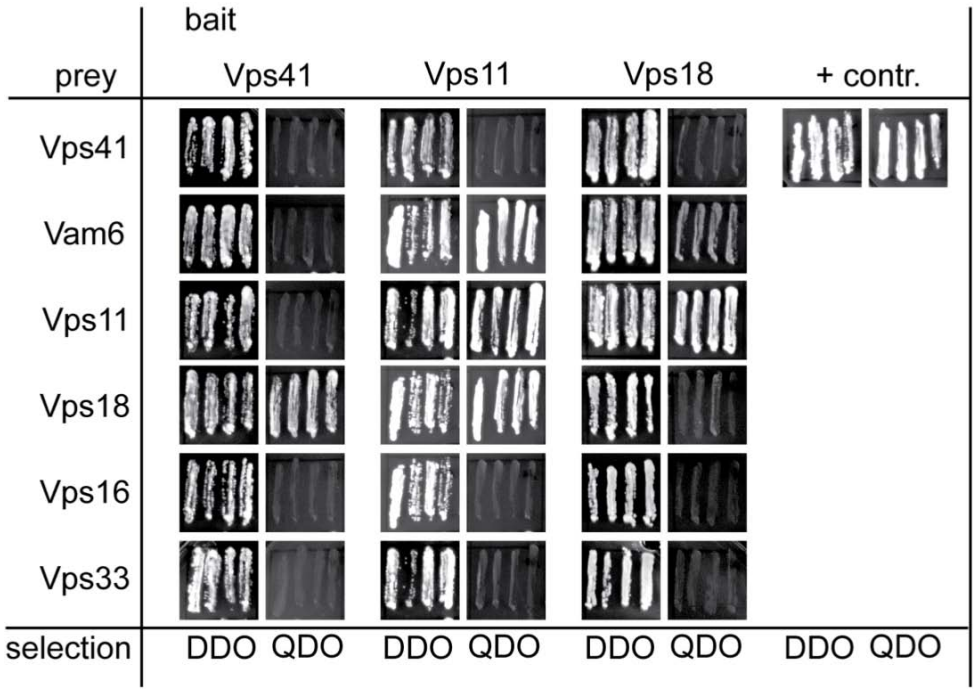

Figure 3.21 | **Yeast-2-Hybrid analysis of HOPS subunits ineractions.** Indicated protein sequences were cloned into the corresponding Yeast-2-Hybrid vector and yeast cell were transformed with two constructs each. Selection on a double drop-out (DDO) plate is employed to screen for positive transformants. Growth on a quadruple drop-out (QDO) plate can only be observed, if the proteins of interest interact.

The Yeast-2-Hybrid experiment yielded several interesting results. Vps41 does only show an interaction with Vps18 and no other HOPS subunit probed for. This finding does only partially match the results from my co-overexpression experiments, where Vps41 only interacted with subcomplexes containing both Vps11 and Vps18, just as if it depends on a binding platform, which consists of Vps11 and Vps18. Furthermore, in a strain overexpression both Vps41 and Vps18, no stable subcomplex was observed. However, considering the overexpression results from **Fig. 3.20**, it appears that Vps41 is only binding to the Vam6-Vps11-Vps18 subcomplex to the same extent as Vps18, indicating a that Vps41 might be able to bind Vps18 alone. The interaction between these two

proteins without Vps11 is most likely too weak to withstand the co-purification conditions and therfore becomes only visible in the Yeast-2-Hybrid approach.

Vps11 binds Vam6, Vps18 and itself. The Vam6 as well as the Vps18 binding is in good agreement with my previous results. The observed weak interaction of Vps18 with Vam6 could be due to small amounts of Vps11 entering the nucleus in complex with the prey Vam6, therefore bridging the two otherwise not interacting proteins. No interaction of Vps16 with any of the assayed HOPS subunits can be detected. This could indicate a similar binding characteristic to the proposed Vps11-Vps18 platform or be due to a false-negative result.

3.4.3 HOPS related subcomplexes are naturally occurring in vivo

The knowledge gained from the combined deletion and overproduction TAPurifications yielded intriguing insights into the architecture of the HOPS/CORVET complex. However, by these means, we were not able to answer, if these subcomplexes do also naturally occur in wild type cells. To address this crucial question and to substantiate my previous findings, I employed a TAP strategy called “subtraction method” (Puig et al., 2001). For this, I TAP-tagged Vam6 and additionally tagged Vps16 with a Protein A tag lacking a TEV-protease cleavage site in a wild type strain background. This allowed me to bind both proteins as well as their attached binding partners to IgG-Sepharose. The Vam6-TAP containing complexes that do not harbor Vps16-ProtA should be efficiently eluted off the column by TEV-protease treatment, whilst most of the Vps16-ProtA containing complexes (like the HOPS complex) were supposed to stick to the beads. If the Vps11-Vps18-Vam6 subcomplex was naturally occurring in the cell lysate, an enrichment of this subcomplex should be observed, whereas the full HOPS complex, which yields a dominant majority in the standard Vam6-TAP setup (compare **Fig. 3.17 B**), would be diminished. Indeed, we detected an enrichment of the three proteins both visible by the linear fluorescent Sypro Orange stain (**Fig. 3.22**) as well as Coomassie staining. It has to be noted that all six HOPS subunits are eluted off the column in this experiment. This most likely indicates, that either Vps16-ProtA binding to the IgG beads is not complete and/or that a part of the Vps16-ProtA-containing complex is co-eluting due to secondary effects like the increase in incubation temperature during TEV elution.

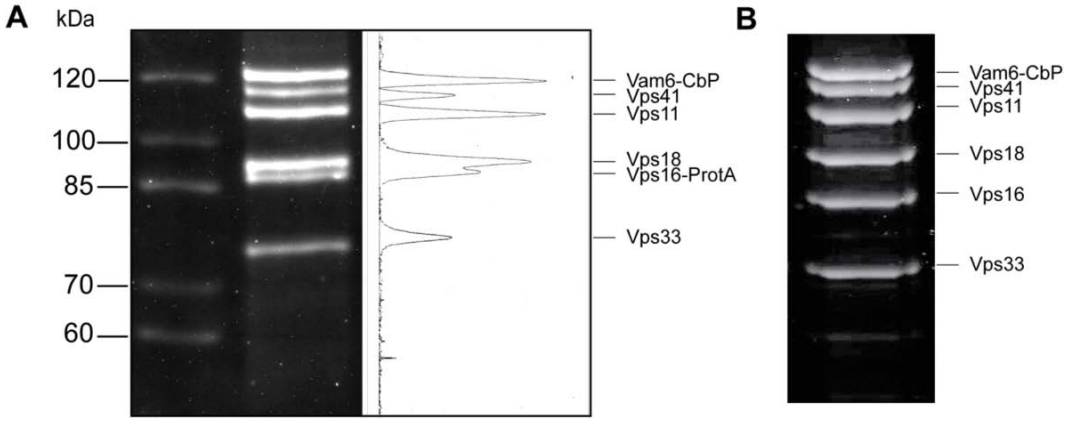

Figure 3.22 | **The Vam6-Vps11-Vps18 subcomplex naturally occurs in vivo. A** A full standard TAP experiment was performed with yeast cells harboring a Tap tagged version of Vam6 as well as a Protein A tagged version of Vps16. Note the different intensities measured for the fluorescence of the Sypro Orange stain, which reflects different amounts of the HOPS subunits in the gel (right side). **B** Control purification of Vam6-TAP without additional subunit tagging. Note that only Coomassie staining is shown here, but the difference in band intensities in **A** were also observed using Coomassie staining.

3.4.4 In vivo localization of overexpressed HOPS subunits

To further address the functionality of the subcomplexes, which formed by co-overexpression of cognate HOPS subunits, I tagged several subunits with a fluorescent GFP-tag in the respective strain backgrounds. The HOPS subunits usually localize to the vacuolar limiting membrane and especially the class C Vps proteins, which are also part of the CORVET complex are additionally found in dots close to the vacuole, most likely representing late endosomes (**Fig. 3.23**, Vps18pr-VPS18-GFP as an example for the other HOPS subunits). Upon overexpression of single subunits, I observed a striking accumulation of the protein in dot-like structures of different sizes and numbers that did not clearly co-localize with the vacuole as monitored using the membrane dye FM 4-64. Overexpressed Vps11-GFP localized for example primarily to a single or few large dots that were only in some cases observed close to the vacuole, whereas overproduced Vps18-GFP localized to several small dots that appeared to be located closer to the slightly fragmented vacuole (**Fig. 3.23**). Interestingly, Vps11-GFP is not accumulated anymore, if co-overexpressed with Vps18 (**Fig. 3.23** fourth panel from top). Overexpression of Vps11-GFP together with Vam6 leads to a high concentration of the

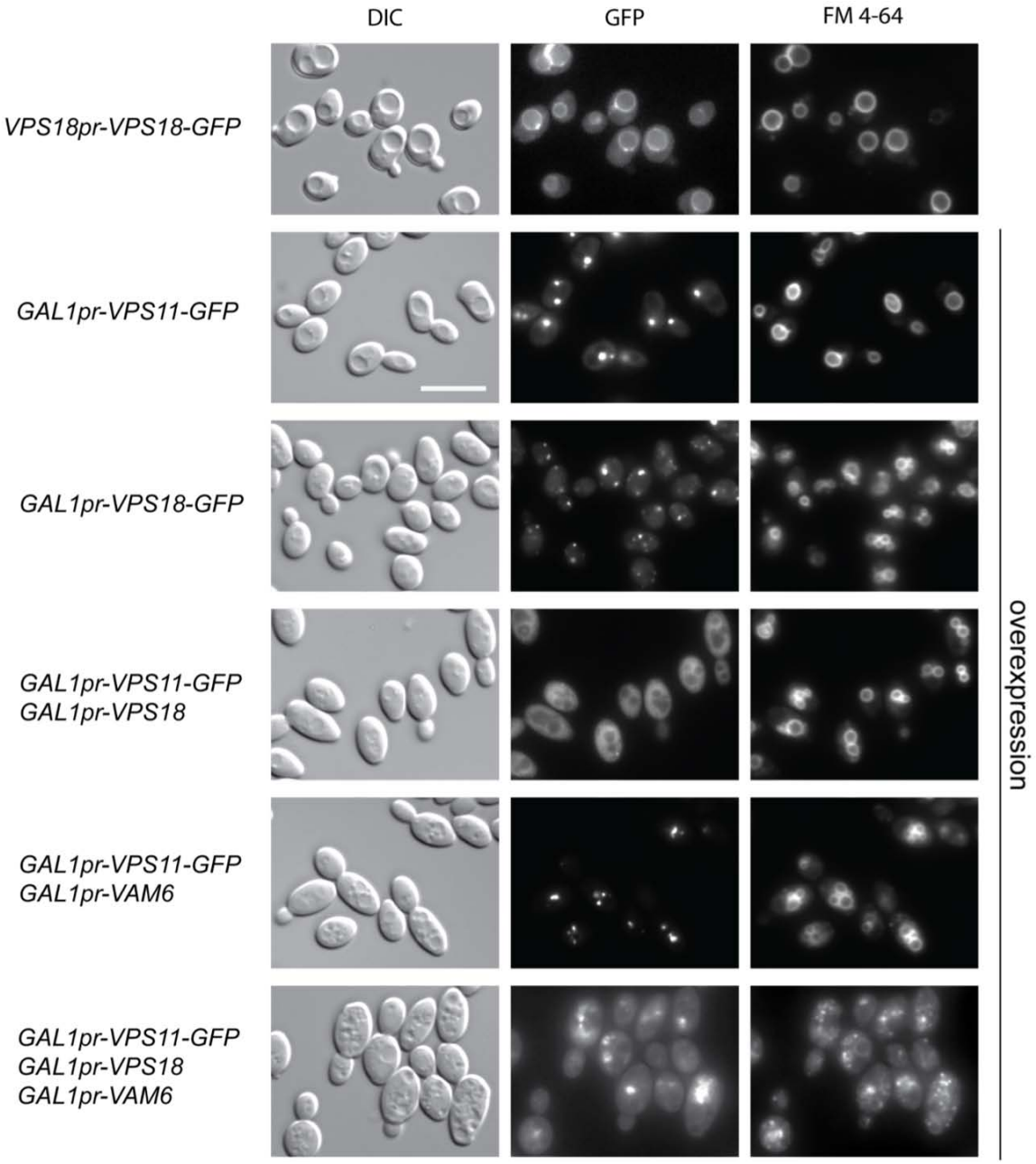

Figure 3.23 | **Localization of selected overexpressed HOPS subunits in different co-overexpression backgrounds.** In the top panel, an example of wild type localization of a HOPS subunit is depicted. Note the different localizations and vacuole fragmentation phenotypes dependent on the overexpression of different subunit combinations. Size bar: 10µm

GFP signal especially at vacuole-vacuole junctions as monitored with FM 4-64. Intriguingly, this phenotype is altered, if Vps18 is co-overexpressed on top. Vps11-GFP now localizes to the boundaries of compartments that are not dot-like, but appear like small vacuoles. As monitored by FM 4-64 staining, endocytic transport seems to be impaired, since the dye accumulates in small vesicles that are not overlapping with the

GFP-stained structures, most likely representing earlier endocytic compartments that are delayed in maturation. Although these results are not simply explained, I suggest that depending on the co-overexpression and therefore accumulation of single HOPS subunits or, more strikingly, HOPS subcomplexes, endocytic transport is delayed or maybe even stuck at different stages towards the vacuole.

3.4.5 In vitro reconstitution of HOPS complex assembly

The co-overexpression approach used above proved to be a powerful tool to identify and characterize stable subcomplexes. Since I was able to purify decent amounts of highly purified subcomplexes, I sought to re-capitulate HOPS complex assembly from subcomplexes, as I expected it to happen inside the cell as part of intracellular membrane trafficking (see discussion 4.4). However, all experiments in which I tried to assemble the holo-complex from purified subcomplexes failed. In these experiments, I employed the Mini-TAP protocol to produce EGTA eluates from a *GAL1pr-VPS41-TAP* and a *GAL1pr-3HA-VPS16-TAP GAL1pr-VPS33* strain. The eluates were then added to IgG-sepharose beads, which were previously incubated with a lysates from a *GAL1pr-VPS11 GAL1pr-VPS18 GAL1pr-VAM6-TAP* strain and washed afterwards. After incubation for 1-4 hours at different temperatures, the beads were washed and bound protein was eluted using TEV protease. Interestingly, I was not able to recover the HOPS complex, indicating that *in vitro* assembly was not feasible in this reaction setup. I consider three possible explanations for this unexpected finding. First, the EGTA contained in the Mini-TAP eluates does impair HOPS subunit interaction; this could be explained for example by the chelating activity of the EGTA towards the zinc ions, which are supposed to be bound to the RING domains of Vps11 and Vps18 (compare introduction, section 1.3.2.5). Second, it is possible that the subcomplexes need further factors to correctly assemble, which are not contained in the purified sample or, third and most unlikely, the subcomplexes are not capable of assembling *in vivo* and consequently do not do so *in vitro*, which would contradict my findings in section 3.4.3. Since the first possible reason could only be challenged by generating further differently tagged strains and the third possible reason did not appear very likely to me, I tried to assemble the complex in a more native, yet an *in vitro* environment first. I decided to bring the overexpressed subcomplexes together as early during the purification procedure as possible. In this experiment, I mixed intact cells of the different subunit/subcomplex overexpressing strains as indicated in **Fig. 3.24**

before glass bead mediated cell lysis and performed an IgG pull-down with the lysate (**Fig. 3.24** lanes C and C'). As controls, pull-downs using the lysates of unmixed cells were performed (**Fig. 3.24** lanes 1-3 and 4-6). Furthermore, to address the question, when the subcomplexes loose their ability to assemble, I carried out a pull-down with a lysate mixture that was produced by mixing lysates from the three employed strains directly after the first pre-clearing step of the single lysates after a 20,000xg centrifugation step (**Fig. 3.24 lanes** L and L').

Indeed, the TEV eluate from the Vam6-TAP bound IgG beads does contain the HA-tagged Version of Vps16, which was contributed from the cell pool that did not contain a TAP tag. This indicates that the observed interaction formed during cell lysis or

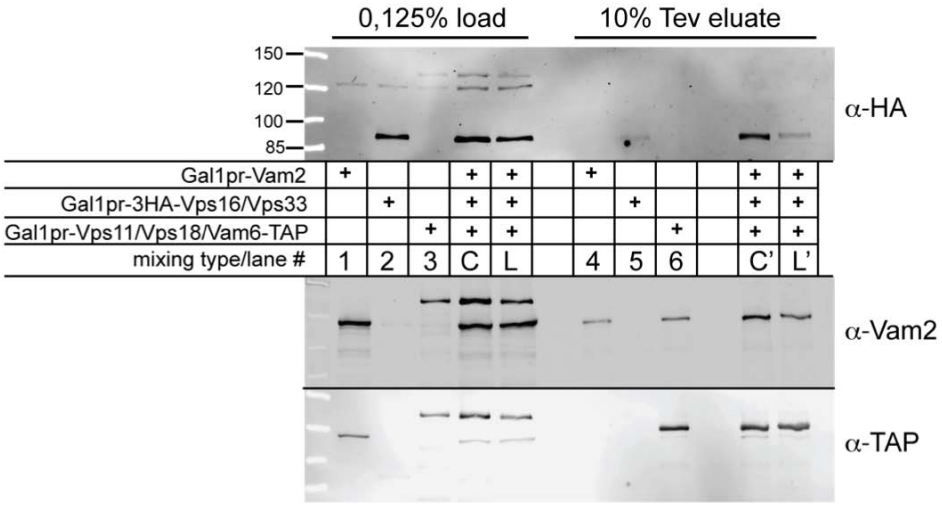

Figure 3.24 | **In vitro HOPS complex assembly**. HOPS subcomplexes do only efficiently assemble into the holo complex, if they are mixed during cell lysis and not upon mixture of pre-cleared lysates. IgG-sepharose pull-downs were performed as in the Mini-TAP protocol and the TEV eluate was loaded onto an SDS-PAGE gel. Western blotting was carried out and the membrane was decorated with the indicated antibodies. Detected protein bands were visualized using fluorescently labeled secondary antibodies and the Odyssey system.

the incubation (**Fig. 3.24** a-HA decoration, upper panel C'). Intriguingly, the amount of 3HA-Vps16 that was co-eluting in the lysates mixture sample (**Fig. 3.24** a-HA decoration, upper panel L') was strongly reduced compared to the cell mixture eluate and did almost match the weak signal of the background of 3HA-Vps16 that bound to the beads without Vam6-TAP (**Fig. 3.24** lane 5), although similar amounts of Vam6-CbP were eluted from the column (**Fig. 3.24** a-TAP decoration, lowest panel compare C' and L'). I concluded that the whole complex assembles in the reaction setup, since also the

amount of Vps41 is enhanced in the cell mixture pull-down compared to the lysates mixing approach (**Fig. 3.24** lanes L and L', a-Vam2, lower panel). Unfortunately, Vps41 unspecifically binds to the IgG-sepharose without a TAP tag (**Fig. 3.24** lane 4) and is also existent in low quantities in the Vam6-TAP eluate, since trace amounts of HOPS complex are co-purified (**Fig. 3.24** lane 6). However, the signal observed for Vps41 in the cell mixture eluate is higher than in the lysates mixture approach or in the controls (compare **Fig. 3.24** lane C' with L' and lanes 4 and 6).

These results strongly suggest, that a factor, which is either inactivated or not extracted from membranes during cell lysis with the detergent containing lysis buffer promotes the assembly of the subcomplexes into the HOPS complex. Alternatively, intracellular membranes themselves or a lipid factor are needed for efficient assembly, but get separated from subcomplexes during prolonged lysis and centrifugation. Further experiments are currently underway to determine the nature of this proposed factor. A first experiment, where recombinant GST-Ypt7 was added to a HOPS reconstitution mixture did not suggest an involvement of the vacuolar Rab protein in this process.

3.5 Functional characterization of HOPS subunits and subcomplexes

3.5.1 Vps41 and Vam6 differentially interact with the vacuolar Rab GTPase Ypt7

In a previous publication (Wurmser et al., 2000), the HOPS subunit Vam6 has been shown to act as a guanyl nucleotide exchange factor (GEF) for the yeast late endosomal/vacuolar Rab protein Ypt7. Moreover, Vps41 as the second HOPS specific subunit (i.e. not being part of the CORVET complex) has very recently been shown to interact with Ypt7 in a different manner than Vam6 (Brett et al., 2008). We therefore asked, if Vps41 is the only Ypt7 interacting subunit beside Vam6 and if it could be assigned to functioning as the subunit, which is mediating Rab-effector properties to the assembled HOPS complex.

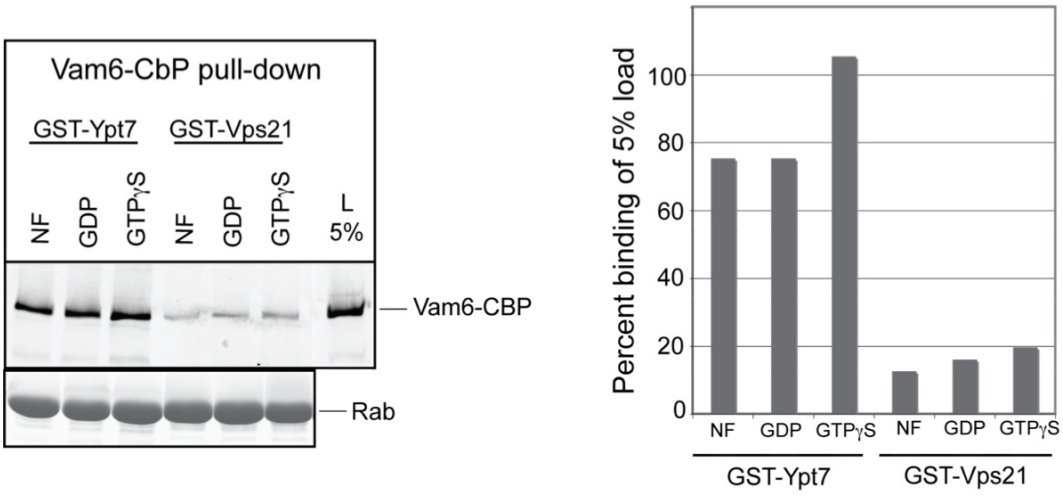

Figure 3.25 | **Rab pull-down of purified Vam6 reveals its affinity for Ypt7.** Purified Vam6-CbP was subjected to a Rab pull-down experiment using Ypt7 and Vps21 as a control. Vam6 specifically binds Ypt7 and exhibits a promiscuous binding pattern to all nucleotide states. L=load, NF=nucleotide free.

Considering our results from section 3.4.1, we were most cautious in interpreting experimental data retrieved from HOPS subunit deletion strains. Therefore, I employed different overproduced and purified HOPS subunits to perform pull-down experiments with recombinantly produced GST-tagged Rab proteins to assess their Rab binding properties. The GTPases were stripped of all nucleotides and either kept nucleotide free or loaded with GDP or the non-hydrolyzable GTP analog GTPγS to mimic the inactive or active state of the Rab protein, respectively. GST-Vps21 or GST-Ypt1, as indicated, were used as controls and were treated just as GST-Ypt7. First, we performed a Rab pull-down experiment with Vam6-CbP from a *GAL1*-overexpression strain, lacking stoichiometric amounts of the other HOPS subunits (**Fig. 3.25**). Indeed, we can report on a protein specific interaction of Ypt7 with Vam6-CbP alone. In our Rab-pull-down experiment, we observe relatively equal binding of single Vam6 to all three nucleotide-binding states of Ypt7. This is in agreement with Y2H data from previous publications (Wurmser et al., 2000) and my own Yeast-2-Hybrid experiments (**Fig. 3.26**). In contrast to this, our finding differs from one pull-down experiment previously published, showing interaction only with the GDP-form of Ypt7 (Wurmser et al., 2000). Nevertheless, my results are in accord with several previous studies concerning the interaction of other GEFs with their respective GTPase (Bos et al., 2007). Moreover, for two other described Rab-GEFs the observed binding pattern appears to be differing from each other, indicating that the Rab-

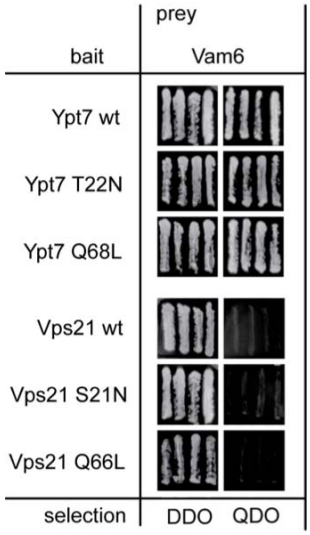

Figure 3.26 | **Vam6 interacts with all Ypt7 variants in the Yeast-2-Hybrid system.** Indicated protein sequences were cloned into the corresponding Yeast-2-Hybrid vector and yeast cell were transformed with two constructs each. Selection on a double drop-out (DDO) plate is employed to screen for positive transformants. Growth on a quadruple drop-out (QDO) plate can only be observed, if the proteins of interest interact.

GEF proteins can function in a variety of binding modes (Hama et al., 1999; Walch-Solimena et al., 1997).

A different result was obtained in the Vps41 Rab-pull-down experiment. In this case, Vps41-CbP was mainly pulled down by GST-Ypt7 in the GTPγS bound form whereas a weak signal was detected for the nucleotide-free form of GST-Ypt7 (**Fig.**

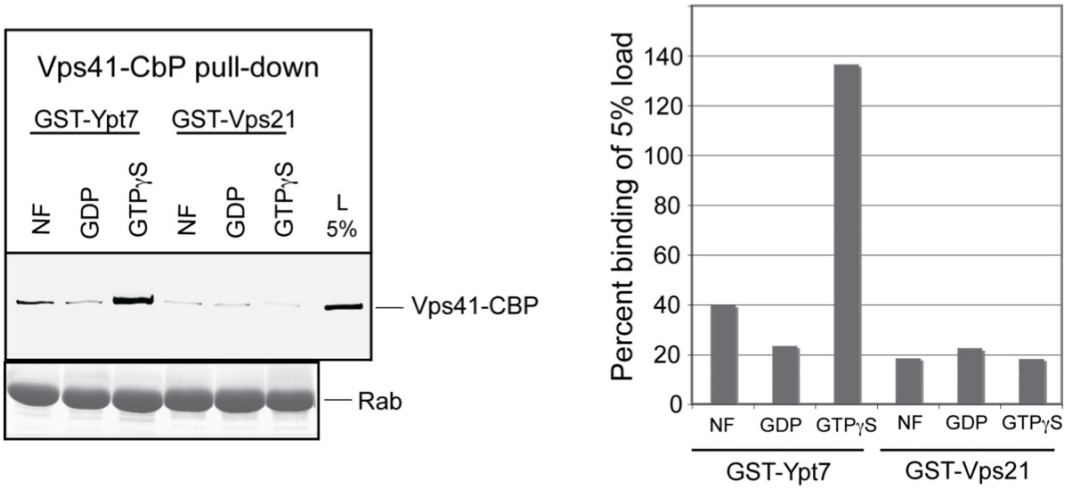

Figure 3.27 | **Vps41 preferentially interacts with the active, GTP-form of Ypt7.** Purified Vps41-CbP was subjected to a Rab pull-down experiment using Ypt7 and Vps21 as a control. Vps41-CbP specifically binds to GTP-Ypt7, suggesting that it functions as the Rab-effector subunit in the HOPS complex. L=load, NF=nucleotide free.

3.27). The interaction of Vps41 with the GDP-bound form of Ypt7 was as low as the background levels, which were detected for the interaction with the other unspecific Rab GTPases. This finding clearly designates Vps41 as a Rab GTPase effector for Ypt7, which is supposed to specifically interact with the activated form, and to exhibit a markedly low affinity for the GDP-bound, inactive form of the Rab protein.

3.5.2 The HOPS complex interacts with Ypt7 via Vps41 alone

I wondered, if the reported interaction of the vacuolar Rab Ypt7 with the HOPS complex was reflecting the same way of interaction that I observed for Vam6 and Vps41. For this purpose, nucleotide specific Rab pull-downs with purified HOPS complex were conducted (**Fig. 3.28**). Intriguingly, I detected strong HOPS interaction with the GTP-form and a weaker interaction with the nucleotide free form of Ypt7, which exactly reflects my findings for Vps41 alone (compare **Fig. 3.25**).

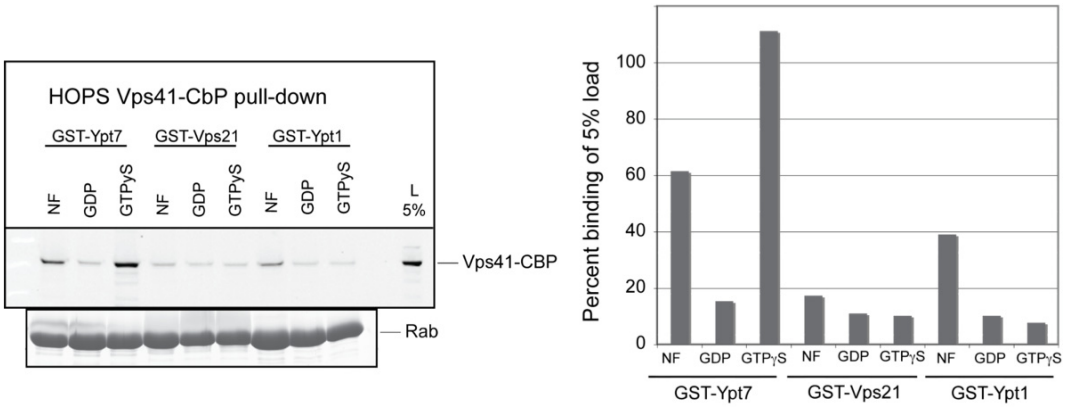

Figure 3.28 | **Purified HOPS complex exhibits the same Ypt7 variant specificity as Vps41.** The HOPS complex exhibits the same binding pattern to Rab proteins as its subunit Vps41. No interaction could be measured to the control Rabs Vps21 or Ypt1. L=load, NF=nucleotide free.

I wondered, why no interaction with the GDP-bound form was detectable, as it has been observed for Vam6 (compare **Fig. 3.25**). I reasoned that either Vam6 binding to Ypt7 was too weak to be detected, compared to the strong Vps41-Ypt7 interaction, or that Vam6 loses its capability to bind Ypt7 in the assembled HOPS complex. To test this, I took advantage of our knowledge of stable subcomplexes and subjected purified Vam6-Vps11 complex to the Rab pull-down assay. Indeed, Vam6-Vps11 binding to any form of Ypt7 was strongly reduced down to background levels (**Fig. 3.29**). Moreover, if I purified

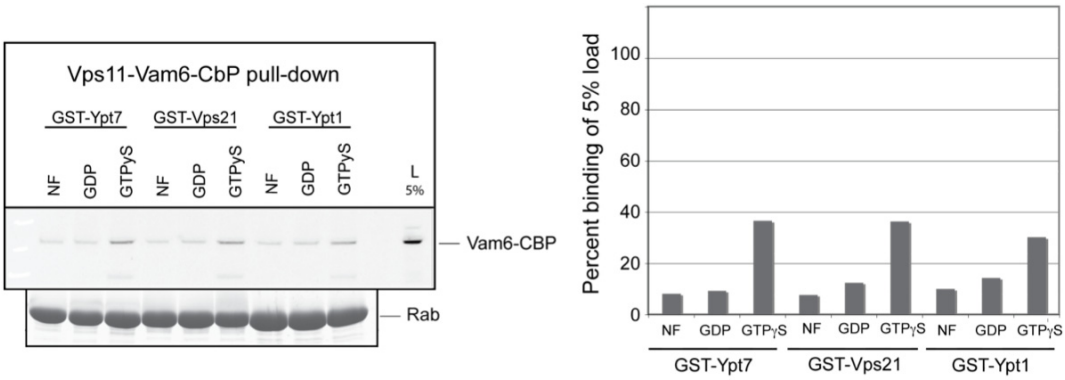

Figure 3.29 | **Vam6 does not bind to Ypt7, if it is in a complex with Vps11.** Binding to Ypt7 of Vam6 that is in complex with Vps11 is reduced to background levels. L=load, NF=nucleotide free.

HOPS complex via Vam6-TAP instead of Vps41-TAP and subjected the complex to a Rab pull-down experiment, Vam6-CbP as a member of the complex exhibits the exact

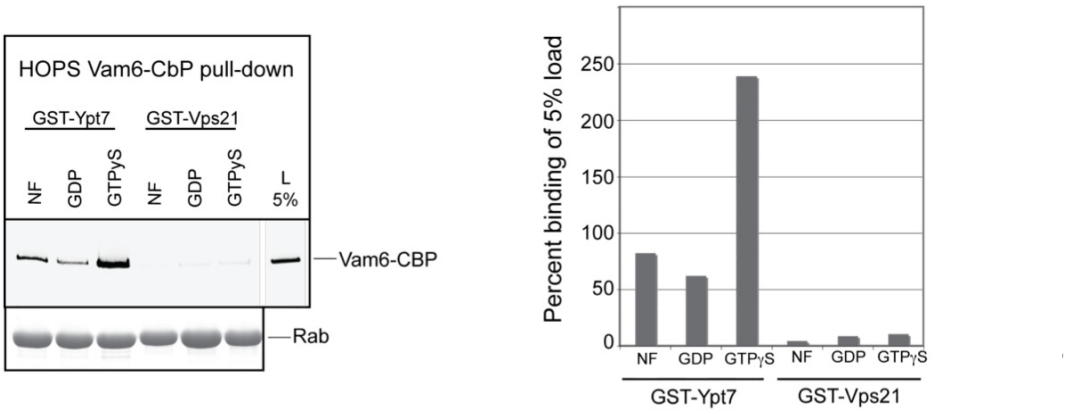

Figure 3.30 | **Vam6 loses its affinity for Ypt7 also if part of the HOPS complex.** Vam6 that is part of the HOPS complex interacts with Ypt7 in the same way as Vps41, suggesting that its ability to act as a GEF for this Rab is abolished as soon as it gets incorporated into the complex. L=load, NF=nucleotide free.

binding characteristics of Vps41 (**Fig. 3.30**). This clearly indicates, that Vam6, if bound to the HOPS complex, is not capable of interacting with Ypt7 by itself any more. In the study by Wurmser *et al*. (Wurmser et al., 2000) it was demonstrated that Vam6 exhibits GEF activity in a vps11Δ background. Therefore, I conclude that Vam6 functions as a GEF as a single protein only and is attenuated in its activity, as soon as it is incorporated into a complex with Vps11 at any level of complexity (i.e. in the Vps11-Vam6, Vps18-

Vps11-Vam6- or the HOPS complex). Our pull-down experiments reveal that the binding of the HOPS complex to Ypt7 is exclusively based on its activity as an effector for this Rab protein. Furthermore, I could now show that this activity entirely depends on its subunit Vps41.

4 Discussion

The results of my thesis work give new substantial insights into the regulation of the HOPS complex by Vps41 phosphorylation, the architecture of the HOPS tethering complex and its subcomplexes. The identification of the novel CORVET tethering complex and the corresponding intermediate complexes filled a gap in our knowledge about endolysosomal tethering and supports previous reports on the mechanism of endosomal maturation upstream of fusion with the vacuole.

4.1 Regulation of the HOPS tethering complex by Vps41 phosphorylation

In a study by Tracy LaGrassa in our lab, it was demonstrated that Vps41 is a substrate for the vacuolar casein kinase Yck3. She was able to show that Vps41 phosphorylation has an influence on the tethering activity of the HOPS complex by employing a hyperosmotic stress experiment (LaGrassa and Ungermann, 2005). To rule out secondary effects of other Yck3 targets in this process and to be able to investigate the effects of Vps41 phosphorylation on the activity of the HOPS complex in more detail, I identified the phosphorylation sites within the protein's sequence (see section 3.1.1). Further experiments that were conducted by my colleague Dr. Margarita Cabrera revealed that an unphosphorylated mutant of Vps41 (Vps41 S-A) concentrates together with the other HOPS subunits at endosome-vacuole fusion sites. Moreover, endosomal structures accumulate at this site, suggesting that fusion activity is altered due to impaired phosphorylation of Vps41 S-A. A phosphomimetic Vps41 mutant (Vps41 S-D) exhibited a contrasting phenotype with a more cytosolic distribution of Vps41 S-D and no sites of accumulation on the vacuolar rim of Vps41 S-D or the other HOPS subunits. Interestingly, the HOPS complex was still assembled in both the unphosphorylated and the phosphomimetic mutant strains (Cabrera et al., 2009). Furthermore, the phosphorylation-independent binding of Vps41 to the active form of the vacuolar Rab GTPase, which I was able to characterize in my studies, allows for a partial rescue of Vps41 S-D localization and enhances the phenotype observed for the unphosphorylated

mutant if high levels of Ypt7 are provided (Cabrera et al., 2009). This suggests, that Vps41 and hence HOPS complex localization and activity are dependent on both Ypt7 and Yck3 phosphorylation activity.

Since Vps41 is needed for AP-3 vesicle formation at the trans Golgi (Darsow et al., 2001; Rehling et al., 1999), the influence of Vps41 phosphorylation on this specific step was investigated. We found that AP-3 cargo transport is impaired in the Vps41 S-A mutant background, which is in good agreement with a reduced mobility of this Vps41 variant (Cabrera et al., 2009). Moreover, this finding implies a positive feedback regulation: Yck3 is transported via the AP-3 pathway and releases Vps41 after it reached the vacuole, therefore allowing it to fulfill its function during AP-3 vesicle formation.

An interesting finding of Bruno Antonny and co-workers sheds light on a possible mechanism of how Vps41 phosphorylation alters its membrane association. In a previous study (Drin et al., 2007), Vps41 was found among other proteins to contain an ALPS-like motif, which can form amphipathic helices that can dip into membranes in a reversible manner and preferentially expose Serine and Threonine residues on the polar surface of the helix. Intriguingly, the ALPS-like motif was predicted to be exactly located at the phosphorylation site identified by me. These findings imply that the mode by which unphosphorylated Vps41 binds to the membrane is by the insertion of an amphipathic helix into the lipid bilayer, a feature that seems to be inhibited by the phosphorylation of the hydrophilic face of the amphipathic helix (Cabrera *et al.*, in preparation).

It is possible that the above-mentioned findings could serve as a general model of how reversible membrane association of proteins can be achieved by site-specific phosphorylation. Since the ALPS motif identified by the Antonny lab always contains Serine and Threonine residues on the polar surface of the amphipathic helix, it appears likely that membrane binding of several other proteins that have been found to contain such a motif could be regulated by yet unidentified phosphorylation events. Our lab is currently following up on this idea by investigating the properties of an ALPS-like sequence in the Vps41 homolog CORVET subunit Vps8. Also the fusion factor Mon1, which I identified as another target of Yck3 activity could be regulated in a similar way, although no ALPS-like motif was yet identified in its amino acid sequence.

4.2 Structural analysis of the HOPS complex

The HOPS complex remained the structurally least characterized tethering complex in the past. Recombinant expression of the subunits was in most cases not feasible due to their high molecular weight and the tendency to aggregate (Dr. Alexey Rak, now Sanofi-Aventis, Paris, personal communication; my own observations). However, these are only some of the features that make the HOPS complex appear quite unique among tethering complexes, and that raised my interest in identifying the structural properties of this very complex.

A substantial amount of time and effort during my thesis work was spent on experiments aiming for the crystallization of single HOPS subunits and the electron microscopic analysis with the complete complex. In preparing the overexpression strains, establishing the purification routine and screening the optimal purification conditions, I was able to pave the ground for current EM experiments with promising results (see section 3.2.2.3). First negative stain electron microscopy pictures are available and the next experiments employing electron tomography should yield even better data, which could finally serve for a refined modeling of the overall complex structure. This structure might give insights into a possible working mode of the complex during tethering. The structures of other tethering factors have been analyzed before (Kim et al., 2006; Kümmel and Heinemann, 2008; Tripathi et al., 2009) (see section 1.3.2) and it will be most interesting, if the HOPS complex structure is in line with these or if it might exhibit a yet unique architecture.

First crystallization trials conducted with the purified HOPS subunit Vps41 were not successful. However, additional crystallization conditions will be tested in further trials to succeed in the analysis of subunits of the HOPS complex. Next to the purification from yeast, fragments of the different subunits are currently recombinantly produced in *E. coli* by my successor colleague Cornelia Bröcker. Together with the knowledge obtained about the interactions between different HOPS subunits in this thesis work, it appears feasible to also co-overexpress cognate subunits or interacting fragments in a bicistronic approach in *E. coli* (see section 3.2.1.1), which might allow for an enhanced purification yield.

4.3 Identification of the novel CORVET complex and intermediate complexes

Together with my colleague Dr. Karolina Peplowska, I was able to identify a novel protein complex with homology to the vacuolar HOPS tethering complex. The existence of this complex and its functioning at the later endosomal compartments is in good agreement with previous studies. The complex interacts with the endosomal Rab GTPase Vps21 (Rab5 homolog) and the Vam6 homolog Vps3 is proposed to act as a guanyl nucleotide exchange factor for Vps21, two findings that stress the similarity also to the functional characteristics of the HOPS complex (Peplowska et al., 2007) (see below).

Interestingly, next to these two complexes, we could identify two additional "intermediate" complexes, that contain one of the complex specific subunits (i.e. Vps3

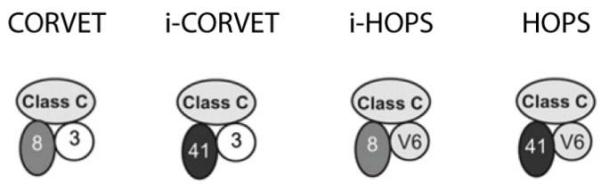

Figure 4.1 | **The different novel complexes identified in this study.** Adapted from Ref. (Peplowska et al., 2007).

and Vps8 for CORVET, Vam6 and Vps41 for HOPS) together with one specific subunit of the other complex (**Fig. 4.1**).

Previous results by Rink *et al.* (Rink et al., 2005) showed that maturation of single endosomes in mammalian cells from an earlier to the late stage was accompanied by an exchange of the Rab GTPase Rab5 for the Ypt7 homolog Rab7 on the endosomal surface. Together with our new data, these findings imply that this Rab exchange depends on or promotes the conversion of tethering complexes during endosomal maturation (**Fig. 4.2**).

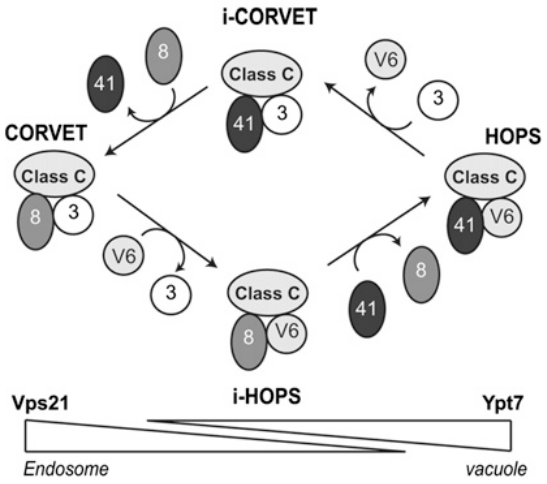

Figure 4.2 | **A possible mode of tethering complex conversion linked to endolysosomal maturation.** Since the endosomal CORVET complex and the vacuolar HOPS complex appear to be linked by the intermediate complexes, it appears likely that they are converted into each other upon endolysosomal maturation events. Figure extracted from Ref. (Peplowska et al., 2007).

However, the identification of stable HOPS subcomplexes and the finding that a *vps41* deletion leads to a trimeric complex consisting of Vam6, Vps11 and Vps18 and not to the formation of the iHOPS complex challenge this model. Although the experiments that identified the iHOPS complex are solid and show the existence of small amounts of this intermediate complex (see section 3.3.3) in wild type cells, the question arises, to which extent such a complex could be involved in the turnover of physiological amounts of tethering complexes (as proposed in **Fig. 4.2**). Especially the fact that the conversion from CORVET on endosomes to HOPS on very late endosomes, a process that should be vigorously happening during endosomal maturation, would rely on this very low abundant intermediate complex raises further doubt. In this regard, my results can be best interpreted, if one would assume that this conversion is happening extremely rapid. Still, iHOPS would have to be very instable to explain, why it could not be detected in a *vps41* deletion background. In fact, my findings about stable subcomplexes suggest a much more dynamic model, were tethering could be mediated by assembling cognate subcomplexes into the HOPS complex, a mode of function that was shown for the exocyst tethering complex (Boyd et al., 2004) and that would as well apply for the CORVET complex. I will further discuss these ideas in the next section.

Considering the model of tether conversion (**Fig. 4.2**), one of the major questions for future experiments is the identification of factors that regulate the maturation events. Since endosomes harbor ubiquitinylated cargo on their surface, which is destined for invagination by the action of ESCRT complexes at the stage of MVB formation, it could be that the enrichment of such cargo on the surface membrane could serve as a trigger for endosomal maturation events.

4.4 Identification of stable subcomplexes and functional characterization of HOPS subunits

Although single HOPS subunits have been show to act upstream of the vacuole in the AP-3 pathway (Vps41) and the CPY pathway (class C-Vps proteins), the finding that the four class-C-Vps proteins function together with Vam6 and Vps41 in the HOPS complex somehow halted the investigation of single subunits in the scientific community. The HOPS tethering complex has therefore been looked upon as a rather static entity residing on the vacuolar membrane to allow for homo- and heterotypic fusion events at the vacuole (Collins et al., 2005; Starai et al., 2008; Stroupe et al., 2006). One aim of my thesis work was to investigate the interactions taking place between different HOPS subunits, which allows the assembly into the holo complex. The striking finding that the deletion of *vps41* leads to the disassembly of the complex into stable subcomplexes, led me to perform additional experiments to reveal further stable subcomplexes. Due to these experiments, I was able to draw a picture of the subunits' interactions taking place in the fully assembled complex (**Fig. 4.3**). In employing a special variant of the TAP technique, I was furthermore able to provide evidence that at least one of the identified subcomplexes (Vam6-Vps11-Vps18) naturally occurs *in vivo* (see section 3.4.3).

These results next to the above-mentioned insights into the connectivity of the CORVET and the HOPS tethering complexes lead me to propose a more dynamic functioning of these two tethers. The exocyst complex, which tethers exocytic vesicles to the plasma membrane, has been shown in several studies to be sequentially assembled during the process of vesicle tethering (Boyd et al., 2004; Munson and Novick, 2006). Similar to the mechanism of *trans*-SNARE formation, the assembled complex only marks the end point of a series of events that are all needed to perform the task of membrane fusion. Our exciting finding about the mechanism of HOPS regulation via the Yck3-

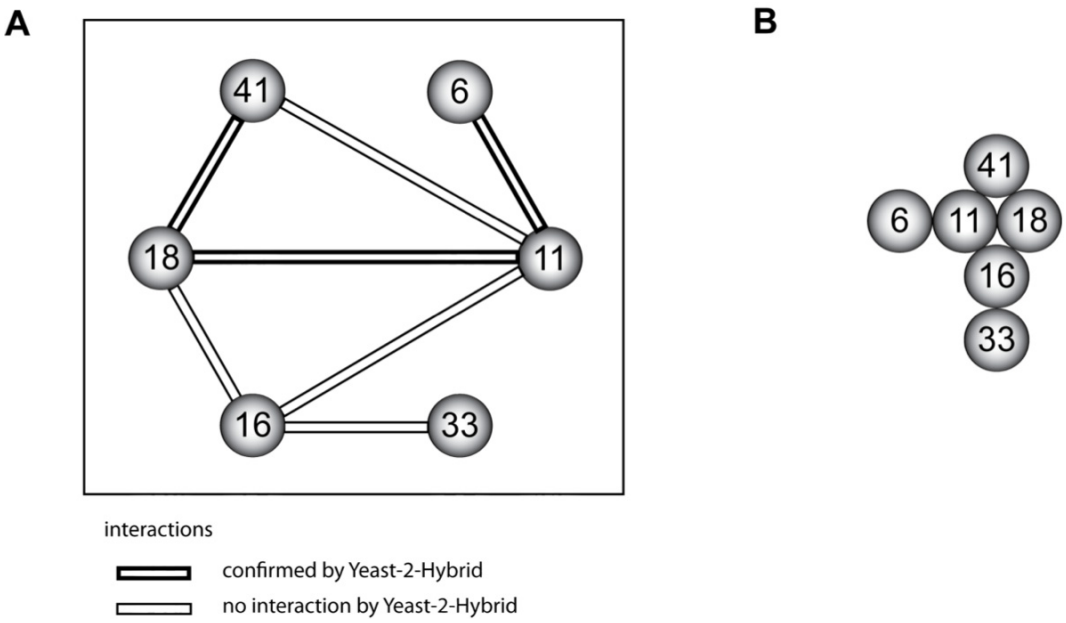

Figure 4.3 | **Interactions between different HOPS subunit as reported in this study. A** interactions that were observed in this thesis work are depicted by double lines. Interactions that were confirmed by Yeast-2-Hybrid analysis are depicted by bold lines. Note that the two subunits Vps16 and Vps41 appear to bind to a platform made of Vps11 and Vps18 together, not to the single proteins. **B** Model of how the subunits could be arranged in the fully assembled HOPS complex base on this thesis work.

dependent phosphorylation of Vps41 could help to understand how the complexes subunits could be made available again after complete assembly.

The idea of a sequential functioning of the HOPS subunits and their subcomplexes is further supported by my finding, that the Ypt7-GEF Vam6 loses its ability to interact with this Rab protein upon binding to its sole binding partner in the HOPS complex,

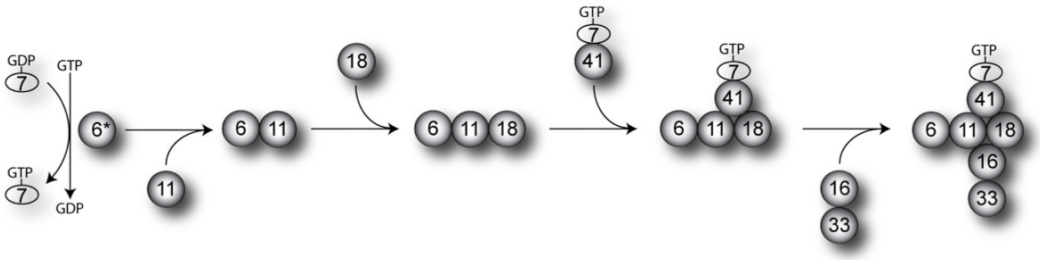

Figure 4.4 | **A Possible mode of sequential assembly of the HOPS tethering complex.** Vam6* is active as a GEF for Ypt7, most likely at the late endosomal membrane, but loses this activity upon binding of Vps11. The other subunits/subcomplexes that might be involved in yet unidentified reactions bind sequentially. Vps41 is recruited to Ypt7-GTP positive membranes and could serve as a dock for the other subcomplexes (compare to Sec3 function in the exocyst, section 1.3.2.4) thereby spatially limiting sites of HOPS complex formation.

Vps11. Hence, the assembled HOPS complex cannot act as GEF for Ypt7 as it has been taken for granted in the past. The subunit Vps41, which I could identify as the only Rab effector subunit of the HOPS complex, could serve as an adaptor, which would bind to Ypt7-GTP-positive membranes, while assembling into the complete HOPS complex during the tethering event (**Fig. 4.4**). By these means, the site of assembly and thereby tethering could be spatially restricted, since only membranes harboring Ypt7-GTP on their surface would be recognized. To substantiate this idea, several future experiments have to be performed, which address the functionality and site of action of the HOPS subcomplexes *in vivo* and identify the factor that promotes HOPS complex assembly during cell lysis *in vitro* (compare section 3.4.5).

4.5 Conclusion

In sum, the data provided in my thesis work provide valuable data for expanding our knowledge about tethering in the endolysosomal system and the architecture and dynamics of the complexes, which are involved in this process. Based on my work on the overexpression and efficient purification of the HOPS complex and its subunits, further structural information will hopefully be accessible in the near future. In combination with my results on the interaction network of HOPS subunits, these data could help clarifying our picture of tethering at the yeast vacuole and yield substantial insights into the process of tethering *per se*.

5 Materials and Methods

5.1 Chemicals and Reagents

Chemicals were purchased from the Sigma-Aldrich Chemie GmbH (Munich, Germany) and Carl Roth (Karlsruhe, Germany) if not differently indicated. All Products used for Molecular cloning, i.e. polymerases, restriction enzymes and accessory products were obtained from Fermentas (St. Leon-Rot, Germany) and NEB (Frankfurt a.M., Germany). Primers were ordered from Thermo-Fisher Scientific (Ulm, Germany). Reagents used for production of media and plates were obtained from MP-Biomedicals (Heidelberg, Germany) and Applichem (Darmstadt, Germany). All plasticware as reaction tubes and pipette tips were acquired from Sarsted (Nümbrecht, Germany). Cultivation flasks and other glassware was provided by VWR (Darmstadt, Germany).

5.2 Yeast and bacteria culture

5.2.1 Media

For yeast cultures, the following media were utilized:

5.2.1.1 Complex media

Yeast Extract Peptone Dextrose (D-Glucose) (YPD) for standard yeast culture. For 1l medium, 10g yeast extract, 20g peptone and 20g D-Glucose were dissolved in 1l ultrapure water and the pH was adjusted to 5.5 using 1M HCl.

Yeast Extract Peptone Galactose (YPG) for yeast culture of Gal1pr-overexpressor strains. For 1l medium, 10g yeast extract, 20g peptone and 20g D-Galactose were dissolved in 1l ultrapure water and the pH was adjusted to 5.5 using 1M HCl.

For the production of plates, 15g Agar were added per liter medium before autoclaving.

YPD and YPG were supplemented with antibiotics, if necessary. For a list of antibiotics and working concentrations, see below.

5.2.1.2 Synthetic media

Synthetic Dextrose complete drop-out medium (SDC-X) for selecting strains harboring a plasmid- or genomically encoded auxotrophy marker (e.g. after transformation). For 1l medium, 6.75g yeast nitrogen base w/o amino acids, 20g D-Glucose and ca. 0,75 complete supplement media lacking the specific marker metabolite (CSM, exact amount depends on the drop-out medium used) were dissolved in 1l ultrapure water and the pH was adjusted to 5.5 using 1M NaOH

For E. coli cultures, lysogeny broth (LB) (BERTANI, 1951) medium was used, supplemented with the antibiotic of choice. For 1l medium, 5g yeast extract, 10g tryptone and 10g NaCl were dissolved in 1l ultrapure water and the pH was adjusted to 7 using 1M HCl.

5.2.2 Antibiotics

The following antibiotics were used in yeast or bacterial cultures in the indicated concentrations:

Ampicillin	100µg/ml
Chloramphenicol	30µg/ml
Geneticin (G418)	200µg/ml
Hygromycin B	300µg/ml
Kanamycin	35µg/ml
Nourseothricin (ClonNat)	100µg/ml

5.2.3 Yeast and bacteria culture

Yeast and bacteria liquid cultures were incubated at 30°C or 37°C, respectively. In both cases, the cultivation flasks or tubes were put on an Innova shaker (New Brunswick

Scientific, Edison, NJ, U.S.A.) set to a rotation of 180rpm. For cultures up to 2ml volume, a benchtop Thermo-Shaker (Eppendorf, Hamburg, Germany) was employed.

5.2.4 Generation of strains

Genetic manipulation of strains was performed genomically by homologous recombination of PCR products, if not indicated differently. C-terminal TAP tagging (Rigaut et al., 1999) was performed with the use of three different template plasmids using either the URA3-, TRP1- (Puig et al., 2001) or KanMX4- (Janke et al., 2004) resistance marker. Primers were designed according to the respective references.

Yeast-2-Hybrid analyses were performed using plasmid pACT2 and pFBT9 (derived from pGBT9, both Clontech labs, Mountain View, CA, U.S.A.; provided by Dr. Francis Barr, University of Liverpool, UK). Open reading frames were amplified from purified genomic DNA from strain BY4741 and ligated into pACT2 or pFBT9 after restriction digest with BamHI and XhoI or BamHI and SalI, respectively. Mutated versions of Rab genes were generated using a site-directed-mutagenesis kit (Quick-Change kit, Stratagene, La Jolla, CA, U.S.A.).

5.3 Biochemical assays

5.3.1 TCA precipitation

For denaturing precipitation of proteins, samples were supplemented with 100% TCA solution to a final concentration of 13%, mixed and incubated for 10 minutes on ice. Samples containing no detergent were supplemented with 10% NP-40 to a final concentration of 0,1% beforehand. Samples were incubated for 10 minutes on ice and centrifuged for 10 minutes at 20,000xg. TCA-containing supernatant was discarded and the pellet was washed once with 1ml 100% Aceton at -20°C. After additional centrifugation at 20,000g for 10 minutes, the pellet was dried at 55°C for several minutes. SDS-sample buffer (Laemmli, 1970) was added after drying was completed.

5.3.2 Total protein extraction from yeast

To assess the protein content of yeast cells both quantitatively and qualitatively, the equivalent of cells contained in 1ml of a cell culture with an optical density (OD) at 600nm wavelength of 1AU (1OD-unit) was subjected to alkaline lysis. The cell suspension was treated with lysis solution containing 0.25M NaOH, 140mM β-ME and 3mM PMSF and lysis was allowed to continue for 10 minutes on ice. Afterwards, TCA precipitation of the lysate was performed. If not otherwise denoted, the equivalent of ½ OD-unit was applied to an SDS-PAGE gel and subsequent Western-blotting was performed.

5.3.3 SDS-PAGE

Gelelectrophoresis was performed using either the HOEFER Mini vertical units from Amersham-Biosciences (GE-Healthcare, Munich Germany) or the Mini-PROTEAN II system (Biorad, Munich, Germany). NuPAGE pre-cast gels (Invitrogen, Karlsruhe, Germany) were employed for 4-12% gradient gel electrophoresis. Pre-cast gels were run according to the manufacturer's protocol, whereas all other gels were run following the Laemmli system (Laemmli, 1970).

5.3.4 Coomassie staining of SDS-PAGE gels

For the staining of proteins separated on an SDS-PAGE gel, the colloidal Coomassie System (Roth, St. Leon-Rot, Germany) was employed according to the manufacturer's description unless denoted otherwise. In brief, 5x Coomassie suspension was diluted in 25% Methanol/ddH20 solution. Gels were incubated overnight together with 100ml of 1x Coomassie suspension per gel. Destaining was performed with 25% Methanol/ddH20 solution. Stained gels were scanned on an EPSON (Meerbusch, Germany) flatbed scanner and pictures were processed using Adobe Illustrator CS software (Adobe, San Jose, CA, U.S.A.).

5.3.5 Sypro Orange staining of SDS-PAGE gels

For the quantitative analysis of proteins separated on an SDS-PAGE gel, the protein dye Sypro Orange (Invitrogen, Karlsruhe, Germany) was employed. Sypro Orange allows for the fluorescence-based detection of proteins, yielding linear signals for a broad range of protein concentrations. Since the dye molecule interacts with the SDS bound to the polypeptide chains, the signal strength is independent of the amino acid sequence to a great extent compared to other staining methods like Coomassie staining. Gels were washed for 30 minutes in SDS-running buffer containing 0,5% SDS compared to 1% normal concentration. After brief rinsing with water, the gels were incubated in 7,5% acetic acid containing SyproOrange dye in 1:5000 dilution for 30 minutes at room temperature. After staining, the gels were briefly rinsed in 7,5% acetic acid and analyzed on a Versadoc fluorescence detection system (Bio-Rad, Munich, Germany) using QuantityOne software by the same manufacturer.

5.3.6 Production of recombinant proteins in *E.coli*

BL21 DE3 Rosetta cells were freshly transformed with the plasmid coding for the protein of interest and plated onto LB agar plates containing the appropriate antibiotics. Single colonies were picked from the transformation plate and the cells were directly suspended in 1l of LB medium containing the appropriate antibiotics. The culture was grown in an Innova Shaker at 37°C, 180rpm for several hours until the OD at 600nm was between 0.4 and 0.8. The cultures were then cooled down to 16-25°C depending on the plasmid encoded protein. Expression was induced with 0.5mM IPTG and cells were grown at 16-25°C, 180rpm overnight or at least additional 4 hours.

5.3.7 Purification of recombinant proteins from *E. coli*

After growth of bacterial culture and expression induction, the cell suspension was harvested by centrifugation in a JLA 8.000 rotor in an Avanti J26 XP centrifuge (both Beckman, Krefeld, Germany) at 5000rpm for 10 minutes. Cells were then washed once with 20ml/l culture ice-cold purification buffer (100mM NaCl, 50mM Hepes/NaOH pH=7.4, 1mM $MgCl_2$) and centrifuged once more as above. The pelleted cells were then carefully resuspended in 10ml/lculture lysis buffer containing 2mM PMSF and 0.2x PIC

avoiding cell aggregates. The cells were then lysed using a Microfluidizer (Microfluidics, Newton, MA, U.S.A.)

5.3.8 Western Blotting

For the detection of proteins by antibody decoration after the transfer of proteins to nitrocellulose membrane from SDS-PAGE gels, the Western blotting technique was employed. The protein containing samples were first subjected to SDS-PAGE for size-dependent separation. Afterwards, a nitrocellulose membrane of similar size as the gel was soaked in Western transfer buffer and put on a wet filter paper. The SDS-PAGE gel was then put on the membrane directly after the electrophoresis run. The gel was overlaid with another sheet of filter paper, turned once by 180 degrees and then put into the blotting chamber (Idea Scientific, Minneapolis, MN, U.S.A.) between several layers of thin cloth sponges. The chamber was then filled with transfer buffer and the transfer was carried out at 400mA, 12-15V for 90minutes. Afterwards, the protein bands were visualized by short incubation of the membrane with 0,3% PonceauS dye in 3% TCA solution and subsequent wash in distilled water. The protein bands of the molecular weight marker were marked with a black pen and free protein binding sites on the membrane were blocked by incubation with 5% milk in PBS buffer for 30 minutes. For protein detection, the blot membrane was then incubated with primary antibody directed against the antigen of interest. In most cases, the primary antibodies were obtained from rabbit serum and diluted 1:3000 to 1:6000 in 5% milk. If affinity purified antibodies were used, the dilution ranged from 1:100 to 1:500. The antibody directed against the HA tag was obtained mouse hybridoma cells and was diluted 1:1000 in 5% BSA. Blots were decorated with primary antibodies generally for 1 hour at room temperatur and washed three times with PBS afterwards. Secondary antibodies were obtained from goat serum and were directed against rabbit or mouse antibodies dependent on the first antibody that was used. These antibodies were coupled to fluorescent dyes; either Alexafluor 680 (Invitrogen, Karlsruhe, Germany) or IRDye800 (LiCor, Bad Homburg, Germany) were used and could be detected on a LiCor Odyssey scanner (LiCor). Incubation of blot membranes with secondary antibody (1:10000 dilution in 5%milk in PBS) was performed for 30 minutes at room temperature. Before detection, the membrane was washed four times for five minutes with PBS.

5.3.9 Subcellular fractionation

This protocol was employed to determine the localization of proteins in the endomemembrane system of yeast cells or to crudely separate vacuoles or endosomes from slower sedimenting organelles. Subcellular fractionating was for example employed to prepare Vps41 and Yck3 containing fractions for a subsequent up-shift assay. The protocol was performed as described in (LaGrassa and Ungermann, 2005). In brief, yeast spheroblasts were prepared and mildly lysed to release the cell content in to the lysis buffer. By subsequent centrifugation at 13,000xg a P13 (pellet at 13,000xg) and an S13 (supernatant at 13,000xg) were generated. If indicated, the S13 fraction was further centrifuged for 1 hour at 100,000xg to generate the P100 and S100 fractions, which contain slower sedimenting organelles as ER Golgi, and plasma membrane fragments and soluble proteins, respectively. The obtained fractions were either directly diluted in 1x Laemmli SDS sample buffer or TCA precipitated. Subsequent SDS-PAGE and Western blotting allowed for the analysis of the samples.

5.3.10 Vps41 upshift assay

P13 fractions obtained via subcellular fractionation (see 5.3.8) were subjected to incubation with ATP and ATP-regenerating system to allow for efficient phosphorylation of Vps41 by Yck3. The samples were incubated for 45 minutes at 26°C for the phosphorylation reaction. Afterwards, samples were centrifuged at 20,000xg for 5 minutes and the resulting pellet was dissolved in 1x Laemmli SDS sample buffer and loaded onto 7,5% SDS-PAGE gels without prior boiling.

5.3.11 Rab GTPase pull-down

GST-Rab fusion proteins (300-350µg per sample) were incubated in 500µl nucleotide loading buffer containing 20mM Hepes/NaOH (pH=7.4), 20mM EDTA and 1mM GDP, GTPγS or no nucleotide for 15 min at 30°C. The GDP and GTPγS samples were adjusted to 25 mM $MgCl_2$, and loaded onto 50µl of washed GSH-sepharose, whereas no $MgCl_2$ was added to the nucleotide free sample prior to loading onto the same amount of GSH-sepharose. After incubation for 1h at 4°C, the GSH-bound nucleotide free form was washed once with 20mM Hepes/NaOH (pH=7.4), 20mM EDTA and the matrix was then

resuspended in 200µl buffer containing 20mM Hepes/NaOH (pH=7.4) 100mM NaCl, 1mM $MgCl_2$. The GDP and GTPγS loaded samples were resuspended in 200µl of the same buffer containing additional 2.5mM GDP or GTPγS, respectively. These nucleotide loaded Rab GTPases bound to GSH-sepharose were then immediately used for pull-down experiments. Protein samples to be applied to Rab GTPase pull-down where prepared in parallel using the Mini-TAP protocol. TEV eluates were directly applied to the immobilized GST-Rab proteins and the bead suspension was incubated for 1h at 4°C on a turning wheel. After the binding reaction, the beads were carefully pelleted by centrifugation and washed three times with 1ml ice-cold buffer (20mM Hepes/NaOH (pH=7.4), 100mM NaCl, 1mM $MgCl_2$ and 0.1% IGEPAL-630 (NP-40 substitute)). Bound proteins were then eluted by incubation with 600µl elution buffer containing 20mM Hepes/NaOH (pH=7.4), 20mM EDTA, 200mM NaCl, 1mM $MgCl_2$ and 0.1% IGEPAL-630 for 20 min at room temperature on a turning wheel. A second elution step was performed with 300µl elution buffer for 10 minutes to elute residual protein. Eluates were then pooled, subjected to TCA precipitation and analyzed by SDS-PAGE and Western blotting.

5.3.12 Tandem affinity purification (TAP)

5.3.12.1 Standard TAP

For native purification of proteins together with non-covalently bound interactors from yeast cells was performed essentially following the protocol of Seraphin and co-workers (Puig et al., 2001). 2 to 4 liters culture of yeast cells harboring the TAP-tagged fusion protein of interest were grown overnight and harvested at an OD600 of 2-5. Cells were washed once with ddH20 once with lysis buffer (150mM NaCl, 50mM Hepes pH=7.4, 2mM MgCl2, 0,15% NP-40 (IGEPAL-630), 1xFY protease inhibitor mix (Serva, Heidelberg, Germany) and 2mM PMSF) and finally centrifuged at 4000xg to pellet the cells. Cell pellets were frozen in liquid nitrogen and stored at -80° C until usage. For lysis, cell pellets were thawed and suspended in lysis buffer additionally containing 1mM DTT in a total volume of 25ml. The cell suspension was transferred to milling buckets and 25ml glass beads with a diameter of 0.4-0.6µm were added. The buckets were closed and fastened in a Pulverisette Mono-planet-mill located in a 4° C cold-room (Fritsch, Idar-Oberstein, Germany). The milling settings were 3 x 500rpm for 4 minutes with 1

minute breaks to allow for sample cooling. Glass beads were separated from the cell lysate by pressing through a standard 50ml syringe. Retained beads were washed with 10ml lysis buffer containing all additives. The lysate was subsequently centrifuged at 4000xg 4° C for 10 minutes to remove unlysed cells and coarse cell debris. The resulting pre-cleared supernatant was then transferred to high-speed ultracentrifugation tubes (Eppendorf, Hamburg, Germany) and centrifuged for 1 hour at 100,000xg in a Ti 50.2 rotor (Beckman, Krefeld, Germany). Before removing the 100,000xg supernantant, the fatty top-phase was removed from the centrifugation tubes using a water-jet vacuum pump. The remaining supernatant was poured off the pellet into a fresh 50ml tube. IgG-spharose beads (GE-Healthcare, Munich, Germany) were washed three times with lysis buffer containing no additives for equilibration. 250-500µl of bead slurry was added to each lysate of approx. 20ml volume. The mixture was incubated one hour at 4°C on a nutator. Afterwards, beads were transferred to small MoBiCol columns (MoBiTec, Göttingen, Germany), drained by gravity flow and washed once with 15ml lysate buffer containing only 0.5mM DTT as additive. The beads were drained, the column closed at the bottom and 150µl lysate buffer (+0.5mM DTT) containing 4µl of a 1mg/ml TEV-protease preparation were added. For the cleavage reaction, the mixture was incubated for 1 hour at 16°C on a turning wheel. Elution from the beads was performed by centrifuging the column in a 1.5ml tube in a tabletop centrifuge at 2000xg for 20 seconds. To raise the elution efficiency, the beads were incubated with additional 100µl of lysis buffer (+0.5mM DTT) briefly mixed and centrifuged as above. Elution fractions were pooled. The TEV eluate was then either used for Gelfiltration analysis, TCA precipitated and used for SDS-PAGE analysis or subjected to an additional purification step as described below:

1M CaCl2 solution was added to the lysate to a final concentration of 2mM CaCl2. Calmodulin sepharose beads were washed 3 times in lysis buffer containing 2mM CaCl2. TEV eluate and 250-350µl of bead slurry per sample were mixed in a new MoBiCol column. The mixture was incubated 1 hour at 4°C on a turning wheel. After the binding reaction, beads were drained by gravity flow and subsequently washed with 10ml lysis buffer containing 1mM DTT and 2mM $CaCl_2$. For the elution, 600µl of EGTA-elution buffer (lysis buffer containing 20mM EGTA) were added per sample and incubated at 30°C for 20 minutes to allow for efficient chelating of Ca^{2+} ions. Eluates were collected as for the TEV elution. A second elution reaction was performed using 300µl of EGTA-

elution buffer and incubation for 10 minutes at 30°C. Both eluates were pooled and used for SDS-PAGE and Western blot analysis after TCA precipitation or other subsequent experiments.

5.3.12.2 Mini TAP

The Mini-TAP was essentially carried out as the standard TAP protocol (see 5.3.12.1). For one purification sample, cell material from 250ml culture at an OD600 of approx. 2 was used (ca. 1/20 of a standard TAP sample) and resuspended the same volume of TAP lysis buffer containing all additives. Lysis was performed on a Disruptor-Genie (Scientific Industries, Bohemia, NY, U.S.A.) in a 2ml reaction tube containing cell suspension and the same volume of glass beads. The following incubation steps are perfomed in 1.5ml reaction tubes instead of MoBiCol columns due to the decreased reaction volume. Wash steps were performed with 3x 1ml with the respective buffers. Incubation conditions were the same as for the standard TAP protocol. Purified proteins were used for Rab GTPase pull-downs or analysis with SDS-PAGE.

5.3.13 Gelfiltration

For the separation of proteins/protein complexes dependent on their molecular weight and for purifying complexes from smaller proteins and metabolites, size exclusion chromatography, or gelfiltration, was employed. Generally, a Superose 6 10/300 GL column (GE Healthcare, Munich, Germany) with a volume of 24ml was used for this procedure if not indicated otherwise. The column was attached to an ÄKTA FPLC system, which was operated from a PC using the Unicorn 5.01 software (both GE Healthcare). The standard flow rate during the gelfiltration run was 0.3ml/minute and up to 0.5ml/minute for washing and equilibration. Since TEV eluate from a TAP experiment was usually applied to the column, TEV-elution buffer (see 5.3.12.1, TAP procedure) containing 4mM DTT was used for the isocratic elution of the sample from the gelfiltration matrix, to avoid the danger of protein precipitation due to a buffer change. Buffers where generally filtered through a 0.22µm filter and subsequently degassed by application of vacuum to prevent damage of the column bed packing by particles or air bubbles. All samples where centrifuged at 20,000xg for 10 minutes prior to loading into the sample loop to pellet insoluble material. Fractions where collected for 0.9 column

volumes i.e. for approx. 21.6ml. The fraction size was 1ml if not indicated differently. All gelfiltration experiments where carried out at 4°C to avoid sample degradation and disintegration of protein complexes. Collected fractions where TCA precipitated afterwards and analyzed by SDS-PAGE alone and/or additional Western blotting.

5.3.14 FM 4-64 staining of live cells

To visualize the yeast vacuole for fluorescence microscopy analysis, the lipophilic styryl dye FM4-64 (N-(3-triethylammoniumpropyl)-4-(6-(4-(diethylamino)phenyl)hexatrienyl) pyrid-inium dibromide, Invitrogen, Karlsruhe, Germany) was employed. Yeast cells were grown in an overnight culture and diluted in the morning with fresh medium to an OD_{600} of approx. 0.25. These cultures were then grown at least 3-4 hours to an OD of 0.5 to 1. The cells were then pelleted by centrifugation at 3000xg for 5 minutes and resuspended in 50µl of fresh medium. 3µl of a 0.3mM FM4-64 solution was added and the cell suspension was incubated in the dark for 30 minutes at 30°C while shaking in a tabletop thermo-shaker (Eppendorf, Hamburg, Germany) ("pulse"). As a crude washing step, 1ml medium was then added, cells briefly centrifuged for pelleting and the supernatant discarded. The cells where then resuspended in 500µl of fresh medium and incubated for 45 minutes in the dark at 30°C while shaking ("chase"). Afterwards, the cells were again pelleted, washed one time with 1ml PBS and finally resuspended in 10-30µl of PBS prior to microscopy.

5.4 Molecular biology

5.4.1 PCR

Primer design and amplification of nucleic acid sequences destined for the integration into the yeast genome after transformation was carried out using a PeqLab PCR machine (PeqLab, Erlangen, Germany) as described in (Janke et al., 2004).

5.4.2 Agarose gelelectrophoresis

To assess the efficiency of PCRs or to monitor restriction enzyme digests, DNA containing samples were subjected to agarose gel electrophoresis. To prepare 1% gels.

0,5g of agarose were mixed with 50ml 1xTAE buffer (20mM Tris, 1mM EDTA, 20mM acetic acid) and heated in a microwave oven at 160Watts for 3-5 minutes. After te agarose was dissolved completely, the solution was cooled down for 1 minute at room temperature and 3µl of a 1% ethidium bromide solution was added. After careful mixing, the mixture was poured into a agarose gel cast stand equipped with a gel slide and the appropriate comb (Hoefer Mini sub system provided by Pharmacia Biotech, now GE-healthcare, Munich, Germany). After cooling for 20-30 minutes, the combs were removed and gels were loaded into the mini sub horizontal gel electrophoresis chamber, which was filled with 1x TAE buffer. Samples were applied into the gel wells and the electrophoretic run was performed at 120V, 30-40mA for 25 minutes. After the run, gels were put into a UV gel documentation system (Peqlab, Erlangen, Germany) and the ethidium bromide stained nucleic acids were visualized.

5.4.3 Bacteria transformation

Standard bacteria strains for cloning procedures (DH5α) or recombinant protein expression (BL21 DE3 Rosetta) were provided as frozen competent cells (competence chemically induced by $CaCl_2$). DNA was added to freshly thawed 50µl bacteria suspension and gently mixed. The mixture was kept on ice for 20 minutes and subjected to a heat shock for 30 seconds at 42°C afterwards. After placing the cell suspension back on ice for additional two minutes, 750µl LB medium without antibiotics was added and the resulting culture was incubated for one hour at 37°C. After the incubation, cells were pelleted by centrifugation at 5000xg for two minutes, resuspended in 150µl sterile water and directly plated onto LB agar plates containing the appropriate antibiotics.

5.4.4 Yeast transformation

Yeast cells were transformed with PCR products or plasmids using Polyethylenglykol (PEG) and Lithium Acetate (LiAc). In brief, overnight yeast cell cultures were diluted in the morning and grown for additional four to five hours. The cells were then harvested by centrifugation, washed once with water and once with 0.1M LiAc solution. Afterwards, appropriate amounts of cells were pelleted by centrifugation and overlaid with a solution containing 50% PEG, 0.1M LiAc and salmon sperm DNA acting as carrier DNA to facilitate the uptake of the DNA of interest. For plasmids, 100-300ng DNA were

employed per transformation. For transformation of PCR products, 15µl of a standard 50µl PCR reaction was used.

5.5 Microscopy

For fluorescence microscopy of cells carrying GFP- and RFP-tagged proteins, cells were grown to logarithmic phase in 5ml complex or selective medium, dependent on the strain background. The cells were harvested by centrifugation and washed once with 1 ml of PBS buffer and resuspended in 10-30µl PBS or stained with FM4-64. Images were acquired using a Leica DM5500 microscope (Leica, Wetzlar, Germany) and a SPOT Pursuit-XS camera (Visitron, Puchheim, Germany) using filters for GFP, FM4-64 and RFP. The pictures were processed using Adobe Photoshop CS3.

5.6 Strains used in this study

Table 5.1 **Strains used in this study**

strain	genotype	reference
CUY100	*BY4727 MATalpha his3Δ200 leu2Δ0 lys2Δ0 met15Δ0 trp1Δ63 ura3Δ0*	Brachman et al., 1998
CUY105	*BY4732 MATa his3Δ200 leu2Δ0 met15Δ0 trp1Δ63 ura3Δ0*	Brachman et al., 1998
CUY490	*MATa his3Δ leu2Δ met15Δ ura3Δ vps41Δ::kanMX*	Euroscarf library
CUY516	*MATa his3Δ leu2Δ met15Δ ura3Δ vam6Δ::kanMX*	Euroscarf library
CUY520	*MATa his3Δ leu2Δ met15Δ ura3Δ vps33Δ::kanMX*	Euroscarf library
CUY521	*MATa his3Δ leu2Δ met15Δ ura3Δ vps16Δ::kanMX*	Euroscarf library
CUY523	*MATa his3Δ leu2Δ met15Δ ura3Δ vps18Δ::kanMX*	Euroscarf library
CUY552	*MATa pep4::HIS3 prb1-Δ1.6R HIS3 lys2-208 trp1Δ101 ura3-52 gal2 can vps41Δ::KANMX6 ura3::pRS406-NOP1pr-VPS41*	LaGrassa and Ungermann, 2005
CUY592	*MATa his3Δ leu2Δ met15Δ ura3Δ yck3Δ::kanMX ura3::pRS406-NOP1pr-GFP-VPS41*	LaGrassa and Ungermann, 2005
CUY764	*MATa his3Δ1 leu2Δ0 met15Δ0 ura3Δ0*	Euroscarf library

CUY785	*MATa pep4::HIS3 prb1-Δ1.6R HIS3 lys2-208 trp1Δ101 ura3-52 gal2 can yck3Δ::kanMX*	LaGrassa and Ungermann, 2005
CUY830	*MATa pep4::HIS3 prb1-Δ1.6R HIS3 lys2-208 trp1Δ101 ura3-52 gal2 can yck3Δ::kanMX4 pRS406-NOP1pr-eGFP-VPS41*	LaGrassa and Ungermann, 2005
CUY856	*MATa pep4::HIS3 prb1-Δ1.6R HIS3 lys2-208 trp1Δ101 ura3-52 gal2 can VPS11::TAP-kanMX*	this study
CUY857	*MATa pep4::HIS3 prb1-Δ1.6R HIS3 lys2-208 trp1Δ101 ura3-52 gal2 can VPS16::TAP-kanMX*	this study
CUY858	*MATa pep4::HIS3 prb1-Δ1.6R HIS3 lys2-208 trp1Δ101 ura3-52 gal2 can VPS18::TAP-kanMX*	this study
CUY859	*MATa pep4::HIS3 prb1-Δ1.6R HIS3 lys2-208 trp1Δ101 ura3-52 gal2 can VPS33::TAP-kanMX*	this study
CUY860	*MATa pep4::HIS3 prb1-Δ1.6R HIS3 lys2-208 trp1Δ101 ura3-52 gal2 can VPS41::TAP-kanMX*	this study
CUY866	*MATa pep4::HIS3 prb1-Δ1.6R HIS3 lys2-208 trp1Δ101 ura3-52 gal2 can VAM6::TAP-kanMX*	this study
CUY927	*MATa pep4::HIS3 prb1-Δ1.6R HIS3 lys2-208 trp1Δ101 ura3-52 gal2 can ura3::pRS406-NOP1pr-VPS41*	LaGrassa and Ungermann, 2005
CUY928	*MATa pep4::HIS3 prb1-Δ1.6R HIS3 lys2-208 trp1Δ101 ura3-52 gal2 can ura3::pRS406-NOP1pr-VPS41 yck3Δ::kanMX*	LaGrassa and Ungermann, 2005
CUY981	*MATa his3Δ1 leu2Δ0 met15Δ0 ura3Δ0 yck3pr::HIS3-GAL1pr*	LaGrassa and Ungermann, 2005
CUY983	*MATa pep4::HIS3 prb1-Δ1.6R HIS3 lys2-208 trp1Δ101 ura3-52 gal2 can yck3pr::TRP1-GAL1pr*	LaGrassa and Ungermann, 2005
CUY1014	*MATa his3Δ leu2Δ met15Δ ura3Δ vps3Δ::kanMX*	LaGrassa and Ungermann, 2005
CUY1048	*MATa his3Δ leu2Δ met15Δ ura3Δ vpr1Δ::kanMX vps41pr::HIS5-PHO5pr-GFP-Myc*	LaGrassa and Ungermann, 2005
CUY1326	*MATa pep4::HIS3 prb1-Δ1.6R HIS3 lys2-208 trp1Δ101 ura3-52 gal2 can vps41Δ::KANMX6 ura3::pRS406-NOP1pr-VPS41 yck3Δ::hphNT*	LaGrassa and Ungermann, 2005
CUY1331	*MATa pep4::HIS3 prb1-Δ1.6R HIS3 lys2-208 trp1Δ101 ura3-52 gal2 can vps41Δ::KANMX6 ura3::pRS406-NOP1pr-VPS41 nop1pr::TRP1-PHO5pr-GFP-Myc*	LaGrassa and Ungermann, 2005

CUY1335	*MATa pep4::HIS3 prb1-Δ1.6R HIS3 lys2-208 trp1Δ101 ura3-52 gal2 can yck3Δ::TRP1*	LaGrassa and Ungermann, 2005
CUY1344	*MATa pep4::HIS3 prb1-Δ1.6R HIS3 lys2-208 trp1Δ101 ura3-52 gal2 can yck3Δ::TRP1 VPS41::TAP-KanMX4*	this study
CUY1381	*MATa his3Δ leu2Δ met15Δ ura3Δ VPS18::GFP-hphNT*	this study
CUY1534	*MATa pep4::HIS3 prb1-Δ1.6R HIS3 lys2-208 trp1Δ101 ura3-52 gal2 can CCZ1::TAP-kanMX4*	this study
CUY1535	*MATa pep4::HIS3 prb1-Δ1.6R HIS3 lys2-208 trp1Δ101 ura3-52 gal2 can MON1::TAP-KanMX4*	this study
CUY1601	*MATa pep4::HIS3 prb1-Δ1.6R HIS3 lys2-208 trp1Δ101 ura3-52 gal2 can yck3Δ::TRP1 CCZ1::TAP-KanMX4*	this study
CUY1602	*MATa pep4::HIS3 prb1-Δ1.6R HIS3 lys2-208 trp1Δ101 ura3-52 gal2 can yck3Δ::TRP1 MON1::TAP-KanMX4*	this study
CUY1761	*MATalpha his3Δ200 leu2Δ0 lys2Δ0 met15Δ0 trp1Δ63 ura3Δ0 vps11pr::HIS3-GAL1pr*	this study
CUY1768	*MATalpha his3Δ200 leu2Δ0 lys2Δ0 met15Δ0 trp1Δ63 ura3Δ0 vps11pr::HIS3-GAL1pr*	this study
CUY1772	*MATalpha his3Δ200 leu2Δ0 met15Δ0 trp1Δ63 ura3Δ0 vps33pr::HIS3-GAL1pr*	this study
CUY1776	*MATalpha his3Δ200 leu2Δ0 lys2Δ0 met15Δ0 trp1Δ63 ura3Δ0 vps11pr::HIS3-GAL1pr vps16pr::TRP1-GAL1pr vps18pr::kanMX-GAL1pr*	this study
CUY1792	*MATa his3Δ1 leu2Δ0 met15Δ0 ura3Δ0 VPS8::TAP-kanMX*	Peplowska et al., 2007
CUY1795	*MATa his3Δ1 leu2Δ0 met15Δ0 ura3Δ0 VPS3::TAP-URA3*	Peplowska et al., 2007
CUY1796	*MATa his3Δ leu2Δ met15Δ ura3Δ vam2Δ::kanMX VPS3::TAP-URA3*	Peplowska et al., 2007
CUY1797	*MATa his3Δ1 leu2Δ0 met15Δ0 ura3Δ0 vps8Δ::kanMX VPS3::TAP-URA3*	Peplowska et al., 2007
CUY1798	*MATa his3Δ1 leu2Δ0 met15Δ0 ura3Δ0 vam6Δ::kanMX VPS3::TAP-URA3*	Peplowska et al., 2007
CUY1799	*MATa his3Δ leu2Δ met15Δ ura3Δ vps33Δ::kanMX VPS3::TAP-URA3*	Peplowska et al., 2007

CUY1800	*MATa his3Δ1 leu2Δ0 met15Δ0 ura3Δ0 VPS41::TAP-URA3*	Peplowska et al., 2007
CUY1801	*MATa his3Δ1 leu2Δ0 met15Δ0 ura3Δ0 vam6Δ::kanMX VAM2::TAP-URA3*	Peplowska et al., 2007
CUY1802	*MATa his3Δ1 leu2Δ0 met15Δ0 ura3Δ0 vps3Δ::kanMX VAM2::TAP-URA3*	Peplowska et al., 2007
CUY1803	*MATa his3Δ1 leu2Δ0 met15Δ0 ura3Δ0 vps8Δ::kanMX VAM2::TAP-URA3*	Peplowska et al., 2007
CUY1804	*MATa his3Δ leu2Δ met15Δ ura3Δ vps33Δ::kanMX VPS41::TAP-URA3*	Peplowska et al., 2007
CUY1846	*MATa his3Δ leu2Δ met15Δ ura3Δ VPS3::TAP-URA3 VPS3::HIS3-GAL1pr*	this study
CUY1847	*MATa his3Δ leu2Δ met15Δ ura3Δ VPS41::TAP-URA3 vps3pr::HIS3-GAL1pr*	Peplowska et al., 2007
CUY1874	*MATa his3Δ leu2Δ met15Δ ura3Δ VPS8::TAP-kanMX vps8pr::HIS3-GAL1pr*	this study
CUY1875	*MATa his3Δ leu2Δ met15Δ ura3Δ VPS8::TAP-kanMX vps3pr::HIS3-GAL1pr*	Peplowska et al., 2007
CUY1876	*MATalpha his3Δ200 leu2Δ0 met15Δ0 trp1Δ63 ura3Δ0 VAM6::TAP-kanMX4 VAM6pr::TRP1-GAL1pr vps11Δ::URA3*	this study
CUY1877	*MATa his3Δ leu2Δ met15Δ ura3Δ VPS8::TAP-kanMX vps3Δ::URA3*	Peplowska et al., 2007
CUY1878	*MATa his3Δ leu2Δ met15Δ ura3Δ VPS3::TAP-URA3 vps11Δ::kanMX*	Peplowska et al., 2007
CUY1896	*MATa his3Δ200 leu2Δ0 met15Δ0 trp1Δ63 ura3Δ0 vps41pr::TRP1-GAL1pr*	this study
CUY1903	*MATa his3Δ200 met15Δ0 trp1Δ63 ura3Δ0 vps41pr::TRP1-GAL1pr vam6pr::KanMX-GAL1pr*	this study
CUY1906	*MATa his3Δ leu2Δ met15Δ ura3Δ vps11Δ::URA3*	this study
CUY1908	*MATa his3Δ200 met15Δ0 trp1Δ63 ura3Δ0 vps41pr::TRP1-GAL1pr vam6pr::KanMX-GAL1pr vps33pr::HIS3-Gal1pr*	this study
CUY1915	*MATa his3Δ1 leu2Δ0 met15Δ0 ura3Δ0 vps3pr::kanMX-Gal1pr*	Peplowska et al., 2007
CUY1916	*MATa his3Δ1 leu2Δ0 met15Δ0 ura3Δ0 VPS8::TAP-kanMX vps41pr::HIS3-GAL1pr*	Peplowska et al., 2007

CUY1918	*MATa pep4::HIS3 prb1-Δ1.6R HIS3 lys2-208 trp1Δ101 ura3-52 gal2 can vps41Δ::kanMX URA3::pRS406-NOP1pr-VPS41-(F124A, F128A)*	Cabrera et al., 2009
CUY1919	*MATa pep4::HIS3 prb1-Δ1.6R HIS3 lys2-208 trp1Δ101 ura3-52 gal2 can vps41Δ::kanMX URA3::pRS406-NOP1pr-VPS41-(S663,664,669A,T662,665A)*	Cabrera et al., 2009
CUY1920	*MATa pep4::HIS3 prb1-Δ1.6R HIS3 lys2-208 trp1Δ101 ura3-52 gal2 can vps41Δ::kanMX URA3::pRS406-NOP1pr-VPS41-(S794A, S798A)*	Cabrera et al., 2009
CUY1921	*MATa pep4::HIS3 prb1-Δ1.6R HIS3 lys2-208 trp1Δ101 ura3-52 gal2 can vps41Δ::kanMX URA3::pRS406-NOP1pr-VPS41-(S364,367,368,371,372A,T376A)*	Cabrera et al., 2009
CUY1922	*MATa pep4::HIS3 prb1-Δ1.6R HIS3 lys2-208 trp1Δ101 ura3-52 gal2 can vps41Δ::kanMX URA3::pRS406-NOP1pr-VPS41-(S117,119,120A)*	Cabrera et al., 2009
CUY1923	*MATa pep4::HIS3 prb1-Δ1.6R HIS3 lys2-208 trp1Δ101 ura3-52 gal2 can vps41Δ::kanMX URA3::pRS406-NOP1pr-VPS41-(F329A,F333A)*	Cabrera et al., 2009
CUY1924	*MATa pep4::HIS3 prb1-Δ1.6R HIS3 lys2-208 trp1Δ101 ura3-52 gal2 can vps41Δ::kanMX URA3::pRS406-NOP1pr-VPS41*	Cabrera et al., 2009
CUY1953	*MATa his3Δ200 met15Δ0 trp1Δ63 ura3Δ0 VAM2::TRP1-GAL1pr VPS41::TAP-URA3 vam6pr::KanMX-GAL1pr vps33pr::HIS3-GAL1pr*	this study
CUY1954	*MATalpha his3Δ200 leu2Δ0 lys2Δ0 met15Δ0 trp1Δ63 ura3Δ0 vps11pr::HIS3-GAL1Pr vps16pr::TRP1-GAL1Pr vps18pr::kanMX-GAL1Pr pRS411 MET15*	this study
CUY1980	*MATa his3Δ leu2Δ met15Δ ura3Δ vps33Δ::kanMX VAM6::TAP-URA3*	this study
CUY1982	*MATa his3Δ leu2Δ met15Δ ura3Δ vps18Δ::kanMX VAM6::TAP-URA3*	this study
CUY1983	*MATa his3Δ leu2Δ met15Δ ura3Δ vps41Δ::kanMX VPS33::TAP-URA3*	this study
CUY1984	*MATa his3Δ leu2Δ met15Δ ura3Δ vam6Δ::kanMX VPS33::TAP-URA3*	this study
CUY1985	*MATa his3Δ leu2Δ met15Δ ura3Δ vps16Δ::kanMX VPS33::TAP-URA3*	this study

CUY1986	*MATa his3Δ leu2Δ met15Δ ura3Δ vps18Δ::kanMX VPS33::TAP-URA3*	this study
CUY1987	*MATalpha his3Δ200 leu2Δ0 met15Δ0 trp1Δ63 ura3Δ0 VAM6::TAP-kanMX4 vps8pr::HIS3-GAL1pr-3HA*	Peplowska et al., 2007
CUY1989	*MATa his3Δ leu2Δ met15Δ ura3Δ vam2Δ::kanMX VAM6::TAP-Ura3*	this study
CUY1998	*MATalpha his3Δ200 leu2Δ0 met15Δ0 trp1Δ63 ura3Δ0 VAM6::TAP-kanMX4 VPS8::3HA-HIS3*	Peplowska et al., 2007
CUY2029	*MATalpha his3Δ200 leu2Δ0 met15Δ0 trp1Δ63 ura3Δ0 vam6pr::kanMX-GAL1pr VAM6::TAP-Trp*	this study
CUY2032	*MATa pep4::HIS3 prb1-Δ1.6R HIS3 lys2-208 trp1Δ101 ura3-52 gal2 can vps41Δ::kanMX URA3::pRS406-NOP1pr-VPS41-(F124A, F128A) TRP1::pRS406-NOP1pr-VPS41-(F124A, F128A)-GFP*	Cabrera et al., 2009
CUY2033	*MATa pep4::HIS3 prb1-Δ1.6R HIS3 lys2-208 trp1Δ101 ura3-52 gal2 can vps41Δ::kanMX URA3::pRS406-NOP1pr-PS41-(S364,367,368,371, 372A,T376A) TRP1::pRS406-NOP1pr-VPS41-(S364,367,368,371,372A,T376A)-GFP*	Cabrera et al., 2009
CUY2034	*MATa pep4::HIS3 prb1-Δ1.6R HIS3 lys2-208 trp1Δ101 ura3-52 gal2 can vps41Δ::kanMX URA3::pRS406-NOP1pr-VPS41-(S117,119,120A) URA3::pRS406-NOP1pr-VPS41-(S117,119,120A)-GFP*	Cabrera et al., 2009
CUY2035	*MATa pep4::HIS3 prb1-Δ1.6R HIS3 lys2-208 trp1Δ101 ura3-52 gal2 can vps41Δ::kanMX URA3::pRS406-NOP1pr-VPS41 TRP1::pRS406-NOP1pr-VPS41-GFP*	Cabrera et al., 2009
CUY2104	*MATa his3Δ leu2Δ met15Δ ura3Δ vps41Δ::kanMX VPS11::TAP-URA3*	this study
CUY2105	*MATa his3Δ leu2Δ met15Δ ura3Δ vps41Δ::kanMX VPS18::TAP-URA3*	this study
CUY2106	*MATa his3Δ leu2Δ met15Δ ura3Δ vps41Δ::kanMX VPS16::TAP-URA3*	this study
CUY2107	*MATa his3Δ leu2Δ met15Δ ura3Δ vam6Δ::kanMX VPS11::TAP-URA3*	this study
CUY2108	*MATa his3Δ leu2Δ met15Δ ura3Δ vam6Δ::kanMX VPS18::TAP-URA3*	this study

CUY2109	*MATa his3Δ leu2Δ met15Δ ura3Δ vam6Δ::kanMX VPS16::TAP-URA3*	this study
CUY2110	*MATa his3Δ leu2Δ met15Δ ura3Δ vps33Δ::kanMX VPS11::TAP-URA3*	this study
CUY2111	*MATa his3Δ leu2Δ met15Δ ura3Δ vps33Δ::kanMX VPS18::TAP-URA3*	this study
CUY2112	*MATa his3Δ leu2Δ met15Δ ura3Δ vps33Δ::kanMX VPS16::TAP-URA3*	this study
CUY2113	*MATa his3Δ leu2Δ met15Δ ura3Δ vps16Δ::kanMX VPS11::TAP-URA3*	this study
CUY2114	*MATa his3Δ leu2Δ met15Δ ura3Δ vps18Δ::kanMX VPS11::TAP-URA3*	this study
CUY2116	*MATa his3Δ leu2Δ met15Δ ura3Δ vam6Δ::kanMX vps8pr::HIS3-GAL1pr-3HA VPS3::TAP-URA3*	Peplowska et al., 2007
CUY2117	*MATalpha his3Δ200 leu2Δ0 met15Δ0 trp1Δ63 ura3Δ0 vam6pr::kanMX-GAL1pr VAM6::TAP-Trp1 VPS8::3HA-HIS3*	Peplowska et al., 2007
CUY2152	*MATa his3Δ200 met5Δ0 trp1Δ63 ura3Δ0 vps41pr::TRP1-GAL1pr VPS41::TAP-URA3*	this study
CUY2153	*MATa his3Δ200 met15Δ0 trp1Δ63 ura3Δ0 vps41pr::TRP1-GAL1pr vam6pr::KanMX-GAL1pr VPS41::TAP-URA3*	this study
CUY2154	*MATa his3Δ leu2Δ met15Δ ura3Δ vps16Δ::kanMX VPS41::TAP-URA3*	this study
CUY2155	*MATa his3Δ leu2Δ met15Δ ura3Δ vps18Δ::kanMX VPS41::TAP-URA3*	this study
CUY2156	*MATa his3Δ leu2Δ met15Δ ura3Δ vps18Δ::kanMX VPS16::TAP-URA3*	this study
CUY2226	*MATa his3Δ leu2Δ met15Δ ura3Δ vps11Δ::URA3 VPS41::TAP-kanMX*	this study
CUY2227	*MATa his3Δ leu2Δ met15Δ ura3Δ vps11Δ::URA3 VAM6::TAP-kanMX*	this study
CUY2228	*MATa his3Δ leu2Δ met15Δ ura3Δ vps11Δ::URA3 VPS16::TAP-kanMX*	this study
CUY2229	*MATa his3Δ leu2Δ met15Δ ura3Δ vps11Δ::URA3 VPS18::TAP-kanMX*	this study
CUY2230	*MATa his3Δ leu2Δ met15Δ ura3Δ vps11Δ::URA3 VpS33::TAP-kanMX*	this study

CUY2231	*MATa his3Δ1 leu2Δ0 met15Δ0 ura3Δ0 VPS8::TAP-kanMX vam6pr::HIS3-GAL1pr-3HA*	this study
CUY2368	*MATa pep4::HIS3 prb1-Δ1.6R HIS3 lys2-208 trp1Δ101 ura3-52 gal2 can vps41Δ::kanMX URA3::pRS406-NOP1pr-VPS41 S367,368D*	Cabrera et al., 2009
CUY2369	*MATa pep4::HIS3 prb1-Δ1.6R HIS3 lys2-208 trp1Δ101 ura3-52 gal2 can vps41Δ::kanMX URA3::pRS406-NOP1pr-VPS41 S367,368A ::GFP-TRP1*	Cabrera et al., 2009
CUY2370	*MATa pep4::HIS3 prb1-Δ1.6R HIS3 lys2-208 trp1Δ101 ura3-52 gal2 can vps41Δ::kanMX URA3::pRS406-NOP1pr-VPS41 S371,372A ::GFP-TRP1*	Cabrera et al., 2009
CUY2379	*MATa pep4::HIS3 prb1-Δ1.6R HIS3 lys2-208 trp1Δ101 ura3-52 gal2 can vps41Δ::kanMX URA3::pRS406-NOP1pr-VPS41 S371A*	Cabrera et al., 2009
CUY2380	*MATa pep4::HIS3 prb1-Δ1.6R HIS3 lys2-208 trp1Δ101 ura3-52 gal2 can vps41Δ::kanMX URA3::pRS406-NOP1pr-VPS41S371A*	Cabrera et al., 2009
CUY2381	*MATa pep4::HIS3 prb1-Δ1.6R HIS3 lys2-208 trp1Δ101 ura3-52 gal2 can vps41Δ::kanMX URA3::pRS406-NOP1pr-VPS41 S371,372D*	Cabrera et al., 2009
CUY2483	*MATa his3Δ leu2Δ met15Δ ura3Δ vam6Δ::kanMX VPS11::TAP-URA3 vam6pr::HIS3-GAL1pr*	this study
CUY2488	*MATalpha his3Δ200 leu2Δ0 lys2Δ0 met15Δ0 trp1Δ63 ura3Δ vps18pr::KanMX-GAL1Pr-3HA*	this study
CUY2489	*MATalpha his3Δ200 leu2Δ0 lys2Δ0 met15Δ0 trp1Δ63 ura3Δ0 vps11pr::HIS3-GAL1Pr vps16pr::natNT2-GAL1Pr vps18pr::kanMX-GAL1Pr-3HA*	this study
CUY2530	*MATa his3Δ200 met15Δ0 trp1Δ63 ura3Δ0 vps33pr::TRP1-GAL1pr*	this study
CUY2531	*MATalpha his3Δ200 leu2Δ0 lys2Δ0 met15Δ0 trp1Δ63 ura3Δ0 vps16pr::kanMX-GAL1Pr-3HA*	this study
CUY2567	*MATalpha his3Δ200 leu2Δ0 lys2Δ0 met15Δ0 ura3Δ0 vps11pr::HIS3-GAL1Pr vps18pr::kanMX-GAL1Pr-3HA VPS11::TAP-URA3*	this study
CUY2568	*MATalpha his3Δ200 leu2Δ0 lys2Δ0 met15Δ0 trp1Δ63 ura3Δ0 VPS16::TAP-URA3*	this study

CUY2569	*MATalpha his3Δ200 leu2Δ0 lys2Δ0 met15Δ0 trp1Δ63 ura3Δ0 VPS18::TAP-URA3*	this study
CUY2570	*MATalpha his3Δ200 leu2Δ0 lys2Δ0 met15Δ0 trp1Δ63 ura3Δ0 VPS33::TAP-URA3*	this study
CUY2571	*MATalpha his3Δ200 leu2Δ0 lys2Δ0 met15Δ0 trp1Δ63 ura3Δ0 VPS41::TAP-URA3*	this study
CUY2572	*MATalpha his3Δ200 leu2Δ0 lys2Δ0 met15Δ0 trp1Δ63 ura3Δ0 VAM6::TAP-URA3*	this study
CUY2659	*MATa his3Δ200 leu2Δ0 met15Δ0 trp1Δ63 ura3Δ0 vps11pr::KanMX-GAL1Pr*	this study
CUY2660	*MATa his3Δ200 leu2Δ0 met15Δ0 trp1Δ63 ura3Δ0 vps16pr::KanMX-GAL1Pr*	this study
CUY2661	*MATa his3Δ200 leu2Δ0 met15Δ0 trp1Δ63 ura3Δ0 vps18pr::KanMX-GAL1Pr*	this study
CUY2673	*MATalpha his3Δ200 leu2Δ0 lys2Δ0 met15Δ0 trp1Δ63 ura3Δ0 vps11pt::HIS3-GAL1Pr vps16pr::natNT2-GAL1Pr*	this study
CUY2674	*MATalpha his3Δ200 leu2Δ0 lys2Δ0 met15Δ0 trp1Δ63 ura3Δ0 vps11pr::HIS3-GAL1Pr vam6pr::natNT2-GAL1Pr*	this study
CUY2675	*MATa/alpha his3Δ200/his3Δ200 met15Δ0/met15Δ0 trp1Δ63/TRP1 ura3Δ0/ura3Δ0 LEU2/leu2Δ0 LYS2/lys2Δ0 vps41pr::TRP1-GAL1pr VPS41::TAP-URA3 vam6pr::KanMX-GAL1pr vps33pr::HIS3-GAL1pr vps11pr::HIS3-GAL1Pr vps16pr::natNT2-GAL1Pr vps18pr::kanMX-GAL1Pr-3HA*	this study
CUY2721	*MATa his3Δ200 leu2Δ0 met15Δ0 trp1Δ63 ura3Δ0 vam6pr::KanMX- GAL1Pr*	this study
CUY2723	*MATalpha his3Δ200 leu2Δ0 lys2Δ0 met15Δ0 trp1Δ63 ura3Δ0 vps11pr::HIS3-GAL1pr vam6pr::natNT2-GAL1pr VPS11::TAP-kanMX*	this study
CUY2724	*MATalpha his3Δ200 leu2Δ0 lys2Δ0 met15Δ0 trp1Δ63 ura3Δ0 vps11::HIS3-GAL1pr vam6pr::natNT2-GAL1pr VAM6::TAP-URA3*	this study
CUY2725	*MATalpha his3Δ200 leu2Δ0 lys2Δ0 met15Δ0 trp1Δ63 ura3Δ0 vps11pr::HIS3-GAL1pr vam6pr::natNT2-GAL1pr VAM6::TAP-TRP1*	this study

CUY2741	*MATalpha his3Δ200 leu2Δ0 lys2Δ0 met15Δ0 trp1Δ63 ura3Δ0 vps11pr::HIS3-GAL1pr vam6pr::natNT2-GAL1pr VPS11::ΔRing-TAP-URA3*	this study
CUY2836	*MATalpha his3Δ200 leu2Δ0 lys2Δ0 met15Δ0 ura3Δ0 vps11pr::HIS3-GAL1pr vps16pr::natNT2-GAL1pr vps18pr::kanMX-GAL1pr-3HA VPS11::TAP-Ura3*	this study
CUY2837	*MATalpha his3Δ200 leu2Δ0 lys2Δ0 met15Δ0 ura3Δ0 vps11pr::HIS3-GAL1pr vps16pr::natNT2-GAL1pr vps18pr::kanMX-GAL1pr-3HA VPS16::TAP-Ura3*	this study
CUY2838	*MATalpha his3Δ200 leu2Δ0 lys2Δ0 met15Δ0 ura3Δ0 vps11pr::HIS3-GAL1pr vps16pr::natNT2-GAL1pr vps18pr::kanMX-GAL1-3HA VPS18::TAP-Ura3*	this study
CUY2839	*MATa his3Δ200 met15Δ0 trp1Δ63 ura3Δ0 vps33pr::TRP1-GAL1pr VPS33::TAP-Ura3*	this study
CUY2841	*MATalpha his3Δ200 leu2Δ0 lys2Δ0 met15Δ0 trp1Δ63 ura3Δ0 vps11pr::HIS3-GAL1pr vam6pr::natNT2-GAL1pr VPS11::TAP-kanMX vps41Δ::URA3*	this study
CUY2858	*MATa his3Δ200 leu2Δ0 met15Δ0 trp1Δ63 ura3Δ0 vps16pr::KanMX-Gal1Pr VPS16::TAP-Ura3*	this study
CUY2872	*MATalpha his3Δ200 leu2Δ0 lys2Δ0 met15Δ0 trp1Δ63 ura3Δ0 vps11pr::HIS3-GAL1pr vam6pr::natNT2-GAL1pr VAM6::TAP-URA3 vps41Δ::KanMX*	this study
CUY2873	*MATa his3Δ200 leu2Δ0 met15Δ0 trp1Δ63 ura3Δ0 vam6pr::KanMX-GAL1Pr VAM6::URA3-TAP*	this study
CUY2874	*MATa his3Δ200 leu2Δ0 met15Δ0 trp1Δ63 ura3Δ0 VPS11::ΔRING-TAP-Ura3*	this study
CUY2875	*MATa his3Δ200 leu2Δ0 met15Δ0 trp1Δ63 ura3Δ0 VPS18::ΔRING-TAP-Ura3*	this study
CUY2876	*MATa/alpha his3Δ200/his3Δ200 met15Δ0/met15Δ0 trp1Δ63/TRP1 ura3Δ0/ura3Δ0 LEU2/leu2Δ0 LYS2/lys2Δ0 vps11pr::HIS3-GAL1Pr vps16pr::natNT2 GAL1Pr vps18pr::kanMX-GAL1Pr-3HA vps33pr::TRP1-GAL1pr VPS33::TAP-Ura3*	this study
CUY2916	*MATalpha his3Δ200 leu2Δ0 lys2Δ0 met15Δ0 trp1Δ63 ura3Δ0 vps11pr::HIS3-GAL1pr VPS3::KanMX-GAL*	this study

CUY2952	*MATalpha his3Δ200 leu2Δ0 lys2Δ0 met15Δ0 trp1Δ63 ura3Δ0 vps11pr::HIS3-GAL1pr vps3pr::KanMX-GAL1pr VPS3::TAP-Ura3*	this study
CUY2975	*MATalpha his3Δ200 leu2Δ0 met15Δ0 trp1Δ63 ura3Δ0 vam6pr::TRP1-GAL1pr-TAP*	this study
CUY2989	*MATalpha his3Δ200 leu2Δ0 lys2Δ0 met15Δ0 ura3Δ0 vps11pr::HIS3-GAL1pr vps16pr::natNT2-GAL1pr vps18pr::kanMX-GAL1pr-3HA VPS33::TAP-URA*	this study
CUY3021	*MATa/alpha his3Δ200/his3Δ200 met15Δ0/met15Δ0 trp1Δ63 ura3Δ0/ura3Δ0 lys2Δ0 leu2Δ0 vps33pr::TRP1-GAL1pr vps11pr::HIS3-GAL1pr vps16pr::natNT2-GAL1pr vps18pr::kanMX-GAL1pr-3HA VPS11::TAP-Ura3*	this study
CUY3022	*MATa/alpha his3Δ200/his3Δ200 met15Δ0/met15Δ0 trp1Δ63 ura3Δ0/ura3Δ0 leu2Δ0 lys2Δ0 vps33pr::TRP1-GAL1pr vps11pr::HIS3-GAL1pr vps16pr::natNT2-GAL1pr vps18pr::kanMX-GAL1pr-3HA VPS16::TAP-Ura3*	this study
CUY3023	*MATa/alpha his3Δ200/his3Δ200 met15Δ0/met15Δ0 trp1Δ63 ura3Δ0/ura3Δ0 leu2Δ0 lys2Δ0 vps33pr::TRP1-GAL1pr vps11pr::HIS3-GAL1pr vps16pr::natNT2-GAL1pr vps18pr::kanMX-GAL1pr-3HA VPS18::TAP-Ura3*	this study
CUY3028	*MATa/alpha his3Δ200/his3Δ200 met15Δ0/met15Δ0 leu2Δ0 lys2Δ0 trp1Δ63 ura3Δ0/ura3Δ0 vps41pr::TRP1-GAL1pr vam6pr::KanMX-GAL1pr vps33pr::HIS3-Gal1pr vps11pr::HIS3-GAL1pr vps16pr::natNT2-GAL1pr vps18pr::kanMX-GAL1pr-3HA*	this study
CUY3050	*MATalpha his3Δ200 leu2Δ0 lys2Δ0 met15Δ0 ura3Δ0 vps11pr::HIS3-GAL1pr vps18pr::kanMX-GAL1pr-3HA*	this study
CUY3067	*MATalpha his3Δ200 leu2Δ0 met15Δ0 trp1Δ63 ura3Δ0 vam6pr::TRP1-GAL1pr-TAP vps11Δ::URA3*	this study
CUY3070	*MATa/alpha lys2Δ0 met15Δ0 ura3Δ0*	this study
CUY3095	*MATalpha his3Δ200 leu2Δ0 lys2Δ0 met15Δ0 trp1Δ63 ura3Δ0 vps11pr::HIS3-GAL1pr vam6pr::natNT2-GAL1pr VAM6::TAP-URA3 VPS11ΔRING::TRP1*	this study
CUY3210	*MATa his3Δ200 leu2Δ0 met15Δ0 trp1Δ63 ura3Δ0 vps18pr::KanMX-GAL1Pr VPS18::TAP-URA3*	this study

CUY3238	*MATalpha/a his3Δ200/his3Δ200 leu2Δ0/leu2Δ0 met15Δ0/met15Δ0 trp1Δ63/trp1Δ63 ura3Δ0/ura3Δ0 vps33pr::HIS3-GAL1pr vps16pr::KanMX-Gal1Pr VPS16::TAP-Ura3*	this study
CUY3246	*MATa/alpha his3Δ200/his3Δ200 leu2Δ0 lys2Δ0 met15Δ/met15Δ0 trp1Δ63 ura3Δ0/ura3Δ0 vps11pr::HIS3-GAL1pr vps16pr::natNT2-GAL1pr vps18pr::kanMX-GAL1pr-3HA VPS11::ΔRing-TAP-URA3 vps33pr::TRP1-GALpr*	this study
CUY3247	*MATa/alpha his3Δ200/his3Δ200 trp1Δ63 leu2Δ0 lys2Δ0 met15Δ0/met15Δ0 ura3Δ0/ura3Δ0 vps11pr::HIS3-GAL1pr vps16pr::natNT2-GAL1pr vps18pr::kanMX-GAL1pr-3HA VPS18::ΔRING-TAP-URA3 vps33pr::TRP1-GAL1pr*	this study
CUY3248	*MATa/alpha his3Δ200/his3Δ200 leu2Δ0 lys2Δ0 met15Δ0/met15Δ0 ura3Δ0/ura3Δ0 vps11pr::HIS3-GAL1pr vps16pr::natNT2-GAL1pr vps18pr::kanMX-GAL1pr-3HA VPS11::ΔRing-TAP-URA3 vps41pr::TRP1-GAL1pr vam6pr::KanMX-GAL1pr vps33pr::HIS3-Gal1pr*	this study
CUY3249	*MATa/alpha his3Δ200/his3Δ200 leu2Δ0 lys2Δ0 met15Δ0/met15Δ0 ura3Δ0/ura3Δ0 trp1Δ63 vps11pr::HIS3-GAL1pr vps16pr::natNT2-GAL1pr vps18pr::kanMX-GAL1pr-3HA VPS18::ΔRING-TAP-URA3 vps41pr::TRP1-GAL1pr vam6pr::KanMX-GAL1pr vps33pr::HIS3-GAL1pr*	this study
CUY3250	*MATalpha his3Δ200/his3Δ200 leu2Δ0 lys2Δ0 met15Δ0/met15Δ0 ura3Δ0/ura3Δ0 trp1Δ63 vps11pr::HIS3-GAL1pr vps16pr::natNT2-GAL1pr vps18pr::kanMX-GAL1pr-3HA VPS11::ΔRing-TAP-URA3 vps33pr::TRP1-GAL1pr vps3pr::KanMX-GAL1pr vps8pr::NatNT2-GAL1pr-3HA*	this study
CUY3251	*MATalpha his3Δ200/his3Δ200 leu2Δ0 lys2Δ0 met15Δ0/met15Δ0 ura3Δ0/ura3Δ0 trp1Δ63 vps11pr::HIS3-GAL1pr vps16pr::natNT2-GAL1pr vps18pr::kanMX-GAL1pr-3HA VPS18::ΔRING-TAP-URA3 vps33pr::TRP1-GAL1pr vps3pr::KanMX-GAL1pr vps8pr::NatNT2-Gal1pr-3HA*	this study
CUY3297	*MATalpha his3Δ200 leu2Δ0 met15Δ0 trp1Δ63 ura3Δ0 VAM6::TAP-kanMX4 vps41pr::NatNT2-GALLpr*	this study

CUY3298	*MATalpha his3Δ200 leu2Δ0 met15Δ0 trp1Δ63 ura3Δ0 VAM6::TAP-kanMX4 vps41pr::NatNT2-GALSpr*	this study
CUY3323	*MATalpha his3Δ200 leu2Δ0 lys2Δ0 met15Δ0 trp1Δ63 ura3Δ0 vps11pr::HIS3-GAL1pr vps3pr::KanMX-GAL1pr VPS11::ΔRING-TAP-URA*	this study
CUY3335	*MATa/alpha his3Δ200/his3Δ200 leu2Δ0/leu2Δ0 lys2Δ0 met15Δ0/met15Δ0 trp1Δ63 ura3Δ0/ura3Δ0 vam6pr::KanMX- GAL1Pr vps11pr::HIS3-GAL1Pr vps18pr::kanMX-GAL1Pr-3HA VPS11::TAP-URA3*	this study
CUY3336	*MATalpha/a his3Δ200/his3Δ200 leu2Δ0 lys2Δ0 met15Δ0/met5Δ0 trp1Δ63/trp1Δ63 ura3Δ/ura3Δ0 vps18pr::KanMX-GAL1Pr-3HA vps41pr::TRP1-GAL1pr VPS41::TAP-URA3*	this study
CUY3347	*MATa his3Δ200 met15Δ0 trp1Δ63 ura3Δ0 vps33pr::TRP1-GAL1pr VPS33::TAP-Ura3 vps16pr::KanMX-GAL1pr*	this study
CUY3361	*MATalpha/a his3Δ200/his3Δ200 leu2Δ0/leu2Δ0 lys2Δ0 met15Δ0/met15Δ0 trp1Δ63/trp1Δ63 ura3Δ0/ura3Δ0 vps11pr::HIS3-GAL1pr vps18pr::kanMX-GAL1pr-3HA vam6pr::KanMX-GAL1Pr VAM6::URA3-TAP*	this study
CUY3362	*MATalpha/a his3Δ200/his3Δ200 leu2Δ0 lys2Δ0 met15Δ0/met15Δ0 trp1Δ63/trp1Δ63 ura3Δ0/ura3Δ0 vps11pr::HIS3-GAL1pr vps18pr::kanMX-GAL1pr-3HA vps41pr::TRP1-GAL1pr vam6pr::KanMX-GAL1pr VPS41::TAP-URA3*	this study
CUY3363	*MATalpha/a his3Δ200/his3Δ200 leu2Δ0 lys2Δ0 met15Δ0/met5Δ0 trp1Δ63/trp1Δ63 ura3Δ0/ura3Δ0 vps11pr::HIS3-GAL1pr vps18pr::kanMX-GAL1pr-3HA vps41pr::TRP1-GAL1pr VPS41::TAP-URA3*	this study
CUY3364	*MATa/alpha his3Δ200/his3Δ200 leu2Δ0 lys2Δ0 met15Δ0/met15Δ0 trp1Δ63 ura3Δ0/ura3Δ0 vps41pr::TRP1-GAL1pr vam6pr::KanMX-GAL1pr vps11pr::HIS3-GAL1Pr vps18pr::kanMX-GAL1Pr-3HA VPS11::TAP-URA3*	this study
CUY3396	*MATalpha his3Δ200 leu2Δ0 lys2Δ0 met15Δ0 trp1Δ63 ura3Δ0 VPS11::HIS3-GAL vam6pr::natNT2-GAL1pr VAM6::TAP-URA3 vps18pr::TRP1-GAL1*	this study

CUY3407	*MATalpha his3Δ200 leu2Δ0 lys2Δ0 met15Δ0 trp1Δ63 ura3Δ0 vps41pr::TRP1-GAL1pr*	this study
CUY3408	*MATa his3Δ200 leu2Δ0 met15Δ0 trp1Δ63 ura3Δ0 vam6pr::KanMX-GAL1Pr VAM2::URA3-PHO5-GFP*	this study
CUY3435	*MATa his3Δ200 met15Δ0 trp1Δ63 ura3Δ0 vps41pr::TRP1-GAL1pr vam6pr::KanMX-GAL1pr VAM6::TAP-URA3*	this study
CUY3436	*MATa his3Δ200 met15Δ0 trp1Δ63 ura3Δ0 vps41pr::TRP1-GAL1pr vam66pr::KanMX-GAL1pr ypt7pr::PHO5pr-GFP*	this study
CUY3446	*MATalpha/a his3Δ200/his3Δ200 leu2Δ0/leu2Δ0 lys2Δ0 met15Δ0/met15Δ0 trp1Δ63 ura3Δ0/ura3Δ0 vps11pr::HIS3-GAL1Pr vps16pr::natNT2-GAL1Pr vps18pr::kanMX-GAL1Pr-3HA vam6pr::KanMX-GAL1Pr*	this study
CUY3447	*MATalpha/a his3Δ200/his3Δ200 leu2Δ0 lys2Δ0 met15Δ0/met15Δ0 trp1Δ63/trp1Δ63 ura3Δ0/ura3Δ0 vps11pr::HIS3-GAL1pr vps18pr::kanMX-GAL1pr-3HA vps41pr::TRP1-GAL1pr vam66pr::KanMX-GAL1pr VAM6::TAP-URA3*	this study
CUY3448	*MATalpha/a his3Δ200/his3Δ200 leu2Δ0 lys2Δ0 met15Δ0/met15Δ0 trp1Δ63 ura3Δ0/ura3Δ0 vps11pr::HIS3-GAL1Pr vps16pr::natNT2-GAL1Pr vps18pr::kanMX-GAL1Pr-3HA vps41pr::TRP1-GAL1pr vam6pr::KanMX-GAL1pr VAM6::TAP-URA3*	this study
CUY3491	*MATa his3Δ200 leu2Δ0 met15Δ0 trp1Δ63 ura3Δ0 vps11pr::KanMX-GAL1Pr VPS11::TAP-URA3*	this study
CUY3492	*MATa his3Δ200 leu2Δ0 met15Δ0 trp1Δ63 ura3Δ0 vps11pr::KanMX-GAL1Pr VPS11::ΔRING-TAP-URA3*	this study
CUY3493	*MATa his3Δ200 met5Δ0 trp1Δ63 ura3Δ0 vps41pr::TRP1-GAL1pr VPS41::TAP-URA3 vps18pr::HIS-GAL1pr vam66pr::natNT2-GAL1pr*	this study
CUY3588	*MATa/alpha his3Δ200 leu2Δ0 lys2Δ0 met15Δ0 trp1Δ63/trp1Δ63 ura3Δ0/ura3Δ0 vam6pr::KanMX-GAL1Pr VAM6::URA3-TAP*	this study
CUY3590	*MATa/alpha his3Δ200 lys2Δ0 met15Δ0 trp1Δ63/trp1Δ63 ura3Δ0/ura3Δ0 vps33pr::TRP1-GAL1pr VPS33::TAP-Ura3*	this study

CUY3645	*MATa/alpha his3Δ200/his3Δ200 leu2Δ0 lys2Δ0 met15Δ0/met15Δ0 trp1Δ63 ura3Δ0/ura3Δ0 vps11pr::HIS3-GAL1Pr vps16pr::natNT2-GAL1Pr vps18pr::kanMX-GAL1Pr-3HA vps41pr::TRP1-GAL1pr vam6pr::KanMX-GAL1pr vps33pr::HIS3-GAL1pr VAM6::TAP-URA3*	this study
CUY3738	*MATalpha his3Δ200 leu2Δ0 met15Δ0 trp1Δ63 ura3Δ0 VPS11::GFP-hphNT1 vps11pr::TRP-GAL1pr*	this study
CUY3740	*MATa his3Δ200 leu2Δ0 met15Δ0 trp1Δ63 ura3Δ0 VPS18::GFP-hphNT1 vps18pr::TRP-GAL1pr*	this study
CUY3742	*MATa his3Δ1 leu2Δ0 met15Δ0 ura3Δ0 VAM6::GFP-HIS3 vam6pr::kanMX-GAL1pr*	this study
CUY3770	*MATa/alpha his3Δ200/his3Δ200 leu2Δ0/leu2Δ0 lys2Δ0 met15Δ0/met15Δ0 trp1Δ63/trp1Δ63 ura3Δ0/ura3Δ0 vps11pr::HIS3-GAL1Pr vam6pr::natNT2-GAL1Pr VPS18::GFP-hphNT1 vps18pr::TRP-GAL1pr*	this study
CUY3772	*MATa/alpha his3Δ200/his3Δ200 leu2Δ0/leu2Δ0 met15Δ0/met15Δ0 trp1Δ63/trp1Δ63 ura3Δ0/ura3Δ0 vps18pr::KanMX-GAL1Pr VPS11::GFP-hphNT1 vps11pr::TRP-GAL1pr*	this study
CUY3773	*MATa/alpha his3Δ200/his3Δ200 leu2Δ0/leu2Δ0 met15Δ0/met15Δ0 trp1Δ63/trp1Δ63 ura3Δ0/ura3Δ0 vam6pr::KanMX-GAL1Pr VPS11::GFP-hphNT1 vps11pr::TRP-GAL1pr*	this study
CUY3775	*MATa/alpha his3Δ200/his3Δ200 leu2Δ0/leu2Δ0 lys2Δ0 met15Δ0/met15Δ0 trp1Δ63/trp1Δ63 ura3Δ0/ura3Δ0 vps11pr::HIS3-GAL1pr VPS18::GFP-hphNT1 vps18pr::TRP-GAL1pr*	this study
CUY3789	*MATa/alpha his3Δ200/his3Δ200 leu2Δ0/leu20 lys2Δ0 met15Δ0/met15Δ0 trp1Δ63/trp1Δ63 ura3Δ0/ura3Δ0 vps11pr::HIS3-GAL1pr vam6pr::kanMX-GAL1pr VAM6::GFP-TRP1*	this study
CUY3834	*MATalpha his3Δ200 leu2Δ0 lys2Δ0 met15Δ0 ura3Δ0 vps11pr::HIS3-GAL1pr vps18pr::kanMX-GAL1-3HA VPS18::TAP-URA3*	this study
CUY3916	*MATa/alpha his3Δ200/his3Δ200 leu2Δ0 lys2Δ0 met15Δ0/met15Δ0 trp1Δ63/trp1Δ63 ura3Δ0/ura3Δ0 vps33pr::TRP1-GAL1pr vps16pr::kanMX-GAL1Pr-3HA*	this study

6 References

Ahle, S., and E. Ungewickell. 1986. Purification and properties of a new clathrin assembly protein. *EMBO J*. 5:3143-9.

Amerik, A.Y., J. Nowak, S. Swaminathan, and M. Hochstrasser. 2000. The Doa4 deubiquitinating enzyme is functionally linked to the vacuolar protein-sorting and endocytic pathways. *Mol Biol Cell*. 11:3365-80.

Baars, T.L., S. Petri, C. Peters, and A. Mayer. 2007. Role of the V-ATPase in regulation of the vacuolar fission-fusion equilibrium. *Mol Biol Cell*. 18:3873-82.

Banta, L.M., T.A. Vida, P.K. Herman, and S.D. Emr. 1990. Characterization of yeast Vps33p, a protein required for vacuolar protein sorting and vacuole biogenesis. *Mol Cell Biol*. 10:4638-49.

Bayer, M.J., C. Reese, S. Buhler, C. Peters, and A. Mayer. 2003. Vacuole membrane fusion: V0 functions after trans-SNARE pairing and is coupled to the Ca2+-releasing channel. *The Journal of Cell Biology*. 162:211-22.

Beck, R., Z. Sun, F. Adolf, C. Rutz, J. Bassler, K. Wild, I. Sinning, E. Hurt, B. Brügger, J. Béthune, and F. Wieland. 2008. Membrane curvature induced by Arf1-GTP is essential for vesicle formation. *Proc Natl Acad Sci USA*. 105:11731-6.

Behnia, R., and S. Munro. 2005. Organelle identity and the signposts for membrane traffic. *Nature*. 438:597-604.

BERTANI, G. 1951. Studies on lysogenesis. I. The mode of phage liberation by lysogenic Escherichia coli. *J Bacteriol*. 62:293-300.

Boeddinghaus, C., A.J. Merz, R. Laage, and C. Ungermann. 2002. A cycle of Vam7p release from and PtdIns 3-P-dependent rebinding to the yeast vacuole is required for homotypic vacuole fusion. *The Journal of Cell Biology*. 157:79-89.

Bonangelino, C.J., N.L. Catlett, and L.S. Weisman. 1997. Vac7p, a novel vacuolar protein, is required for normal vacuole inheritance and morphology. *Mol Cell Biol*. 17:6847-58.

Bonangelino, C.J., J.J. Nau, J.E. Duex, M. Brinkman, A.E. Wurmser, J.D. Gary, S. Emr, and L. Weisman. 2002. Osmotic stress-induced increase of phosphatidylinositol 3,5-bisphosphate requires Vac14p, an activator of the lipid kinase Fab1p. *The Journal of Cell Biology*. 156:1015-28.

Bos, J., H. Rehmann, and A. Wittinghofer. 2007. GEFs and GAPs: Critical Elements in the Control of Small G Proteins. *Cell*. 129:865-877.

Bowers, K., and T. Stevens. 2005. Protein transport from the late Golgi to the vacuole in the yeast. *Biochimica et Biophysica Acta (BBA) - Molecular Cell Research*. 1744:438-454.

Boyd, C., T. Hughes, M. Pypaert, and P. Novick. 2004. Vesicles carry most exocyst subunits to exocytic sites marked by the remaining two subunits, Sec3p and Exo70p. *The Journal of Cell Biology*. 167:889-901.

Brett, C., R. Plemel, B. Lobinger, M. Vignali, S. Fields, and A. Merz. 2008. Efficient termination of vacuolar Rab GTPase signaling requires coordinated action by a GAP and a protein kinase. *The Journal of Cell Biology*. 182:1141-1151.

Cabrera, M., C. Ostrowicz, M. Mari, T.J. Lagrassa, F. Reggiori, and C. Ungermann. 2009. Vps41 Phosphorylation and the Rab Ypt7 Control the Targeting of the HOPS Complex to Endosome-vacuole Fusion Sites. *Mol Biol Cell*.

Cai, H., K. Reinisch, and S. Ferro-Novick. 2007a. Coats, tethers, Rabs, and SNAREs work together to mediate the intracellular destination of a transport vesicle. *Developmental Cell*. 12:671-82.

Cai, H., S. Yu, S. Menon, Y. Cai, D. Lazarova, C. Fu, K. Reinisch, J.C. Hay, and S. Ferro-Novick. 2007b. TRAPPI tethers COPII vesicles by binding the coat subunit Sec23. *Nature*. 445:941-4.

Cai, H., Y. Zhang, M. Pypaert, L. Walker, and S. Ferro-Novick. 2005. Mutants in trs120 disrupt traffic from the early endosome to the late Golgi. *The Journal of Cell Biology*. 171:823-33.

Cai, Y., H. Chin, D. Lazarova, S. Menon, C. Fu, H. Cai, A. Sclafani, D. Rodgers, E. Delacruz, and S. Ferronovick. 2008. The Structural Basis for Activation of the Rab Ypt1p by the TRAPP Membrane-Tethering Complexes. *Cell*. 133:1202-1213.

Cheever, M.L., T.K. Sato, T. de Beer, T.G. Kutateladze, S.D. Emr, and M. Overduin. 2001. Phox domain interaction with PtdIns(3)P targets the Vam7 t-SNARE to vacuole membranes. *Nat Cell Biol*. 3:613-8.

Chen, X., D. Araç, T.M. Wang, C.J. Gilpin, J. Zimmerberg, and J. Rizo. 2006. SNARE-mediated lipid mixing depends on the physical state of the vesicles. *Biophys J*. 90:2062-74.

Chernomordik, L., and M. Kozlov. 2003. PROTEIN-LIPID INTERPLAY IN FUSION AND FISSION OF BIOLOGICAL MEMBRANES *. *Annu Rev Biochem*. 72:175-207.

Chernomordik, L., and M. Kozlov. 2008. Mechanics of membrane fusion. *Nat Struct Mol Biol*. 15:675-683.

Collins, K., N. Thorngren, R. Fratti, and W. Wickner. 2005. Sec17p and HOPS, in distinct SNARE complexes, mediate SNARE complex disruption or assembly for fusion. *EMBO J*. 24:1775-1786.

Collins, K., and W. Wickner. 2007. Trans-SNARE complex assembly and yeast vacuole membrane fusion. *Proc Natl Acad Sci USA*. 104:8755-60.

Conibear, E., J.N. Cleck, and T.H. Stevens. 2003. Vps51p mediates the association of the GARP (Vps52/53/54) complex with the late Golgi t-SNARE Tlg1p. *Mol Biol Cell*. 14:1610-23.

Conibear, E., and T.H. Stevens. 2000. Vps52p, Vps53p, and Vps54p form a novel multisubunit complex required for protein sorting at the yeast late Golgi. *Mol Biol Cell*. 11:305-23.

Conradt, B., A. Haas, and W. Wickner. 1994. Determination of four biochemically distinct, sequential stages during vacuole inheritance in vitro. *The Journal of Cell Biology*. 126:99-110.

Conradt, B., J. Shaw, T. Vida, S. Emr, and W. Wickner. 1992. In vitro reactions of vacuole inheritance in Saccharomyces cerevisiae. *The Journal of Cell Biology*. 119:1469-79.

Cooper, A.A., and T.H. Stevens. 1996. Vps10p cycles between the late-Golgi and prevacuolar compartments in its function as the sorting receptor for multiple yeast vacuolar hydrolases. *The Journal of Cell Biology*. 133:529-41.

Costaguta, G., C.J. Stefan, E.S. Bensen, S.D. Emr, and G.S. Payne. 2001. Yeast Gga coat proteins function with clathrin in Golgi to endosome transport. *Mol Biol Cell*. 12:1885-96.

Cowles, C.R., G. Odorizzi, G.S. Payne, and S.D. Emr. 1997a. The AP-3 adaptor complex is essential for cargo-selective transport to the yeast vacuole. *Cell*. 91:109-18.

Cowles, C.R., W.B. Snyder, C.G. Burd, and S.D. Emr. 1997b. Novel Golgi to vacuole delivery pathway in yeast: identification of a sorting determinant and required transport component. *EMBO J*. 16:2769-82.

Darsow, T., C.G. Burd, and S.D. Emr. 1998. Acidic di-leucine motif essential for AP-3-dependent sorting and restriction of the functional specificity of the Vam3p vacuolar t-SNARE. *The Journal of Cell Biology*. 142:913-22.

Darsow, T., D.J. Katzmann, C.R. Cowles, and S.D. Emr. 2001. Vps41p function in the alkaline phosphatase pathway requires homo-oligomerization and interaction with AP-3 through two distinct domains. *Mol Biol Cell*. 12:37-51.

Darsow, T., S.E. Rieder, and S.D. Emr. 1997. A multispecificity syntaxin homologue, Vam3p, essential for autophagic and biosynthetic protein transport to the vacuole. *The Journal of Cell Biology*. 138:517-29.

Dell'Angelica, E.C., J. Klumperman, W. Stoorvogel, and J.S. Bonifacino. 1998. Association of the AP-3 adaptor complex with clathrin. *Science*. 280:431-4.

Dennison, S.M., M.E. Bowen, A. Brunger, and B.R. Lentz. 2006. Neuronal SNAREs do not trigger fusion between synthetic membranes but do promote PEG-mediated membrane fusion. *Biophys J*. 90:1661-75.

Deshaies, R.J., S.L. Sanders, D.A. Feldheim, and R. Schekman. 1991. Assembly of yeast Sec proteins involved in translocation into the endoplasmic reticulum into a membrane-bound multisubunit complex. *Nature*. 349:806-8.

Devos, D., S. Dokudovskaya, F. Alber, R. Williams, B. Chait, A. Sali, and M. Rout. 2004. Components of coated vesicles and nuclear pore complexes share a common molecular architecture. *Plos Biol*. 2:e380.

Dietrich, L.E., R. Gurezka, M. Veit, and C. Ungermann. 2004. The SNARE Ykt6 mediates protein palmitoylation during an early stage of homotypic vacuole fusion. *EMBO J*. 23:45-53.

Dietrich, L.E., T.J. LaGrassa, J. Rohde, M. Cristodero, C.T. Meiringer, and C. Ungermann. 2005. ATP-independent control of Vac8 palmitoylation by a SNARE subcomplex on yeast vacuoles. *J Biol Chem*. 280:15348-55.

Dilcher, M., B. Köhler, and G.F. von Mollard. 2001. Genetic interactions with the yeast Q-SNARE VTI1 reveal novel functions for the R-SNARE YKT6. *J Biol Chem*. 276:34537-44.

Dove, S.K., F.T. Cooke, M.R. Douglas, L.G. Sayers, P.J. Parker, and R.H. Michell. 1997. Osmotic stress activates phosphatidylinositol-3,5-bisphosphate synthesis. *Nature*. 390:187-92.

Drake, M.T., Y. Zhu, and S. Kornfeld. 2000. The assembly of AP-3 adaptor complex-containing clathrin-coated vesicles on synthetic liposomes. *Mol Biol Cell*. 11:3723-36.

Drin, G., J.F. Casella, R. Gautier, T. Boehmer, T.U. Schwartz, and B. Antonny. 2007. A general amphipathic alpha-helical motif for sensing membrane curvature. *Nat Struct Mol Biol*. 14:138-46.

Dulubova, I., T. Yamaguchi, D. Arac, H. Li, I. Huryeva, S.W. Min, J. Rizo, and T.C. Sudhof. 2003. Convergence and divergence in the mechanism of SNARE binding by Sec1/Munc18-like proteins. *Proc Natl Acad Sci USA*. 100:32-7.

Dulubova, I., T. Yamaguchi, Y. Wang, T.C. Südhof, and J. Rizo. 2001. Vam3p structure reveals conserved and divergent properties of syntaxins. *Nat Struct Biol*. 8:258-64.

Fasshauer, D., W. Antonin, M. Margittai, S. Pabst, and R. Jahn. 1999. Mixed and non-cognate SNARE complexes. Characterization of assembly and biophysical properties. *J Biol Chem*. 274:15440-6.

Fasshauer, D., D. Bruns, B. Shen, R. Jahn, and A.T. Brünger. 1997a. A structural change occurs upon binding of syntaxin to SNAP-25. *J Biol Chem*. 272:4582-90.

Fasshauer, D., H. Otto, W.K. Eliason, R. Jahn, and A.T. Brünger. 1997b. Structural changes are associated with soluble N-ethylmaleimide-sensitive fusion protein attachment protein receptor complex formation. *J Biol Chem*. 272:28036-41.

Fasshauer, D., R.B. Sutton, A.T. Brunger, and R. Jahn. 1998. Conserved structural features of the synaptic fusion complex: SNARE proteins reclassified as Q- and R-SNAREs. *Proc Natl Acad Sci USA*. 95:15781-6.

Finger, F.P., T.E. Hughes, and P. Novick. 1998. Sec3p is a spatial landmark for polarized secretion in budding yeast. *Cell*. 92:559-71.

Fratti, R., K. Collins, C.M. Hickey, and W. Wickner. 2007. Stringent 3Q.1R composition of the SNARE 0-layer can be bypassed for fusion by compensatory SNARE mutation or by lipid bilayer modification. *J Biol Chem*. 282:14861-7.

Fratti, R., Y. Jun, A.J. Merz, N. Margolis, and W. Wickner. 2004. Interdependent assembly of specific regulatory lipids and membrane fusion proteins into the vertex ring domain of docked vacuoles. *The Journal of Cell Biology*. 167:1087-98.

Fukuda, M. 2008. Membrane traffic in the secretory pathway. *Cell. Mol. Life Sci.* 65:2801-2813.

Fukuda, R., J.A. McNew, T. Weber, F. Parlati, T. Engel, W. Nickel, J.E. Rothman, and T.H. Söllner. 2000. Functional architecture of an intracellular membrane t-SNARE. *Nature*. 407:198-202.

Garrett, M.D., J.E. Zahner, C.M. Cheney, and P.J. Novick. 1994. GDI1 encodes a GDP dissociation inhibitor that plays an essential role in the yeast secretory pathway. *EMBO J*. 13:1718-28.

Gerhardt, B., T.J. Kordas, C.M. Thompson, P. Patel, and T. Vida. 1998. The vesicle transport protein Vps33p is an ATP-binding protein that localizes to the cytosol in an energy-dependent manner. *J Biol Chem*. 273:15818-29.

Gromley, A., C. Yeaman, J. Rosa, S. Redick, C.T. Chen, S. Mirabelle, M. Guha, J. Sillibourne, and S.J. Doxsey. 2005. Centriolin anchoring of exocyst and SNARE complexes at the midbody is required for secretory-vesicle-mediated abscission. *Cell*. 123:75-87.

Haas, A., B. Conradt, and W. Wickner. 1994. G-protein ligands inhibit in vitro reactions of vacuole inheritance. *The Journal of Cell Biology*. 126:87-97.

Haas, A., and W. Wickner. 1996. Homotypic vacuole fusion requires Sec17p (yeast alpha-SNAP) and Sec18p (yeast NSF). *EMBO J*. 15:3296-305.

Hama, H., G.G. Tall, and B.F. Horazdovsky. 1999. Vps9p is a guanine nucleotide exchange factor involved in vesicle-mediated vacuolar protein transport. *J Biol Chem*. 274:15284-91.

Hammer, J.A., and X.S. Wu. 2002. Rabs grab motors: defining the connections between Rab GTPases and motor proteins. *Current Opinion in Cell Biology*. 14:69-75.

Heuser, J.E., and R.G. Anderson. 1989. Hypertonic media inhibit receptor-mediated endocytosis by blocking clathrin-coated pit formation. *The Journal of Cell Biology*. 108:389-400.

Hirst, J., M.R. Lindsay, and M.S. Robinson. 2001. GGAs: roles of the different domains and comparison with AP-1 and clathrin. *Mol Biol Cell*. 12:3573-88.

Hofmann, M., K. Peplowska, J. Rohde, B. Poschner, C. Ungermann, and D. Langosch. 2006. Self-interaction of a SNARE Transmembrane Domain Promotes the Hemifusion-to-fusion Transition. *Journal of Molecular Biology*. 364:1048-1060.

Holthuis, J.C., G. van Meer, and K. Huitema. 2003. Lipid microdomains, lipid translocation and the organization of intracellular membrane transport (Review). *Mol Membr Biol*. 20:231-41.

Hurley, J., and S. Emr. 2006. The ESCRT complexes: structure and mechanism of a membrane-trafficking network. *Annual review of biophysics and biomolecular structure*. 35:277-98.

Jahn, R., and R. Scheller. 2006. SNAREs — engines for membrane fusion. *Nat Rev Mol Cell Biol*. 7:631-643.

Janke, C., M. Magiera, N. Rathfelder, C. Taxis, S. Reber, H. Maekawa, A. Moreno-Borchart, G. Doenges, E. Schwob, E. Schiebel, and M. Knop. 2004. A versatile toolbox for PCR-based tagging of yeast genes: new fluorescent proteins, more markers and promoter substitution cassettes. *Yeast*. 21:947-962.

Jørgensen, M.U., S.D. Emr, and J.R. Winther. 1999. Ligand recognition and domain structure of Vps10p, a vacuolar protein sorting receptor in Saccharomyces cerevisiae. *Eur J Biochem*. 260:461-9.

Jun, Y., R. Fratti, and W. Wickner. 2004. Diacylglycerol and its formation by phospholipase C regulate Rab- and SNARE-dependent yeast vacuole fusion. *J Biol Chem*. 279:53186-95.

Jun, Y., N. Thorngren, V. Starai, R. Fratti, K. Collins, and W. Wickner. 2006. Reversible, cooperative reactions of yeast vacuole docking. *EMBO J*. 25:5260-5269.

Jun, Y., and W. Wickner. 2007. Assays of vacuole fusion resolve the stages of docking, lipid mixing, and content mixing. *Proc Natl Acad Sci USA*. 104:13010-5.

Kanaseki, T., and K. Kadota. 1969. The "vesicle in a basket". A morphological study of the coated vesicle isolated from the nerve endings of the guinea pig brain, with special reference to the mechanism of membrane movements. *The Journal of Cell Biology*. 42:202-20.

Kato, M., and W. Wickner. 2003. Vam10p defines a Sec18p-independent step of priming that allows yeast vacuole tethering. *Proc Natl Acad Sci USA*. 100:6398-403.

Kim, D.W., T. Massey, M. Sacher, M. Pypaert, and S. Ferro-Novick. 2001. Sgf1p, a new component of the Sec34p/Sec35p complex. *Traffic*. 2:820-30.

Kim, Y.G., S. Raunser, C. Munger, J. Wagner, Y.L. Song, M. Cygler, T. Walz, B.H. Oh, and M. Sacher. 2006. The architecture of the multisubunit TRAPP I complex suggests a model for vesicle tethering. *Cell*. 127:817-30.

Kirchhausen, T. 2000. Three ways to make a vesicle. *Nat Rev Mol Cell Biol*. 1:187-98.

Kirchhausen, T., and S.C. Harrison. 1981. Protein organization in clathrin trimers. *Cell*. 23:755-61.

Klionsky, D., R. Cueva, and D.S. Yaver. 1992. Aminopeptidase I of Saccharomyces cerevisiae is localized to the vacuole independent of the secretory pathway. *The Journal of Cell Biology*. 119:287-99.

Klionsky, D.J. 2005. The molecular machinery of autophagy: unanswered questions. *Journal of Cell Science*. 118:7-18.

Kohtz, D.S., and S. Puszkin. 1988. A neuronal protein (NP185) associated with clathrin-coated vesicles. Characterization of NP185 with monoclonal antibodies. *J Biol Chem*. 263:7418-25.

Koumandou, V.L., J. Dacks, R.M. Coulson, and M. Field. 2007. Control systems for membrane fusion in the ancestral eukaryote; evolution of tethering complexes and SM proteins. *BMC Evol Biol*. 7:29.

Kümmel, D., and U. Heinemann. 2008. Diversity in structure and function of tethering complexes: evidence for different mechanisms in vesicular transport regulation. *Curr Protein Pept Sci*. 9:197-209.

Laage, R., and C. Ungermann. 2001. The N-terminal domain of the t-SNARE Vam3p coordinates priming and docking in yeast vacuole fusion. *Mol Biol Cell*. 12:3375-85.

Laemmli, U.K. 1970. Cleavage of structural proteins during the assembly of the head of bacteriophage T4. *Nature*. 227:680-5.

LaGrassa, T.J., and C. Ungermann. 2005. The vacuolar kinase Yck3 maintains organelle fragmentation by regulating the HOPS tethering complex. *The Journal of Cell Biology*. 168:401-14.

Lee, M.C., L. Orci, S. Hamamoto, E. Futai, M. Ravazzola, and R. Schekman. 2005. Sar1p N-terminal helix initiates membrane curvature and completes the fission of a COPII vesicle. *Cell*. 122:605-17.

Lee, S.A., J. Kovacs, R.V. Stahelin, M.L. Cheever, M. Overduin, T.G. Setty, C.G. Burd, W. Cho, and T.G. Kutateladze. 2006. Molecular mechanism of membrane docking by the Vam7p PX domain. *J Biol Chem*. 281:37091-101.

Lutzmann, M., R. Kunze, A. Buerer, U. Aebi, and E. Hurt. 2002. Modular self-assembly of a Y-shaped multiprotein complex from seven nucleoporins. *EMBO J*. 21:387-97.

Machner, M., and R. Isberg. 2007. A Bifunctional Bacterial Protein Links GDI Displacement to Rab1 Activation. *Science*. 318:974-977.

Marcusson, E.G., B.F. Horazdovsky, J.L. Cereghino, E. Gharakhanian, and S.D. Emr. 1994. The sorting receptor for yeast vacuolar carboxypeptidase Y is encoded by the VPS10 gene. *Cell*. 77:579-86.

Markgraf, D.F., K. Peplowska, and C. Ungermann. 2007. Rab cascades and tethering factors in the endomembrane system. *FEBS Letters*. 581:2125-30.

Matanis, T., A. Akhmanova, P. Wulf, E. Del Nery, T. Weide, T. Stepanova, N. Galjart, F. Grosveld, B. Goud, C. De Zeeuw, A. Barnekow, and C. Hoogenraad. 2002. Bicaudal-D regulates COPI-independent Golgi–ER transport by recruiting the dynein–dynactin motor complex. *Nat Cell Biol*. 4:986-992.

Mayer, A., and W. Wickner. 1997. Docking of yeast vacuoles is catalyzed by the Ras-like GTPase Ypt7p after symmetric priming by Sec18p (NSF). *The Journal of Cell Biology*. 136:307-17.

Mayer, A., W. Wickner, and A. Haas. 1996. Sec18p (NSF)-driven release of Sec17p (alpha-SNAP) can precede docking and fusion of yeast vacuoles. *Cell*. 85:83-94.

McMahon, H.T., and I.G. Mills. 2004. COP and clathrin-coated vesicle budding: different pathways, common approaches. *Current Opinion in Cell Biology*. 16:379-91.

McNew, J.A., T. Weber, F. Parlati, R.J. Johnston, T.J. Melia, T.H. Söllner, and J.E. Rothman. 2000. Close is not enough: SNARE-dependent membrane fusion requires an active mechanism that transduces force to membrane anchors. *The Journal of Cell Biology*. 150:105-17.

Medkova, M., Y.E. France, J. Coleman, and P. Novick. 2006. The rab exchange factor Sec2p reversibly associates with the exocyst. *Mol Biol Cell*. 17:2757-69.

Merz, A.J., and W. Wickner. 2004a. Resolution of organelle docking and fusion kinetics in a cell-free assay. *Proc Natl Acad Sci USA*. 101:11548-53.

Merz, A.J., and W. Wickner. 2004b. Trans-SNARE interactions elicit Ca2+ efflux from the yeast vacuole lumen. *The Journal of Cell Biology*. 164:195-206.

Morozova, N., Y. Liang, A. Tokarev, S. Chen, R. Cox, J. Andrejic, Z. Lipatova, V. Sciorra, S. Emr, and N. Segev. 2006. TRAPPII subunits are required for the specificity switch of a Ypt–Rab GEF. *Nat Cell Biol*. 8:1263-1269.

Morsomme, P., and H. Riezman. 2002. The Rab GTPase Ypt1p and tethering factors couple protein sorting at the ER to vesicle targeting to the Golgi apparatus. *Developmental Cell*. 2:307-17.

Munson, M., and P. Novick. 2006. The exocyst defrocked, a framework of rods revealed. *Nat Struct Mol Biol*. 13:577-581.

Murphy, J.E., I.T. Pleasure, S. Puszkin, K. Prasad, and J.H. Keen. 1991. Clathrin assembly protein AP-3. The identity of the 155K protein, AP 180, and NP185 and demonstration of a clathrin binding domain. *J Biol Chem*. 266:4401-8.

Nakamura, N., A. Hirata, Y. Ohsumi, and Y. Wada. 1997. Vam2/Vps41p and Vam6/Vps39p are components of a protein complex on the vacuolar membranes and involved in the vacuolar assembly in the yeast Saccharomyces cerevisiae. *J Biol Chem*. 272:11344-9.

Nichols, B.J., C. Ungermann, H.R. Pelham, W.T. Wickner, and A. Haas. 1997. Homotypic vacuolar fusion mediated by t- and v-SNAREs. *Nature*. 387:199-202.

Nickel, W., T. Weber, J.A. McNew, F. Parlati, T.H. Söllner, and J.E. Rothman. 1999. Content mixing and membrane integrity during membrane fusion driven by pairing of isolated v-SNAREs and t-SNAREs. *Proc Natl Acad Sci USA*. 96:12571-6.

Ortiz, D., M. Medkova, C. Walch-Solimena, and P. Novick. 2002. Ypt32 recruits the Sec4p guanine nucleotide exchange factor, Sec2p, to secretory vesicles; evidence for a Rab cascade in yeast. *The Journal of Cell Biology*. 157:1005-15.

Ostrowicz, C.W., C.T. Meiringer, and C. Ungermann. 2008. Yeast vacuole fusion: a model system for eukaryotic endomembrane dynamics. *Autophagy*. 4:5-19.

Pearse, B.M. 1976. Clathrin: a unique protein associated with intracellular transfer of membrane by coated vesicles. *Proc Natl Acad Sci USA*. 73:1255-9.

Peplowska, K., D. Markgraf, C. Ostrowicz, G. Bange, and C. Ungermann. 2007. The CORVET Tethering Complex Interacts with the Yeast Rab5 Homolog Vps21 and Is Involved in Endo-Lysosomal Biogenesis. *Developmental Cell*. 12:739-750.

Peters, C., T.L. Baars, S. Bühler, and A. Mayer. 2004. Mutual control of membrane fission and fusion proteins. *Cell*. 119:667-78.

Pfeffer, S.R., A.B. Dirac-Svejstrup, and T. Soldati. 1995. Rab GDP dissociation inhibitor: putting rab GTPases in the right place. *J Biol Chem*. 270:17057-9.

Pobbati, A.V., A. Stein, and D. Fasshauer. 2006. N- to C-terminal SNARE complex assembly promotes rapid membrane fusion. *Science*. 313:673-6.

Price, A., D. Seals, W. Wickner, and C. Ungermann. 2000a. The docking stage of yeast vacuole fusion requires the transfer of proteins from a cis-SNARE complex to a Rab/Ypt protein. *The Journal of Cell Biology*. 148:1231-8.

Price, A., W. Wickner, and C. Ungermann. 2000b. Proteins needed for vesicle budding from the Golgi complex are also required for the docking step of homotypic vacuole fusion. *The Journal of Cell Biology*. 148:1223-29.

Prigent, M. 2003. ARF6 controls post-endocytic recycling through its downstream exocyst complex effector. *The Journal of Cell Biology*. 163:1111-1121.

Pruyne, D.W., D.H. Schott, and A. Bretscher. 1998. Tropomyosin-containing actin cables direct the Myo2p-dependent polarized delivery of secretory vesicles in budding yeast. *The Journal of Cell Biology*. 143:1931-45.

Puig, O., F. Caspary, G. Rigaut, B. Rutz, E. Bouveret, E. Bragado-Nilsson, M. Wilm, and B. Séraphin. 2001. The tandem affinity purification (TAP) method: a general procedure of protein complex purification. *Methods*. 24:218-29.

Quenneville, N.R., T.Y. Chao, J.M. McCaffery, and E. Conibear. 2006. Domains within the GARP subunit Vps54 confer separate functions in complex assembly and early endosome recognition. *Mol Biol Cell*. 17:1859-70.

Ram, R.J., B. Li, and C.A. Kaiser. 2002. Identification of Sec36p, Sec37p, and Sec38p: components of yeast complex that contains Sec34p and Sec35p. *Mol Biol Cell*. 13:1484-500.

Raymond, C.K., I. Howald-Stevenson, C.A. Vater, and T.H. Stevens. 1992. Morphological classification of the yeast vacuolar protein sorting mutants: evidence for a prevacuolar compartment in class E vps mutants. *Mol Biol Cell*. 3:1389-402.

Reese, C., F. Heise, and A. Mayer. 2005. Trans-SNARE pairing can precede a hemifusion intermediate in intracellular membrane fusion. *Nature*. 436:410-4.

Reggiori, F., and H.R. Pelham. 2002. A transmembrane ubiquitin ligase required to sort membrane proteins into multivesicular bodies. *Nat Cell Biol*. 4:117-23.

Rehling, P., T. Darsow, D.J. Katzmann, and S.D. Emr. 1999. Formation of AP-3 transport intermediates requires Vps41 function. *Nat Cell Biol*. 1:346-53.

Rieder, S.E., and S.D. Emr. 1997. A novel RING finger protein complex essential for a late step in protein transport to the yeast vacuole. *Mol Biol Cell*. 8:2307-27.

Rigaut, G., A. Shevchenko, B. Rutz, M. Wilm, M. Mann, and B. Séraphin. 1999. A generic protein purification method for protein complex characterization and proteome exploration. *Nat Biotech*. 17:1030-2.

Rink, J., E. Ghigo, Y. Kalaidzidis, and M. Zerial. 2005. Rab Conversion as a Mechanism of Progression from Early to Late Endosomes. *Cell*. 122:735-749.

Rizo, J., and T.C. Südhof. 2002. Snares and Munc18 in synaptic vesicle fusion. *Nat Rev Neurosci*. 3:641-53.

Ross, J., M. Ali, and D. Warshaw. 2008. Cargo transport: molecular motors navigate a complex cytoskeleton. *Current Opinion in Cell Biology*. 20:41-47.

ROTH, T.F., and K.R. PORTER. 1964. YOLK PROTEIN UPTAKE IN THE OOCYTE OF THE MOSQUITO AEDES AEGYPTI. L. *The Journal of Cell Biology*. 20:313-32.

Rothman, J.E. 1994. Mechanisms of intracellular protein transport. *Nature*. 372:55-63.

Rothman, J.H., I. Howald, and T.H. Stevens. 1989. Characterization of genes required for protein sorting and vacuolar function in the yeast Saccharomyces cerevisiae. *EMBO J*. 8:2057-65.

Roumanie, O., H. Wu, J.N. Molk, G. Rossi, K. Bloom, and P. Brennwald. 2005. Rho GTPase regulation of exocytosis in yeast is independent of GTP hydrolysis and polarization of the exocyst complex. *The Journal of Cell Biology*. 170:583-94.

Sacher, M., J. Barrowman, W. Wang, J. Horecka, Y. Zhang, M. Pypaert, and S. Ferro-Novick. 2001. TRAPP I implicated in the specificity of tethering in ER-to-Golgi transport. *Molecular Cell*. 7:433-42.

Sacher, M., Y.G. Kim, A. Lavie, B.H. Oh, and N. Segev. 2008. The TRAPP Complex: Insights into its Architecture and Function. *Traffic*. 9:2032-2042.

Sato, T.K., T. Darsow, and S.D. Emr. 1998. Vam7p, a SNAP-25-like molecule, and Vam3p, a syntaxin homolog, function together in yeast vacuolar protein trafficking. *Mol Cell Biol*. 18:5308-19.

Sato, T.K., P. Rehling, M.R. Peterson, and S.D. Emr. 2000. Class C Vps protein complex regulates vacuolar SNARE pairing and is required for vesicle docking/fusion. *Molecular Cell*. 6:661-71.

Schott, D., J. Ho, D. Pruyne, and A. Bretscher. 1999. The COOH-terminal domain of Myo2p, a yeast myosin V, has a direct role in secretory vesicle targeting. *The Journal of Cell Biology*. 147:791-808.

Scott, B.L., J.S. Van Komen, H. Irshad, S. Liu, K.A. Wilson, and J.A. McNew. 2004. Sec1p directly stimulates SNARE-mediated membrane fusion in vitro. *The Journal of Cell Biology*. 167:75-85.

Scott, S.V., M. Baba, Y. Ohsumi, and D. Klionsky. 1997. Aminopeptidase I is targeted to the vacuole by a nonclassical vesicular mechanism. *The Journal of Cell Biology*. 138:37-44.

Scott, S.V., A. Hefner-Gravink, K.A. Morano, T. Noda, Y. Ohsumi, and D. Klionsky. 1996. Cytoplasm-to-vacuole targeting and autophagy employ the same machinery to deliver proteins to the yeast vacuole. *Proc Natl Acad Sci USA*. 93:12304-8.

Scott, S.V., D.C. Nice, J.J. Nau, L.S. Weisman, Y. Kamada, I. Keizer-Gunnink, T. Funakoshi, M. Veenhuis, Y. Ohsumi, and D. Klionsky. 2000. Apg13p and Vac8p are part of a complex of phosphoproteins that are required for cytoplasm to vacuole targeting. *J Biol Chem*. 275:25840-9.

Seals, D.F., G. Eitzen, N. Margolis, W.T. Wickner, and A. Price. 2000. A Ypt/Rab effector complex containing the Sec1 homolog Vps33p is required for homotypic vacuole fusion. *Proc Natl Acad Sci USA*. 97:9402-7.

Seaman, M.N. 2005. Recycle your receptors with retromer. *Trends in Cell Biology*. 15:68-75.

Seeger, M., and G.S. Payne. 1992. A role for clathrin in the sorting of vacuolar proteins in the Golgi complex of yeast. *EMBO J*. 11:2811-8.

Shen, J., D.C. Tareste, F. Paumet, J.E. Rothman, and T.J. Melia. 2007. Selective activation of cognate SNAREpins by Sec1/Munc18 proteins. *Cell*. 128:183-95.

Simpson, F., N.A. Bright, M.A. West, L.S. Newman, R.B. Darnell, and M.S. Robinson. 1996. A novel adaptor-related protein complex. *The Journal of Cell Biology*. 133:749-60.

Simpson, F., A.A. Peden, L. Christopoulou, and M.S. Robinson. 1997. Characterization of the adaptor-related protein complex, AP-3. *The Journal of Cell Biology*. 137:835-45.

Siniossoglou, S., S.Y. Peak-Chew, and H.R. Pelham. 2000. Ric1p and Rgp1p form a complex that catalyses nucleotide exchange on Ypt6p. *EMBO J*. 19:4885-94.

Siniossoglou, S., and H.R. Pelham. 2001. An effector of Ypt6p binds the SNARE Tlg1p and mediates selective fusion of vesicles with late Golgi membranes. *EMBO J*. 20:5991-8.

Siniossoglou, S., and H.R. Pelham. 2002. Vps51p links the VFT complex to the SNARE Tlg1p. *J Biol Chem*. 277:48318-24.

Sivaram, M.V., J.A. Saporita, M.L. Furgason, A.J. Boettcher, and M. Munson. 2005. Dimerization of the exocyst protein Sec6p and its interaction with the t-SNARE Sec9p. *Biochemistry*. 44:6302-11.

Sivars, U., D. Aivazian, and S.R. Pfeffer. 2003. Yip3 catalyses the dissociation of endosomal Rab-GDI complexes. *Nature*. 425:856-9.

Söllner, T., M.K. Bennett, S.W. Whiteheart, R.H. Scheller, and J.E. Rothman. 1993a. A protein assembly-disassembly pathway in vitro that may correspond to sequential steps of synaptic vesicle docking, activation, and fusion. *Cell*. 75:409-18.

Söllner, T., S.W. Whiteheart, M. Brunner, H. Erdjument-Bromage, S. Geromanos, P. Tempst, and J.E. Rothman. 1993b. SNAP receptors implicated in vesicle targeting and fusion. *Nature*. 362:318-24.

Song, X., W. Xu, A. Zhang, G. Huang, X. Liang, J.V. Virbasius, M.P. Czech, and G.W. Zhou. 2001. Phox homology domains specifically bind phosphatidylinositol phosphates. *Biochemistry*. 40:8940-4.

Starai, V., C.M. Hickey, and W. Wickner. 2008. HOPS proofreads the trans-SNARE complex for yeast vacuole fusion. *Mol Biol Cell*. 19:2500-8.

Starai, V., Y. Jun, and W. Wickner. 2007. Excess vacuolar SNAREs drive lysis and Rab bypass fusion. *Proc Natl Acad Sci USA*. 104:13551-8.

Stepp, J.D., K. Huang, and S.K. Lemmon. 1997. The yeast adaptor protein complex, AP-3, is essential for the efficient delivery of alkaline phosphatase by the alternate pathway to the vacuole. *The Journal of Cell Biology*. 139:1761-74.

Stevens, T., B. Esmon, and R. Schekman. 1982. Early stages in the yeast secretory pathway are required for transport of carboxypeptidase Y to the vacuole. *Cell*. 30:439-48.

Stroupe, C., K. Collins, R. Fratti, and W. Wickner. 2006. Purification of active HOPS complex reveals its affinities for phosphoinositides and the SNARE Vam7p. *EMBO J*. 25:1579-1589.

Subramanian, S., C.A. Woolford, and E.W. Jones. 2004. The Sec1/Munc18 protein, Vps33p, functions at the endosome and the vacuole of Saccharomyces cerevisiae. *Mol Biol Cell*. 15:2593-605.

Sun, B., L. Chen, W. Cao, A.F. Roth, and N.G. Davis. 2004. The yeast casein kinase Yck3p is palmitoylated, then sorted to the vacuolar membrane with AP-3-dependent recognition of a YXXPhi adaptin sorting signal. *Mol Biol Cell*. 15:1397-406.

Sutton, R.B., D. Fasshauer, R. Jahn, and A.T. Brunger. 1998. Crystal structure of a SNARE complex involved in synaptic exocytosis at 2.4 A resolution. *Nature*. 395:347-53.

Suvorova, E.S., R. Duden, and V.V. Lupashin. 2002. The Sec34/Sec35p complex, a Ypt1p effector required for retrograde intra-Golgi trafficking, interacts with Golgi SNAREs and COPI vesicle coat proteins. *The Journal of Cell Biology*. 157:631-43.

Takai, Y., K. Kaibuchi, A. Kikuchi, and M. Kawata. 1992. Small GTP-binding proteins. *Int Rev Cytol*. 133:187-230.

Tang, F., Y. Peng, J.J. Nau, E.J. Kauffman, and L. Weisman. 2006. Vac8p, an armadillo repeat protein, coordinates vacuole inheritance with multiple vacuolar processes. *Traffic*. 7:1368-77.

Teis, D., S. Saksena, and S. Emr. 2008. Ordered Assembly of the ESCRT-III Complex on Endosomes Is Required to Sequester Cargo during MVB Formation. *Developmental Cell*. 15:578-589.

TerBush, D.R., T. Maurice, D. Roth, and P. Novick. 1996. The Exocyst is a multiprotein complex required for exocytosis in Saccharomyces cerevisiae. *EMBO J*. 15:6483-94.

Tripathi, A., Y. Ren, P.D. Jeffrey, and F. Hughson. 2009. Structural characterization of Tip20p and Dsl1p, subunits of the Dsl1p vesicle tethering complex. *Nat Struct Mol Biol*. 16:114-23.

Ungar, D., T. Oka, E.E. Brittle, E. Vasile, V.V. Lupashin, J.E. Chatterton, J.E. Heuser, M. Krieger, and M.G. Waters. 2002. Characterization of a mammalian Golgi-localized protein complex, COG, that is required for normal Golgi morphology and function. *The Journal of Cell Biology*. 157:405-15.

Ungar, D., T. Oka, M. Krieger, and F. Hughson. 2006. Retrograde transport on the COG railway. *Trends in Cell Biology*. 16:113-20.

Ungermann, C., B.J. Nichols, H.R. Pelham, and W. Wickner. 1998a. A vacuolar v-t-SNARE complex, the predominant form in vivo and on isolated vacuoles, is disassembled and activated for docking and fusion. *The Journal of Cell Biology*. 140:61-9.

Ungermann, C., A. Price, and W. Wickner. 2000. A new role for a SNARE protein as a regulator of the Ypt7/Rab-dependent stage of docking. *Proc Natl Acad Sci USA*. 97:8889-91.

Ungermann, C., K. Sato, and W. Wickner. 1998b. Defining the functions of trans-SNARE pairs. *Nature*. 396:543-8.

Ungermann, C., G.F. von Mollard, O.N. Jensen, N. Margolis, T.H. Stevens, and W. Wickner. 1999. Three v-SNAREs and two t-SNAREs, present in a pentameric cis-SNARE complex on isolated vacuoles, are essential for homotypic fusion. *The Journal of Cell Biology*. 145:1435-42.

Ungermann, C., and W. Wickner. 1998. Vam7p, a vacuolar SNAP-25 homolog, is required for SNARE complex integrity and vacuole docking and fusion. *EMBO J*. 17:3269-76.

Veit, M., R. Laage, L. Dietrich, L. Wang, and C. Ungermann. 2001. Vac8p release from the SNARE complex and its palmitoylation are coupled and essential for vacuole fusion. *EMBO J*. 20:3145-55.

Vembar, S.S., and J.L. Brodsky. 2008. One step at a time: endoplasmic reticulum-associated degradation. *Nat Rev Mol Cell Biol*.

Vetter, I.R., and A. Wittinghofer. 2001. The guanine nucleotide-binding switch in three dimensions. *Science*. 294:1299-304.

Vowels, J.J., and G.S. Payne. 1998. A dileucine-like sorting signal directs transport into an AP-3-dependent, clathrin-independent pathway to the yeast vacuole. *EMBO J*. 17:2482-93.

Wada, Y., Y. Ohsumi, and Y. Anraku. 1992. Genes for directing vacuolar morphogenesis in Saccharomyces cerevisiae. I. Isolation and characterization of two classes of vam mutants. *J Biol Chem*. 267:18665-70.

Walch-Solimena, C., R.N. Collins, and P.J. Novick. 1997. Sec2p mediates nucleotide exchange on Sec4p and is involved in polarized delivery of post-Golgi vesicles. *The Journal of Cell Biology*. 137:1495-509.

Walter, P., and G. Blobel. 1980. Purification of a membrane-associated protein complex required for protein translocation across the endoplasmic reticulum. *Proc Natl Acad Sci USA*. 77:7112-6.

Wang, C.W., P.E. Stromhaug, E.J. Kauffman, L. Weisman, and D.J. Klionsky. 2003a. Yeast homotypic vacuole fusion requires the Ccz1-Mon1 complex during the tethering/docking stage. *The Journal of Cell Biology*. 163:973-85.

Wang, C.W., P.E. Stromhaug, J. Shima, and D.J. Klionsky. 2002a. The Ccz1-Mon1 protein complex is required for the late step of multiple vacuole delivery pathways. *J Biol Chem*. 277:47917-27.

Wang, L., A.J. Merz, K. Collins, and W. Wickner. 2003b. Hierarchy of protein assembly at the vertex ring domain for yeast vacuole docking and fusion. *The Journal of Cell Biology*. 160:365-74.

Wang, L., E.S. Seeley, W. Wickner, and A.J. Merz. 2002b. Vacuole fusion at a ring of vertex docking sites leaves membrane fragments within the organelle. *Cell*. 108:357-69.

Wang, L., C. Ungermann, and W. Wickner. 2000. The docking of primed vacuoles can be reversibly arrested by excess Sec17p (alpha-SNAP). *J Biol Chem*. 275:22862-7.

Wang, Y., I. Dulubova, J. Rizo, and T.C. Südhof. 2001a. Functional analysis of conserved structural elements in yeast syntaxin Vam3p. *J Biol Chem*. 276:28598-605.

Wang, Y.X., E.J. Kauffman, J.E. Duex, and L.S. Weisman. 2001b. Fusion of docked membranes requires the armadillo repeat protein Vac8p. *J Biol Chem*. 276:35133-40.

Weber, T., B.V. Zemelman, J.A. McNew, B. Westermann, M. Gmachl, F. Parlati, T.H. Söllner, and J.E. Rothman. 1998. SNAREpins: minimal machinery for membrane fusion. *Cell*. 92:759-72.

Weimbs, T., S.H. Low, S.J. Chapin, K.E. Mostov, P. Bucher, and K. Hofmann. 1997. A conserved domain is present in different families of vesicular fusion proteins: a new superfamily. *Proc Natl Acad Sci USA*. 94:3046-51.

Weisman, L. 2006. Organelles on the move: insights from yeast vacuole inheritance. *Nat Rev Mol Cell Biol*. 7:243-52.

Weisman, L.S., R. Bacallao, and W. Wickner. 1987. Multiple methods of visualizing the yeast vacuole permit evaluation of its morphology and inheritance during the cell cycle. *The Journal of Cell Biology*. 105:1539-47.

Weisman, L.S., and W. Wickner. 1988. Intervacuole exchange in the yeast zygote: a new pathway in organelle communication. *Science*. 241:589-91.

Wen, W., L. Chen, H. Wu, X. Sun, M. Zhang, and D.K. Banfield. 2006. Identification of the yeast R-SNARE Nyv1p as a novel longin domain-containing protein. *Mol Biol Cell*. 17:4282-99.

Whittaker, R.H., and L. Margulis. 1978. Protist classification and the kingdoms of organisms. *BioSystems*. 10:3-18.

Whyte, J.R., and S. Munro. 2002. Vesicle tethering complexes in membrane traffic. *Journal of Cell Science*. 115:2627-37.

Wickner, W. 2002. Yeast vacuoles and membrane fusion pathways. *EMBO J*. 21:1241-7.

Woese, C.R., O. Kandler, and M.L. Wheelis. 1990. Towards a natural system of organisms: proposal for the domains Archaea, Bacteria, and Eucarya. *Proc Natl Acad Sci USA*. 87:4576-9.

Wurmser, A.E., T.K. Sato, and S.D. Emr. 2000. New component of the vacuolar class C-Vps complex couples nucleotide exchange on the Ypt7 GTPase to SNARE-dependent docking and fusion. *The Journal of Cell Biology*. 151:551-62.

Ybe, J.A., F.M. Brodsky, K. Hofmann, K. Lin, S.H. Liu, L. Chen, T.N. Earnest, R.J. Fletterick, and P.K. Hwang. 1999. Clathrin self-assembly is mediated by a tandemly repeated superhelix. *Nature*. 399:371-5.

Yogosawa, S., M. Kawasaki, S. Wakatsuki, E. Kominami, Y. Shiba, K. Nakayama, S. Kohsaka, and C. Akazawa. 2006. Monoubiquitylation of GGA3 by hVPS18 regulates its ubiquitin-binding ability. *Biochemical and Biophysical Research Communications*. 350:82-90.

Acknowledgments

First of all, I would like to thank my supervisor Christian Ungermann for the opportunity to work in his lab on such an exciting project. More than that, he taught me so much more about science and how to work in science than I had thought I could ever learn. Thank you for being such a supportive and understanding mentor during this time.

Furthermore, I would like to thank Professor Dr. Ed Hurt for being the first referee of this thesis and for the opportunity to take advantage of the knowledge and facilities in his lab, which helped me establish important methods used in this study.

Many people have accompanied my route both in Heidelberg and in Osnabrück. It is them, who I want to thank for being part of my life in so many different regards. I cannot possibly mention everyone, but I especially want to thank Gabi Müller and Nadine Decker for being so helpful in the lab both on the professional as well as on the personal level. My fellow co-workers who made their way up to Osnabrück together with me, Christoph Meiringer, Karolina Peplowska, Daniel Markgraf, Haitong Hou, and Kangaraj Subramanian, I want to thank you for all the great moments we shared in- and outside the lab. Thank you all for your friendship and loyalty.

I want to thank the new crew here in Osnabrück for the pleasant lab atmosphere and especially Kathrin Auffarth and Angela Perz for help at the bench but also for making this lab work so well.

Most of all, I thank my wife Claudine for her never-ending support and understanding, her strength and her belief in me. Thank you for being who you are and thank you for being with me.

Our little son Felix accompanied us during the last year of my PhD. I want to thank him for brightening every moment of our lives ever since his birth.

Finally, I would like to say thank you to my parents for their ongoing support and their never-ending belief in my abilities, which have made me who I am.